Probabilistic Seismic Hazard Analysis for Zimbabwe

By

VICTOR PHILIP MAPURANGA

University of Pretoria

Submitted in partial fulfilment of the requirements for the degree of

MASTER OF SCIENCE (MSc) IN PHYSICS

Department of Physics in the Faculty of

Natural and Agricultural Sciences at the

University of Pretoria

Pretoria

May 2014

Supervisor: Professor A Kijko

DECLARATION

I, Victor Philip Mapuranga, declare that the thesis/dissertation, which I hereby submit for the degree Master of Science in Physics at the University of Pretoria, is my own work and has not previously been submitted by me for a degree at this or any other tertiary institution.

SIGNATURE: …….

DATE: ……

SUMMARY

In this study, the seismic hazards of Zimbabwe are presented as maps showing probabilistic peak ground acceleration (PGA). Seismic hazards maps have a 10% chance of exceeding the indicated ground acceleration over a 50 year period, and are prepared using a homogenized 101 year catalogue compiled for seismic moment magnitude M_w. Two approaches of probabilistic seismic hazard assessment were applied.

The first was the widely used "deductive" approach (Cornell, 1968) which integrates geological and geophysical information together with seismic event catalogues in the assessment of seismic hazards. Application of the procedure includes several steps. As a first step, this procedure requires the delineation of potential seismic zones, which is strongly influenced by historic patterns and based on independent geologic evidence or tectonic features such as faults (Atkinson, 2004; Kijko and Graham, 1998).

The second method was the "parametric-historic" approach of Kijko and Graham (1998, 1999) which has been developed for regions with incomplete catalogues and does not require the subjective delineation of active seismic zones. It combines the best features of the deductive Cornell-McGuire procedure and the historic method of Veneziano *et al.* (1984).

Four (4) ground motion prediction equations suitable for hard rock conditions in a specified region were applied in the assessment of seismic hazards. The highest levels of hazards in Zimbabwe are in the south-eastern border of the country with Mozambique, the Lake Kariba area and the mid-Zambezi basin in the vicinity of the Save-Limpopo mobile belt. Results show that assessment of seismic hazard using parametric-historic procedure to a large extent gives a “mirror” of the seismicity pattern whereas using the classic Cornell-McGuire procedure gives results that reflect the delineated pattern of seismic zones and the two methods are best used complementary of each other depending on available input data.

ACKNOWLEDGEMENTS

I would like to express my most sincere appreciation to my supervisor, Professor Andrzej Kijko. His help has been more than I could have hoped for. Always available and willing to offer his assistance and guidance even beyond scientific matters has been exactly what every student would need. I would also like to thank my dear mother, my brothers Michael, Martin and especially Leon for his unwavering support materially and morally, without which this would have been impossible. I also want express my appreciation towards Miss. Yvette Beever, Mrs Ingrid Booysen for the GIS assistance and Ms. Elizabeth Marx for the editorial work. I would also like to acknowledge all other people that have been supportive and who offered advice from behind the scenes such as: Mr. B Manzunzu, Miss. Smit, Miss. T Mulabisana, Mr. D Gonese, as well as the staff at the Council of Geoscience amongst the many others that I have not mentioned by name.

LIST OF ABBREVIATIONS AND ACRONYMS

BUL	Bulawayo
CDF	Cumulative Distribution Function
CZ	Central Zone
DEM	Digital Elevation Model
DSHA	Deterministic Seismic Hazard Assessment
EARS	East African Rift System
FMD	Frequency Magnitude Distribution
GMPE	Ground Motion Prediction Equation
G-R	Gutenberg Richter
ISC	International Seismological Centre
K-S	Kijko-Sellevoll
K-S-B	Kijko-Sellevoll-Bayes
MFR	Magnitude Frequency relationship
MZV	Mid-Zambezi Valley
NMZ	Northern Marginal Zone
PDF	Probability Density Function
PGA	Peak Ground Acceleration
PSHA	Probabilistic Seismic Hazard Assessment
SMZ	Southern Marginal Zone
SSAC	Senior Seismic Hazard Analysis Committee

TABLE OF CONTENTS

TABLE OF FIGURES

Chapter 1

Introduction

1.1 Introduction and background

According to the Munich Reinsurance Company Issue (2000), increased seismic vulnerability of most urban structures especially in developing countries is a major reason of apprehension. Such a quandary therefore means emphasis should be given to the reduction of vulnerability in urban areas. This, according to Ingleton (1999), requires an analysis of potential losses in order to make recommendations for prevention, preparedness and response through a risk evaluation assessment. Risk is defined as the expected losses (of lives, person injured, property damaged and economic activity disrupted) due to seismic hazard for a given area and reference period. Based on mathematical calculations, risk is the product of hazards, vulnerability and the cost of the elements at risk (WMO, 1999).

Seismic vulnerability in generalised terms can be defined as the likelihood of some group of elements at risk, such as buildings, to undergo adverse effects due to potential earthquakes (Sandi *et. al*, 2007). Assessment of seismic vulnerability of existing infrastructure would help in disaster mitigation and management by planning mitigation measures before the occurrence of a fatal seismic event. The cost of the elements at risk refers to the human activity located in the zones of seismic hazard and represents the quantity and quality of the "goods" (population, facilities, and lifelines) exposed to risk.

In this study we shall limit our focus on seismic hazard assessment which involves the quantitative evaluation of ground shaking hazards (primary hazard; earthquake damage to the site and secondary hazards such as: surface faulting, liquefaction, landslides and fires) at a specific location. It also provides an approximation of ground motion at a site of interest by incorporating information such as historical earthquake records, tectonics, geology, and attenuation characteristics of seismic waves.

Earthquake damage can affect many fields which are correlated to each other. The most universal and basic damages are to buildings, and human casualties. In order to reduce earthquake damage, the first step

for a region should be to understand what would happen if a significant earthquake were to strike the city. As a second step, effective earthquake risk management activities and measures that would aid in damage reduction that are based on the findings of the first step, should be identified. Assessing the magnitude of potential damage should not be thought of as the final goal of the damage estimation process, but rather as the beginning of the earthquake disaster management planning.

Seismic hazard analysis can be done using two distinct methodologies; the deterministic approach, and the probabilistic approach. The deterministic approach uses an accepted earthquake scenario, whereas the probabilistic approach quantifies the rate (or probability) of exceeding various ground motion levels at a site, given all possible earthquakes. Seismic hazards affects lifeline facilities such as electric power and gas networks, railroads, highways, bridges, water and sewage.

To begin the process of earthquake disaster management planning, a scenario earthquake for the area should be decided on. Reoccurrence of a past significant earthquake or active fault earthquake is commonly assumed. The epicenter, magnitude, occurrence time (day or night) should also be determined. Usually, ground shaking intensity or PGA (peak ground acceleration) at the site generally becomes greater as the magnitude becomes larger or the distance from the site to the epicenter becomes smaller.

Ground shaking is also greatly influenced by the ground conditions of the site. Thus, seismic hazards will be estimated from the parameters of the scenario earthquake and ground conditions. Damage will be estimated for hazards and the existing structures in the area and depends not only on the number of structures but also types of the buildings or lifeline facilities, using vulnerability functions derived from each type of structure. Vulnerability functions reflect the relationship between seismic intensity and the degree of damage to the structure. Casualties such as deaths and injuries are also estimated if the population distribution is known. Thus, the total amount and distribution of damage can be estimated if the chosen scenario earthquake was to occur.

The seismicity of Zimbabwe is generally moderate with some notable events occurring near the Zimbabwe – Mozambique border, the Nyamandlovu area as well as the northern part of the country which covers the Zambezi area. The country lies at the southern tip of the East African Rift System (Vail, 1967; Fairhead & Girdler, 1969; Fairhead & Henderson, 1977, Hlatywayo, 1997). In terms of seismicity, the country can be divided into three broad seismic zones as shown on figure 1.1 below namely, the eastern area of the country, the Zambezi basin and the central area. Seismic activity is mainly centred along its borders with Mozambique, to the east, in the Deka fault zone in the Hwange area, to the northwest and over the mid-Zambezi basin in the Lake Kariba area.

Seismic events of magnitude higher than 5.0 have occurred in the mid-Zambezi basin. Events in this area show normal faulting (Shudofsky, 1985; Hlatywayo, 1995). Studies on incipient rifting in the mid-Zambezi Basin confirm tectonic activity similar to that along the East Africa Rift System to the north (Fairhead & Girdler, 1969; Fairhead & Henderson, 1977). The south-eastern border area of Zimbabwe forms the western flank of the rift extension from Lake Malawi (Hlatywayo, 1996). Peak ground acceleration (PGA) values in excess of 0.1g for a return period of 100 years were reported for both the Deka Valley and the Mid-Zambezi Basin (Hlatywayo, 1997).

A number of seismic hazard assessments have been carried out in Zimbabwe with the Global Seismic Hazard Assessment Programme (Midzi *et al*., 1999) being the most notable. Hlatywayo (1995) carried out seismic hazard assessment for central and southern Africa region. Notably, events that have occurred in Zimbabwe since the 1995 assessment includes the 25 June 2004 and 15 March 2008 Nyamandlovu earthquakes m_b = 4.3, which were felt as far as Bulawayo, 120km away. The 22 February 2006 Mozambique earthquake m_b = 7.0, which killed 4 people near the Zimbabwe border in Mozambique and caused a lot of destruction especially in Chipinge and surrounding areas is regarded as one of the biggest events in Africa. Also we have the 2006 Wedza earthquake, which occurred in area where the seismicity is very low. The magnitude of this event was around M_L= 4.0. The event was felt as far as Marondera, a town about 75km from the epicentre. Near the epicentre of this event, the shaking was so intense such that a lot of people were frightened by the event.

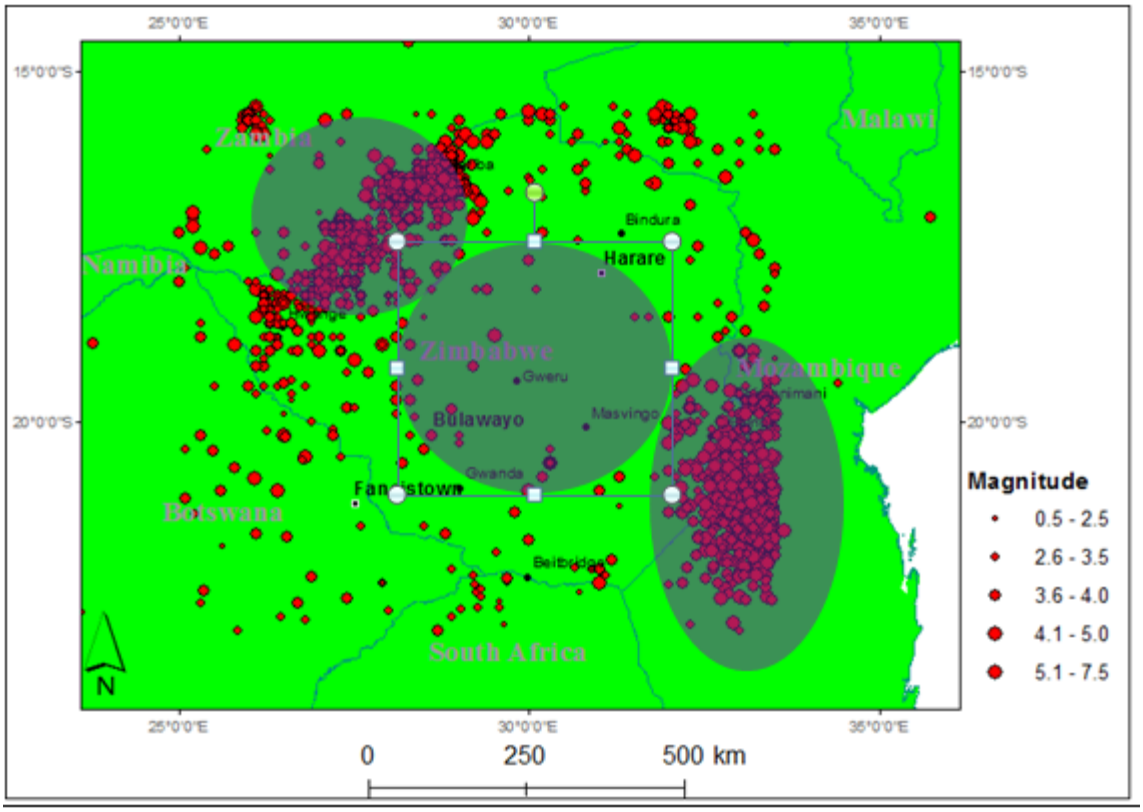

Figure 1.1: Map showing the 3 broad seismic regions of Zimbabwe

Most of these events occurred in areas that had been previously regarded as aseismic and thus not included as source zones in previous studies. Increased industrial activity and urbanisation of the population and the growth of a number of high rise buildings together with the increased construction of dams and mining activity, accentuate the need for seismic hazard mitigation in the form of seismic zoning maps, peak ground motions and seismic activity rates.

Chapter 2

Literature Review

2.1 Introduction

Seismic hazard assessment has a number of applications, among them, seismic micro-zonation studies, which are important for decision-making on land use, evaluation of the level of earthquake preparedness, economical consideration of earthquake-resistant design, retrofit strategy, economic loss estimation in the event of future earthquakes, and also for the design of ordinary structures where site-specific studies are not warranted (SamamYangmaei-Sabegh *et al.*, 2010). There are two basic methodologies which one can follow when carrying out seismic hazard analysis of a region as stated earlier, which are the deterministic approach as well as the probabilistic approach, though the probabilistic approach is much more widely used compared to the deterministic approach.

According to Bulajic and Manic (2006) even if one chooses to use probabilistic seismic hazard assessment (PSHA) or deterministic seismic hazard analysis (DSHA), the basic input data that must be collected are practically the same. The data would include all past earthquakes within an area of several hundred kilometre radius around the site of a structure of interest, the seismotectonic and geological features of the region as well as the local soil conditions for different sites and the ground attenuation characteristics. Before any further step in the analysis is undertaken, the seismic source zones and their properties must be defined using all the available data.

2.2 Deterministic seismic hazard analysis

In the deterministic approach, the strong-motion parameters are estimated for the maximum credible earthquake, assumed to occur at the closest possible distance from the site of interest, without considering the likelihood of its occurrence during a specified exposure period (Gupta, 2002). It must be noted that there is no generally accepted deterministic seismic hazard analysis approach that is appropriate for all parts of the world as it is practiced in diverse ways in different parts of the world. The DSHA approach can be aimed at finding the maximum possible strong earthquake ground motion at a site of interest (Reiter, 1990; Anderson, 1997; Anderson *et al.*, 2000) or at finding the values of the selected ground

motion parameter that are compatible with the results of the corresponding probabilistic seismic hazard analysis (Trifunac, 1989; McGuire, 1995).

When DSHA is used to find the maximum possible ground motion in a given region, then the largest possible earthquake must be estimated for each of the active faults and seismic zones within the region with a radius of up to 450 km, assuming it occurs at the closest distance to a site of interest and the magnitude and distance combination that produces the largest value of the ground motion parameter used to evaluate seismic hazard can be found using the appropriate attenuation relations. DSHA can also be used to find earthquakes that will not necessarily produce the largest possible ground motion at a site but will contribute significantly to the seismic hazard assessment that has been calculated using the PSHA.

Even though this approach sounds straightforward it is overshadowed by the complexity and uncertainty in selecting the appropriate earthquake scenario (Kijko, 2011). Furthermore the reliable estimation of the maximum credible earthquake, definition of source characteristics as well as estimating corresponding ground motion are all concepts that are associated with large uncertainties. The probability of the so-called "scenario earthquake" that would have been estimated for a site by the PSHA method occurring in time is often low compared to the hazards that a given structure may face and this all creates the need for an alternative approach, the probabilistic methodology, which is free from discrete selection of scenario earthquakes.

2.3 Probabilistic seismic hazard analysis

The main goal of probabilistic seismic hazard analysis (PSHA) is to quantify the probability of exceeding various ground motion levels at a site, given all possible earthquake scenarios. It allows for uncertainties in the size, location and rate of recurrence of earthquakes and in the variation of ground motion characteristics with earthquake size and location to be explicitly considered for the evaluation of seismic hazard. Additionally, it provides a framework for these uncertainties to be identified, quantified and combined in a rational manner to provide a more complete picture of the seismic hazard.

There are different types of PSHA methodologies that are in use today. These methods can either be deductive or historic (Veneziano *et al*. 1984). The most commonly followed procedure for deductive PSHA is normally referred to as the classic Cornell-McGuire approach (Cornell, 1968; McGuire, 1976) and forms the theoretical basis of the deductive methods and allows the use of geological, geophysical

information in addition to seismic catalogues. It is essentially carried out in four steps which are outlined in the following sections (Reiter, 1990; Kramer, 1996; Kijko, 2011).

2.3.1 Identification and delineation of seismic source zones

The initial step in this procedure is the identification and delineation of seismic source zones which are normally associated with geologic and tectonic features such as active faults which may affect the site under consideration and averaging all the available information. Uniform distribution of seismicity is assigned to each earthquake source, implying that earthquakes are equally likely to occur at any point within the source zone.

All available information on active faults must be taken into account such that they are characterized in terms of geometry (in three dimensions), segmentation, and sense of slip as well a function describing rupture length or area as a function of magnitude (McGuire, 1993). Geological maps, expressing the age of the formations, trenches, geophysical data and digital elevation model (DEM) allow better location of faults. Other useful data for this purpose is shown in Figure 2.1. In cases where this information is limited or unavailable, the alternative procedure would be to identify areal sources (usually demarcated as polygons) where earthquake characteristics are taken to be similar and account for uncertainties in the characterization process.

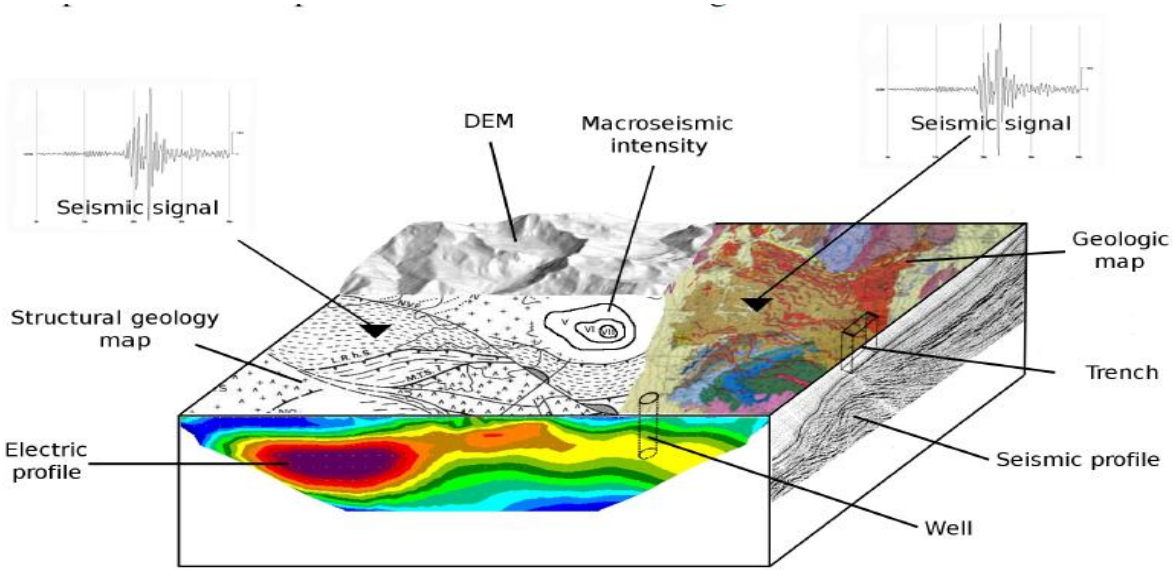

Figure 2.1: 3D diagram representing the some useful data for using in delineating zones

(Le Goff *et al*. 2007)

The identification and delineation of seismic source zones is at the core of deductive methods such as the Cornell-McGuire approach. Unfortunately this also forms the major disadvantage of this approach. This is because in most parts of the world tectonic provinces as well as active faults have not been mapped and the causes of seismicity are not well understood. This results in the process of identification and delineation of source zones being a subjective matter. Nonetheless, even renowned experts rarely agree on the boundaries of source zones for the same region.

The specification of different source zones for the same area will most often result in a hazard assessment that is significantly different for the same area. In addition, often, seismicity within the seismic sources is not distributed uniformly, as required by the classic Cornell-McGuire procedure (Kijko, 2011). Figure 2.3 below shows two different seismic hazard maps that have been produced for Italy by two different research groups due to specification of different seismogenic zones.

Also the causes of seismicity and the processes that govern how an earthquake's energy propagates from its origin beneath the earth's surface to various points near and far on the surface are not well understood. The limited information that does exist can be-and often is-legitimately interpreted differently by different experts, and these differences of interpretation translate into important uncertainties in the numerical results from a PSHA (SSHAC, 1997).

2.3.2 Determination of seismic parameters for each seismic zone

In the second step, the seismicity parameters (mean seismic activity rate λ, Gutenberg-Richter parameter b, level of completeness of the available earthquake catalogue m_{min}, as well as the maximum earthquake magnitude m_{max}) are evaluated for each seismic zone that was defined in the first step. Assessment of these parameters requires a seismic event catalogue containing origin times, event magnitudes, spatial location of earthquakes so that the probability density function (PDF) of distance to the specified site can be calculated (Kijko, 2008).

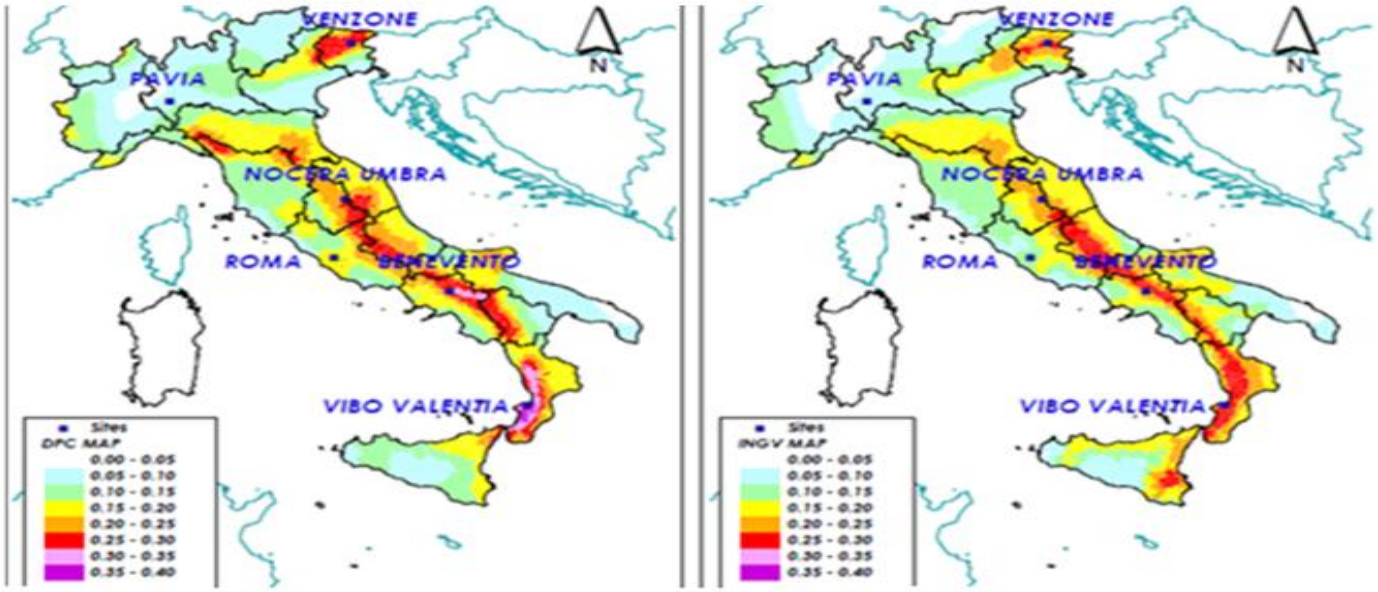

Figure 2.3: Two hazard maps for Italy with different specification of source zones by different research groups (Theodorakatou, 2007)

It is assumed that earthquake occurrence in time is random and follows a Poisson process such that earthquakes occur independently of each other, implying that occurrence of a future event is not related to another one that may have occurred in the past and earthquake magnitudes follow a doubly truncated Gutenberg-Richter distribution (Gutenberg and Richter, 1944):

$$\log N = a - bM, \tag{2.1}$$

where N is the number of events with magnitude greater than or equal to M where a and b are parameters. This relationship is critical in seismology as it is used to describe both tectonic and induced seismicity (Kijko and Smit, 2012), it can be applied in different time scales, and holds true over a large interval of earthquake magnitudes.

The parameter a, is the measure of the level of seismicity, while b describes the ratio between the number of small and large events. It is further assumed that the magnitude M lies within the range (m_{min}, m_{max}) where m_{min}denotes level of completeness of the earthquake catalogue and m_{max} is the area characteristic maximum possible seismic event magnitude.

The *b*-value varies within the range 0.5 to 1.5 depending on the tectonic environment under consideration (Scholz, 1968) but is typically 1.0 for seismically active regions. This means, for example, that for every magnitude 4.0 event there will be 10 magnitude 3.0 events and 100 magnitude 2.0 events. A notable special case in the variation of the b-value occurs in earthquake swarms where it can be as high as 2.5, indicating a large proportion of small earthquakes to larger ones.

2.3.3 (a) Estimating the level of completeness (m_{min}) of an earthquake catalogue

Due to the lack of complete documentation, the probability of "lost" earthquakes increases as one goes back in time making the catalogue progressively less representative of actual seismicity. The level of completeness is defined as the lowest magnitude above which all earthquakes in a space-time volume are reliably detected therefore an earthquake catalogue is said to be complete for a given period if all earthquakes that occurred within that time space are accurately and comprehensively recorded in the catalogue (Weimer & Wyss, 2000).

Errors in the estimation of the level of completeness lead to under sampling if too high due to unnecessarily discarding usable data, or to artefacts in *a*- and *b*-values if too low (e.g. Habermann, 1987).The catalogue normally consists of historic as well as instrumental records. When instrumental data is being considered then the detection capability is taken to be the determining factor for the level of completeness.

Historic events are normally taken to be those that began before the end of the nineteenth century and are frequently compiled using past newspapers, diaries, church records as well as journals. This is a painstaking process which must be done with utmost care involving interpreting descriptions of past earthquakes in terms of numerical values of intensity that can be incorporated into the catalogue as well as filtering these sources of information for useful and relevant facts. It is not uncommon for sources written long after an earthquake to report the date incorrectly or to confuse and mix different reports as well as for some events to be exaggerated (Theodorakatou, 2007). For example, in South Africa, Singh *et al.* (2009) reported that the frequency of occurrence for events exceeding magnitude 5 is lower in recent times compared to records of historical events.

There are different methodologies which are followed for the estimation of m_{min}. The first one is built on the information gleaned from the earthquake catalogue and m_{min} is said to be defined as the

minimum magnitude at which the (complementary) cumulative frequency magnitude distribution (FMD) departs from the exponential decay (e.g. Zuniga and Wyss, 1995) and in this approach the Gutenberg-Richter relation is taken to be valid. Examples that have followed this procedure include Wiemer and Katsumata (1999); Wiemer and Wyss (2000); Cao and Gao (2002); Marsan (2003); Amorèse (2007) amongst others.

Rydelek and Sacks (1989, 1992) used changes between the day and night-time sensitivity of networks to estimate completeness while Sereno and Bratt (1989); Harvey and Hansen, (1994) utilized comparison of amplitude-distance curves and the signal-to-noise ratio or amplitude threshold studies to estimate the level completeness. These methods form a category of waveform-based methods that require estimating the signal-to-noise ratio for numerous events at many stations and are generally not suitable for use as part of a seismicity study (Wiemer and Wyss, 2000).Theodorakatou (2007) suggests that the best way to evaluate the level of completeness is to use independent historical information. Even though that is rarely accessible as any statistical approach based exclusively on catalogue data is in some way a "vicious cycle" as use of an incomplete data base is being used to evaluate its incompleteness.

2.3.4 (b) Estimating of rate of seismic activity λ and b-value of Gutenberg-Richter

The activity rate λ refers to number of annual earthquakes equal and above m_{min} assuming that they are independent and follow a Poisson distribution. Whereas the *b*-value of the Gutenberg-Richter (G-R) magnitude-frequency relationship (MFR) in (2.1). It seems that the *b*-value represents properties of the seismic medium in some respect, like stress and/or material conditions in the focal region (Kulhanek, 2005; Scholz, 1968; Schorlemmer *et al*. 2005).

A number of challenges are observed in most earthquake catalogues such as incompleteness of the dataset as well as uncertainties in magnitude determination of events especially in historical (macroseismic) events mainly due to incomplete documentation of past records, inaccuracies and misinterpretation of damages that took place as a result of an earthquake into numerical values of magnitude. The instrumental period may also have errors as a result of unification of magnitudes. Both the instrumental and historic sections may also contain "gaps". The instrumental part may further be subdivided into sub-catalogues which have different levels of completeness as shown in Figure 2.3.4 below.

All these challenges need to be taken into account in the evaluation of λ and b. The maximum likelihood approach is the commonly utilised methodology for the approximation of these two parameters. Several workers such as Weichert (1980); Kijko and Sellevoll (1989, 1992) as well as McGuire (2004) and most recently Kijko and Smit (2012) have utilized this approach to come up with the most flexible way that takes cognisance of the scenarios discussed above.

The maximum likelihood estimator of λ is equal to n/t, where n is number of events that occurred within time interval t (Benjamin and Cornell, 1970). To calculate the b-value, there are various techniques but Aki's (1965) classic estimator is considered as the preferred estimator. If the maximum magnitude is known, then the b-value can be evaluated from the solution of

$$\frac{1}{\beta} = \bar{m} - m_{min} + \frac{(m_{max}-m_{min})exp[-\beta(m_{max}-m_{min})]}{1-exp[-\beta(m_{max}-m_{min})]}, \tag{2.2}$$

where $\beta=b\ ln\ 10$ and $\bar{m}$ is the mean magnitude of the whole sample greater than or equal to m_{min}. The solution of 2.2 can be calculated using the Aki-Utsu estimator (Aki, 1965; Utsu, 1965).

$$\beta = \frac{1}{\bar{m}-m_{min}}, \tag{2.3}$$

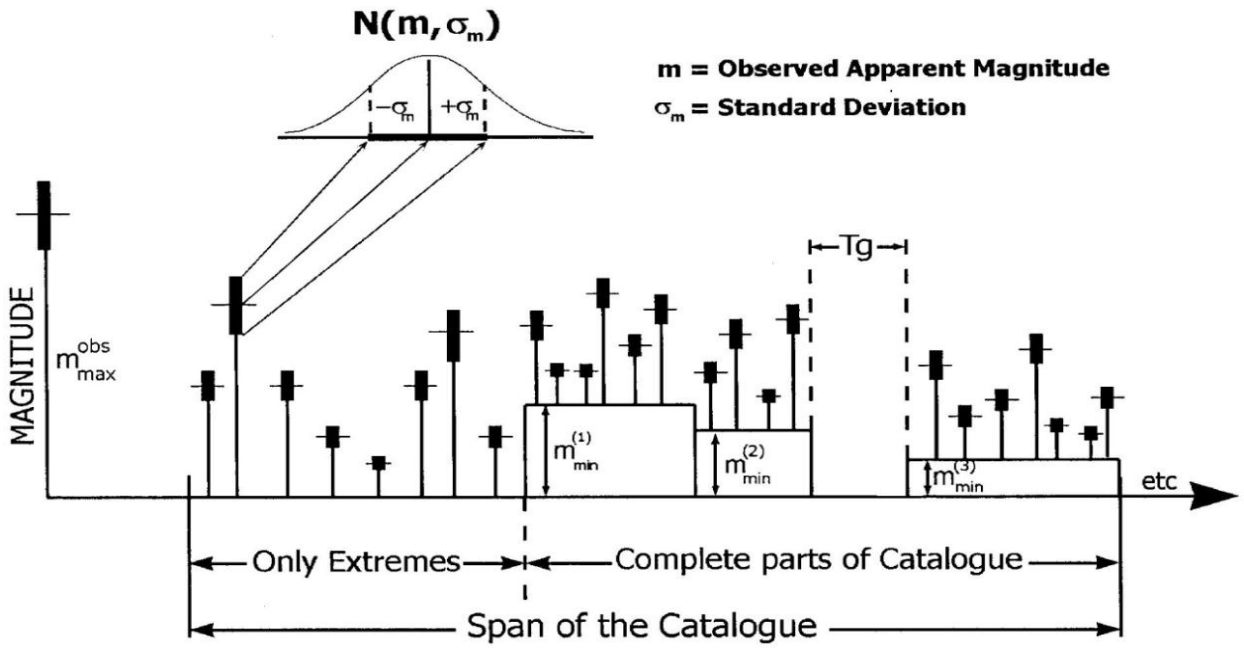

Figure 2.3.4: Illustration of data which can be used to obtain maximum likelihood estimators of recurrence parameters by the procedure developed by Kijko and Sellevoll (1992)

2.3.5 (c) Estimation of the area-characteristic maximum possible magnitude (m_{max})

The maximum possible magnitude is a critical parameter in seismic hazard studies and its accurate evaluation is pertinent in earthquake engineering, disaster mitigation as well as in insurance applications. The terminology is sometimes used synonymously with maximum credible earthquake. The earthquake engineers (EERI Committee, 1984), defines the maximum magnitude as the upper limit of magnitude for a given seismic source such as a fault, such that it assumes a sharp cut-off magnitude for a seismic source which cannot be exceeded by any seismic event and is set by the strength of the crustal rocks in terms of the maximum strain that they are able to withstand (Richter, 1958).The maximum magnitude is estimated using a combination of factors but at the present moment there is no one universally accepted procedure that is available for the evaluation of m_{max} but the available methodologies can generally be classified into two categories i.e. deterministic and probabilistic methods.

Deterministic procedures involve use of empirical formulas that relate earthquake magnitude to various tectonic, geological, geophysical as well as structural information and fault parameters. The empirical relationships that are used for different regions and faults can sometimes be simulated on a computer for different types of faults (Ward, 1997). The geological information is used to identify distinctive tectonic features, which control the value of m_{max}. (Wheeler, 2009; Kijko, 2011). Most times, unfortunately the value of m_{max} estimated from deterministic procedures are often inaccurate and can have uncertainties of up to one unit on the Richter scale (Kijko and Graham, 1998).

When using probabilistic procedures, the value of m_{max} is calculated by applying statistical methods on data that is of a pure seismological nature. Procedures of extreme value statistics are used and a suitable technique for a particular situation would depend on available information on past seismicity and or the statistical distribution model. Only two estimators of m_{max} are discussed here from Kijko and Graham (1998).

Assuming that the largest observed magnitude m_{max}^{obs} is equal to the largest magnitude that can be expected and on the distribution of the largest among *n* observations is of the form (Pisarenko *et al*, 1996)

$$\hat{m}_{max} = m_{max}^{obs} + \frac{1}{n f_M(m_{max}^{obs})}, \tag{2.4}$$

where $f_m(m_{max}^{obs})$ is the probability density function (PDF) of the earthquake magnitude distribution which is given below

$$f_M(m) = \frac{\beta \exp[(-(m-m_{\min})]}{1-\exp[(-\beta(m_{max}-m_{min}]}, \tag{2.5}$$

Substituting (2.5) into (2.4) we get

$$\hat{m}_{max} = m_{max}^{obs} + \frac{1-\exp[(-\beta(m_{max}-m_{min}]}{\beta \exp[(-(m-m_{\min})]}, \tag{2.6}$$

The variance of $\hat{m}_{max}$ in (2.6) takes the form

$$VAR\,(\hat{m}_{max}) = \sigma_M^2 + \frac{1}{n^2}\left[\frac{1-\exp[(-\beta(m_{max}-m_{min}]}{\beta \exp[(-(m-m_{\min})]}\right]^2 . \tag{2.7}$$

Where σ_M represents the epistemic uncertainty in the determination of m_{max}^{obs} and the last term on the right side is the aleatory uncertainty of the maximum magnitude.

The second more complex procedure is based on the formalism by Cooke (1979)

$$\hat{m}_{max} = m_{max}^{obs} + \int_{m_{min}}^{m_{max}^{obs}} [F_M(m)]^n dm \tag{2.8}$$

Where $F_M(m)$ denotes the CDF of the random magnitude variable *m*. For the frequency-magnitude Gutenberg–Richter relation, the respective CDF of magnitude which is bounded from above by m_{max}, is (Page 1968)

$$F_M(m) = \begin{cases} 0, \\ \frac{1-\beta \exp[(-(m-m_{\min})]}{1-\exp[(-\beta(m_{max}-m_{min}} \\ 1, \end{cases} \quad \begin{cases} for\ m < m_{min} \\ for\ m_{min} \le m \le m_{max} \\ for\ m < m_{max} \end{cases} \tag{2.9}$$

Combining (2.8) and (2.9) we then have to calculate the integral

$$\Delta = \int_{m_{min}}^{m_{max}} \left[\frac{1-\exp[(-\beta(m_{max}^{obs}-m_{min}]}{1-\exp[(-(m_{max}-m_{\min})]}\right]^n dm \tag{2.10}$$

Which does not have a simple solution but is estimated according to Cramer (1961) to give

$$\Delta = \frac{E_1(n_2) - E_1(n_1)}{\beta \exp(-n_2)} + m_{min} \exp(-n) \quad (2.11)$$

Where n_1 = n/{1- exp [-β($m_{max} - m_{min}$)]}, $n_2 = n_1$ exp [-β($m_{max} - m_{min}$], and $E_1(.)$ denotes an exponential integral function. Following equation (2.9), for the Gutenberg–Richter frequency-magnitude relation, the estimator of m_{max} is obtained as an iterative solution of the equation.

$$\widehat{m}_{max} = m_{max}^{obs} + \frac{E_1(n_2) - E_1(n_1)}{\beta \exp(-n_2)} + m_{min} \exp(-n) \quad (2.12)$$

Kijko and Sellevoll (1989) introduced equation (2.12) and it has subsequently been used in more than 65 countries around the world. The solution is often termed the Kijko–Sellevoll estimator of maximum magnitude, or, in short, K-S. The variance of estimator (2.12) has two components, epistemic and aleatory and is of the form (Kijko 2004)

$$VAR\ (\widehat{m}_{max}) = \sigma_M^2 + [\frac{E_1(n_2) - E_1(n_1)}{\beta \exp(-n_2)} + m_{min} \exp(-n)]^2 \quad (2.13)$$

where σ_M denotes standard error in the determination of the largest observed magnitude m_{max}^{obs}.

The two procedures outlined above are applicable in a number of situations such as when the number of earthquakes *n* is not known. In such a case we substitute λt in place of *n*, where t is the time span of the catalogue. In so doing, one indirectly assumes that earthquake occurrence in time follows a Poissonian distribution. The major weakness of statistical procedures as outlined above is the fact that in most cases the available earthquake catalogues are too short to reliably estimate the maximum magnitude and in such cases we resort to the use of Bayesian statistical methods (Cornell, 1994; Kijko and Singh, 2011) which allow the incorporation of various supporting data such as geological, geophysical, paleoseismicity and tectonic information.

2.3.6 Calculation of the appropriate ground motion prediction equation (GMPE)

As a third step, in order for one to evaluate the seismic hazard or prepare a zoning map of a region, it is necessary to know the attenuation and scaling characteristics of the various strong motion parameters with distance, earthquake size and the geological conditions (Gupta, 2002). The popular parameters of interest

include peak ground acceleration, peak ground velocity, peak ground displacement; spectral acceleration amongst others and (2.14) below gives a simple and commonly used form of GMPEs.

$$\text{In } Z = c_1 - c_2 M - c_3 InR - c_4 R + c_5 F + c_6 S + \varepsilon \tag{2.14}$$

Where Z is the ground motion parameter; M is the earthquake magnitude, R is the shortest earthquake distance from the source to the site; F is responsible for the faulting mechanism; S describes the site effects and ε is the random error with zero mean and standard deviation $\sigma_{In\,Z}$ with two components for the aleatory and epistemic error.

The coefficients c_1 to c_6 in (2.14) are dependent on a particular tectonic setting of the site. Recent GMPEs have more complex forms e.g. Atkinson and Boore (2006). The selected GMPE can then be used to find the cumulative distribution function (CDF) for the ground motion parameter that is being evaluated such as peak ground acceleration (PGA), peak ground displacement, peak ground velocity. This process of selecting the appropriate ground motion relation (also sometimes referred to as the attenuation relationship) is one of the major contributors to uncertainties in PSHA.

Three factors affect the attenuation of seismic waves as they propagate; these are; the earthquake source, the propagation path from the source to the site and the geological conditions beneath the site. Ground motion models have been often developed by regression on recorded accelerograms to predict the expected earthquake ground motion parameter of interest at a site (Douglas, 2007).

An important concern when selecting these models is the possible dependence of ground motion on geographical region. In such a scenario the median ground motion for the region of interest could be the same as that in the region where a ground model is from and the aleatoric variability of ground motion is similar. The question can be particularly difficult to tackle in many regions of the world where little observed strong motion data is available such as most of Africa since there are few records to validate the choice of model. Douglas (2007) suggests that it is currently more defensible to use a well-constrained model based on data from other regions rather than use predicted motion from local often poorly constrained models.

There are various techniques that are in use for the prediction of ground motion which can be basically grouped into two categories: the mathematical approach, where a model is analytically based on physical principles and the experimental one (where a mathematical model) not necessarily based on physical

insight is fitted to experimental data. A concise summary of most techniques that are applied currently can be found in Douglas and Aochi (2008).

2.3.7 (a) The Stochastic method

The ability to simulate strong ground motion is an important area of seismology and strong motion records are helpful in the design of earthquake resistant buildings. Unfortunately these strong motion data records are normally scarce or even unavailable in most parts of the world, hence the need to use simulation techniques. The stochastic method simulates ground motion for frequencies of engineering interest (generally, $f > 0.1$ Hz) by combining parametric or functional descriptions of the ground motion's amplitude spectrum with a random phase spectrum modified such that the motion is distributed over a duration related to the earthquake magnitude and to the distance from the source (Boore, 2003). This technique has become widely used for the simulation of ground motion especially for regions lacking data for damaging earthquakes (Douglas, 2007). The major and critical characteristic for this method is its ability to describe in the form of equations the earthquake processes and wave propagation involved in a given scenario in terms, source path and site.

Strong ground motion is simulated by estimating a Fourier spectrum of ground motion using models of the source spectrum that is transferred to site by considering geometric decay inelastic attenuation of seismic waves as they propagate. The parameters that define the source spectrum, the geometric and inelastic attenuation are based on simple physical models of the earthquake process and wave propagation and these parameters are estimated by analysing many seismograms.

After the Fourier spectrum at a site is estimated time histories are then computed by adjusting and enveloping white noise to give the desired spectrum and duration of shaking. Since the method does not account for phase effects due to propagation rupture (i.e. Doppler shift of frequencies) or wave propagation, the results for near source region may not be appropriate. Since only body waves are usually considered, the long period ground motion, and could be poorly estimated by the stochastic method (Douglas, 2007).

2.3.8 (b) Empirical method

This method is closely based on strong motion observation. The empirical techniques are a straight forward way to predict ground motion in future earthquakes and they are assume that shaking caused by future earthquakes will be similar to that observed in the previous events such that predictions of ground motion are done by choosing or constructing a model, which should fit the observed ground motion data (Douglas and Aochi, 2008).Records are chosen from databanks containing accelerograms that are appropriate for the considered site. Selection is made by considering the magnitude and distance of the scenario event. Records with elastic response spectra that match a design spectrum are often preferred. After the selection, scaling of the amplitude is often performed to correct for differences to the design ground motion parameters (e.g. PGA).

The empirical method has its limitations in predicting near-source records from large events. It difficult to find records to match scenario characteristics in addition to magnitude and distance and databanks for most regions are small. It is implicitly assumed that host and target regions have similar characteristics (or that ground motions are not dependent on the region) and also difficult to ascertain whether certain records are applicable elsewhere due to particular site or source effects.

2.3.9 (c) Physics-based techniques

This class of methods has become increasingly popular in recent years as knowledge of the physical processes involved in earthquake propagation and the availability of powerful computational as well as simulation technology has become available. They have the advantage of being able to model various earthquake scenarios as they require more parameters to be defined compared to empirical methods which can generally regarded to be much simpler compared to physics-based methods. They require the simulation of the generation of the seismic wave through fault rupture as well as the propagation of the seismic wave hence parameters such as the point of nucleation of the fault and rupture velocity will have to be defined by necessity.

2.3.10 (d) Comparison of some ground motion models that are applicable to Zimbabwe

Since we have very limited strong motion data, it is preferable to use a well-constrained models based on data from another regions with similar seismotectonic characteristics, rather than a local, but poorly-

constrained model (Douglas, 2007). Atkinson and Boore (1995; 1997 and 2006) as well as Somerville *et al.* (2001) have derived models for the eastern part of North Africa which can be used to describe stable continental regions with low levels of seismic activity. Three other relationships have been derived using data from Africa by Mavonga (2007) for the Western Rift Valley, Twesigomwe (1997) for Uganda, and Jonathan (1996) for eastern and southern Africa.

Jonathan (1996) used the random vibration theory using earthquakes that had been recorded by digital stations, constant stress drop source model from Brune (1970) to estimate the ground motion attenuation parameters as a function of magnitude, M and hypocentral distance, R. He obtained the relation:

$$ln\ a = 3.024 + 1.30\ M_w - 1.351\ ln\ R - 0.0008\ R \quad (2.15)$$

Mavonga (2007) derived an attenuation relationship for the western part of the East African Rift Valley by simulating strong motion of large earthquakes using recordings of small earthquakes. Small earthquake recordings adjacent to the expected large earthquakes were treated as empirical Green's functions (EGF) between the source and that site and unlike Jonathan (1996) he evaluated the stress drop which is a critical input in the generation of the attenuation relation as it contributes to influencing the simulated seismograms. The resulting equation takes the form

$$In\ Y = c_1 + c_2 M + aR \quad (2.16)$$

Where c_1 and c_2 are constants, Y is the ground motion parameter and R is the hypocentral distance.

Twesigomwe (1997) calculated the attenuation relationship for Uganda which is situated between two seismically active branches of the East African Rift System; the Western Rift (stretching from Aswa Fault Zone in the north to Lake Tanganyika in the south), and the Eastern Rift (stretching from Lake Turkana in the north to Lake Eyasi in the south. He adopted a semi-theoretical approach to develop the attenuation relationship for Uganda, slightly modifying the relationship by Krinitzky *et al* (1988) for eastern Canada as it also has similar hard rock conditions that are comparable to Uganda as well as shear wave velocity and Q values determined by other works such as Gumper and Pomeroy (1970) as well as Xie and Mitchell (1990). He evaluated

$$In\ a = 2.832 + 0.866\ M_s - In\ R - 0.0025\ R + \varepsilon \quad (2.17)$$

Where ε is a normally distributed error term with an expectance of zero and standard deviation *a* the constant term and scaling coefficient of M_s relate to the near field excitation of the earthquake wave motion, which is considered to be more or less independent of tectonic conditions (Hanks and Johnston, 1992; Bungum *et al.*, 1992).

The GMPEs derived by Atkinson and Boore (1995, 1997) are widely known and have been used frequently in the past to describe ground motion for stable continental regions. They were developed as predictive ground motion relations for Eastern North America from an empirically based stochastic ground-motion model which are suitable for stable continental regions of low seismicity. These relations were in part supposed to improve on previous models in terms of addressing concerns about wave propagation in layered crust where it had been found that ground motion amplitude was dependent on depth (EPRI, 1993).

Kijko *et al.* (2000) after observing that the original Atkinson and Boore (1995, 1997) model did not adequately describe the physical processes of wave propagation in instances which involve earthquakes of small to moderate magnitudes such that it did not always fit the shape of the attenuation curve modified it by recalculating the coefficients of the original attenuation model. Their model does not include the quadratic term of the original Atkinson and Boore (1995, 1997) but allows different values of the coefficient c_4 in front of the element ln*(R)* (where *R* is the hypocentral distance) and is found to be a better fit of the for values of PGA and response spectra. Their modified relation which we shall refer to as the Atkinson and Boore (1995, 1997) modified has the form

$$In\,(a) = c_1 + c_2 m + c_3 R + In\,R$$

Where *a* is peak ground acceleration in units of *g*, c_1, c_2, c_3 are the attenuation coefficients, *m* is earthquake magnitude and *R* is the hypocentral distance.

Ambraseys *et al.* (1996) came up with an attenuation model using a dataset representative of Europe which is meant to be used in the construction of hazard-consistent design spectra in that region and the Middle East. This model is suitable for shallow European earthquakes which are comparable to Zimbabwe. The model is of the form

$$log(y) = c_1 + c_2 M + c_3 r + c_4 log(r) + \sigma \qquad (2.18)$$

where *y* is the parameter being predicted, *M* is surface wave magnitude and $r = \sqrt{d^2 + h^2}$ is the shortest distance from the station to the surface projection of the fault rupture, in km, and *h* is a constant to be determined with coefficients c_1, c_2, c_3 and c_4 and σ is the standard deviation. Their model includes both geometric and anelastic distance terms in addition to adopting linear magnitude scaling as well as a magnitude-independent shape. To decouple the determination of distance dependence from the determination of magnitude dependence the regression technique by Sarma (1994) was used. This model has the added feature of being able to take into consideration local geology site conditions.

Atkinson and Boore (2006) developed ground-motion relations for hard rock sites in eastern North America including estimates of their aleatory uncertainty using a stochastic finite-fault model which is important in improving the reliability of estimates for large-magnitude events at close distances. This was an improvement on Atkinson and Boore (1995) which were based on a stochastic point-source model since new seismographic data was incorporated to provide information on source and path effects thereby improving the definition of attenuation trends in eastern North America. The major difference between these two relations is that high-frequency amplitudes were found to be lower than they had predicted in earlier studies due to a slightly lower average stress drop parameter (140 bars versus 180 bars) and a steeper near-source attenuation.

Deif *et al.* (2011) developed an attenuation relationship for the Aswan area in Egypt. Like most of Africa they did not have strong motion data and so they used seismological modelling as an alternative approach. They used the stochastic technique to generate suites of ground motion histories. The relationship is for events spanning $4.0 \leq M_w \leq 7.0$ and a distance of up to 100km to the surface projection of the fault. Their equation is of the form

$$log(PGA) = 1.24 + 0.358M_w - log(R) - 0.008R + 0.22P \qquad (2.19)$$

where PGA is in cm/s^2; M_w is moment magnitude, *R* is the closest distance between rupture projection and site of interest and *P* is a dummy variable.

Somerville *et al.* (2001) developed ground motion relation for the central and eastern United States by first developing earthquake source scaling relations for use in generating ground motions which allowed them to construct earthquake source models without resorting to *a priori* assumptions about the shape of the source spectrum, as is done in the stochastic approach. The scaling relations were then used to generate suites of ground motion history using a broadband Green's function method that has a rigorous

basis in theoretical and computational seismology and has been extensively validated against recorded strong motion data (Somerville *et al*., 1996) which were used to generate the ground motion prediction relations.

2.3.11 Integration of uncertainties contributed by each zone

In the final step, the individual uncertainty contributions in earthquake location, earthquake magnitude as well as ground motion relation from each zone are integrated into a probability that the ground motion parameter of interest will be exceeded during a given time interval at the site of interest. The total probability theorem is used in this integration process. Attenuation relationships are always a major contributor in PSHA due to randomness in the mechanism of rupture and from variability and heterogeneity of the source, travel path and site conditions and this must be accounted for (Theodorakatou, 2007).

2.4 A brief review of the theory behind the Cornell-McGuire PSHA procedure

Suppose Z is used to characterize a particular ground motion parameter such as peak ground acceleration, peak ground velocity, spectral acceleration etc. The probability that a specified value z(in the domain of Z) will be exceeded is given by $P\,[Z \geq z]$ which is calculated for a particular earthquake magnitude occurring at a source and multiplied by the probability of that particular earthquake occurring. Using the Total Probability Theorem, this calculation is repeated for a range of earthquake location and magnitudes at a site and summed up to give an expression of the form of McGuire (1968):

$$P\,[Z \geq z] = \int_{m_{min}}^{m_{max}} \int_{R|M} P\,[Z \geq z|\, m, r] f_M(m) f_{R|M}(r|m)\, dr\, dm \qquad (2.20)$$

where $P\,[Z \geq z|\, m, r]$ is the conditional probability that a chosen ground motion level z of a ground motion parameter Z at a site due to an earthquake of a given magnitude m occurring at an epicentral distance r; $f_M(m)$ and $f_{R|M}(r|m)$ are the PDF of earthquake magnitude and the conditional PDF of the epicentral distance respectively.

In most engineering applications, it is assumed that the magnitudes of earthquakes follow the Gutenberg-Richter relation which is given in (2.1), therefore it follows that $f_M(m)$ is a negative, exponential distribution, shifted from zero to m_{min} and truncated from the top by m_{max}, (Page, 1968)

$$f_M(m) = \frac{\beta \exp[(-(m - m_{\min})]}{1 - \exp[(-\beta(m_{max} - m_{min}]}$$

which is the same as 2.5 above, where $\beta = b \ln 10$. Assuming that earthquake occurrence follows a Poisson distribution in every seismic source, then the probability that *z*, a specified level of ground motion at a site will be exceeded at least once within a time interval *t* will be

$$P\,[Z > z;\ t = 1] = 1 - \exp\,[-t \cdot \lambda(y)] \qquad (2.21)$$

From 2.21 above, if $t = 1$, we get the plot of the annual rate of exceedance against the ground motion parameter z which is a hazard curve for PSHA.

2.5 The parametric-historic procedure

This method falls under the category of PSHA technique and basically combines the best features of the ‘‘deductive’’ (Cornell, 1968) and ‘‘historical’’ (Veneziano *et al*., 1984) procedures (Kijko and Graham, 1998). The U.S. Geological Survey national seismic hazard maps by Frankel *et al*. (1996) were done using a procedure which is very close to the parametric-historic procedure. This procedure was used as a time the U.S. nuclear industry was struggling with the consequences of the subjective definition of source zones as it aimed to reassess the seismic safety of existing nuclear power plants throughout the eastern United States (Atkinson, 2004).

The two major outstanding features are: firstly, its capability to take into account the limitations of data such as incompleteness of catalogues and inaccuracies of epicentral location and earthquake magnitude. Secondly, it does not require the subjective judgement involved in the mapping of seismic source zones by mapping the specific active faults. Taking into account the limitations of data incompleteness allows one to use the whole seismic event catalogue available for the area being assessed, including historical observations as well as the instrumental data recorded during the past decades.

The Cornell-McGuire procedure requires the assessment of seismic parameters for each delineated seismic source zone and this cannot be done when faced with an incomplete seismic history or for a small area. In such a case, the way forward is normally to increase the boundary of the seismic zone under evaluation and this would then be in direct conflict with the requirement of independent delineation of source zones and in addition leads to underestimation of seismic hazard (Xu and Gao, 1997).

The major limitation of the parametric-historic procedure, in its current state, is on the choice of ground motion prediction equations (GMPEs) that do not allow non-linear magnitude scaling (Saman Yaghmaei-Sabegh *et al.*, 2010). In order to calculate the probability of exceedance of a ground motion parameter (which is the main objective of PSHA), say maximum possible PGA for a site, then its value can be obtained by applying the design (floating) earthquake procedure, assuming the occurrence of the strongest possible earthquake at very close distance from the site. The probabilities of exceedance of the maximum possible PGA values can also be calculated to illustrate the uncertainty of maximum PGA estimation. Some of the exhaustive statistical techniques that can be used for the evaluation of the maximum regional earthquake magnitude, m_{max} are described the following papers: Kijko and Graham (1998) and Kijko (2004).

The procedure is done by firstly evaluating the area-specific parameters for the site where hazard is being evaluated. This step is essentially similar to the Cornell-McGuire procedure and makes it of a parametric nature. The second step is computing amplitude of the distribution of ground motion parameter such as peak ground acceleration (PGA) at a specific site. It is worth noting at this stage that since parameters are calculated by maximum likelihood using Bayesian formalism, this allows for the incorporation of additional geological and geophysical data as well as alternative parameterization.

2.5.1 Assessment of area-specific seismic parameters

In deriving the formulae for assessing the seismic parameters, it is assumed that earthquake occurrence follows a Poisson distribution and that that earthquake magnitude distribution follows a doubly truncated Gutenberg-Richter frequency-magnitude relationship. The cumulative distribution function (CDF) of the largest magnitudes occurring at least once over a time t is taken from Kijko and Sellevoll (1989, 1992) given by

$$F_M^{max}\left(m\middle|m_{0,}m_{max},t\right)=\frac{\exp\{-\lambda_0 t[1-F_M(m|m_0,m_{max})]\}-\exp(-\lambda_0 t)}{1-\exp(-\lambda_0 t)} \quad (2.22)$$

where $\lambda_0 \equiv \lambda(m_0)=\lambda[1\text{-}F_M(m_0\,|m_{min},m_{max})]$ is the mean activity rate of earthquake occurrence, m_0 is lower earthquake magnitude in the extreme part of the catalogue and $m_0 \geq m_{min}$ which is the minimum threshold magnitude of the entire catalogue and it should be less than the level of completeness in all the sub-catalogues as illustrated in Figure 2.2. Usually the values of λ_0 and t in the denominator are high hence the denominator is ignored.

Assuming the error in magnitude has a normal distribution with standard deviationσ_M from Tinti and Mulargia (1985a, b) then using Kijko and Sellevoll (1992), Gibowicz and Kijko (1994) it follows that the PDF and CDF are respectively given by

$$f_M(m|m_{min},m_{max},\sigma_M)=f_M(m|m_{min},m_{max})\frac{e^{\chi^2}}{2}\left[\text{erf}\left(\frac{m_{max}-m}{\sqrt{2\sigma_M}}+\chi\right)+\text{erf}\left(\frac{m-m_{min}}{\sqrt{2\sigma_M}}-\chi\right)\right] \quad (2.23)$$

$$F_M(m|m_{min},m_{max},\sigma_M)=F_M(m|m_{min},m_{max})\{A_1\,\text{erf}\left(\frac{m-m_{min}}{\sqrt{2\sigma_M}}+1\right)+A_2\,\text{erf}\left(\frac{m_{max}-m}{\sqrt{2\sigma_M}}-1\right)\} \quad (2.24)$$

where $A_1=\exp(-\beta m_{min})$, $A_2=\exp(-\beta m_{max})$, erf $(\cdot)$ is the error function, $\chi=\frac{\beta\sigma_M}{\sqrt{2}}$ and the magnitude m is bounded above and below.

If m_{min} is the cut-off value of apparent magnitude then the normalised PDF and CDF respectively become,

$$\tilde{f}_M\left(m\middle|m_{min},m_{max},\sigma_M\right)=\{^{0\ for\ m\leq m_{min}}_{\frac{f_M(m|m_{min},m_{max},\sigma_M)}{1-F_M(m|m_{min},m_{max},\sigma_M)}\ for\ m\geq m_{max}} \quad (2.25)$$

$$\tilde{F}_M\left(m\middle|m_{min},m_{max},\sigma_M\right)=\frac{F_M(m|m_{min},m_{max},\sigma_M)-F_M(m_{min}|m_{min},m_{max},\sigma_M)}{1-F_M(m_{min}|m_{min},m_{max},\sigma_M)} \quad (2.26)$$

Using the relation from Tinti and Mulargia (1985 a, b) and replacing the "true" activity rate $\lambda\ (m)$ with the apparent one $\tilde{\lambda}(m)$ we have

$$\tilde{\lambda}(m) = \lambda(m)\exp(\chi^2) \tag{2.27}$$

Combining the CDF of the largest magnitudes occurring over a time interval t given in (2.22) and the CDF for the for normalised apparent magnitude in (2.26) we have the PDF of the strongest earthquake with, magnitude m$\geq m_0$as

$$\tilde{f}_M^{max}(m|m_0, m_{max}, t_M) = \frac{\tilde{\lambda}_0 t \tilde{f}_M(m|m_0, m_{max}, t, \sigma_M)\exp[-\tilde{\lambda}_0 t(1-F_M(m|m_0, m_{max}, t, \sigma_M))]}{1-\exp(-\tilde{\lambda}_0 t)} \tag{2.28}$$

From (2.28) the likelihood function of the strongest earthquakes is given by,

$$L_0(\lambda, \beta) = const\pi_{j=1}^{n_0} \tilde{f}_M^{max}\left(m_{0j}\middle|m_0, m_{max}, t_{0j}, \sigma_{M0j}\right) \tag{2.29}$$

w here m_{0j} is the apparent magnitude of the strongest earthquake which has standard deviation σ_{M0j} and occurs within a time interval t_j.The number of earthquakes that occur in the extreme of the catalogue are given by j=1,…,n_0 with λ and β being independent of the normalization factor $const$. The procedure takes into account the incompleteness of catalogues as shown in Figure 2.2. The sub-catalogues are each assumed to be have a level of completeness $m_{min}^{(i)}$, time span T_i , apparent magnitude m_{ij} which is greater than or equal to the level of completeness $m_{min}^{(i)}$ and σ_{mij}. The likelihood function of earthquake magnitudes in the sub-catalogues is given by

$$L_i(\lambda, \beta) = \left[const\ \pi_{j=1}^{n_0} \tilde{f}_M^{max}\left(m_{ij}\middle|m_{min}^{(i)}, m_{max}, \sigma_{Mij}\right)\right] \cdot [const(\tilde{\lambda}_i t_i)^{n_i} \exp(-\tilde{\lambda}_i t_i)] \tag{2.30}$$

Combining all the likelihood functions in all parts of the catalogue we have a function

$$L(\lambda,\beta) = \pi_{i=0}^{n_s} L_i(\lambda,\beta) \tag{2.31}$$

The largest earthquake m_{max}^{obs} is the maximum likelihood estimate of m_{max} since (2.31) decreases monotonically as $m_{max} \to \infty$ while $\hat{\lambda}$ and $\hat{\beta}$ are the values of λ and β that will maximize the likelihood function (2.31). Using the K-S estimator for m_{max} given in (2.12) and equating to zero the first derivatives of (2.31) with respect to λ and β we obtain the two equations given by Kijko and Sellevoll (1989) that are solved using an iterative scheme to find the parameters $\hat{\lambda}$ and $\hat{\beta}$.

2.5.2 Assessment of seismic hazard at a site

This is the second step of the parametric-historic procedure and site-specific PSHA requires knowledge of the attenuation of the selected ground-motion parameter, usually PGA, as a function of earthquake magnitude and its distance. According to the adopted methodology, the attenuation law of PGA is assumed to be of the type,

$$\ln(\text{PGA}) = c_1 + c_2 \cdot m + \phi(r) + \varepsilon \tag{2.32}$$

where c_1 and c_2 denote empirical coefficients, m is the earthquake magnitude, $\phi(r)$ is a function of earthquake, epicentral or hypocentral distance and ε is a normally distributed random error.

To express seismic hazard in terms of PGA, the aim would be to calculate the conditional probability that an earthquake of random magnitude, occurring at a random distance from the site, will cause a PGA value equal to, or greater than, the chosen threshold value, PGA_{min}, at the site. We accept the standard assumption (e.g., Page, 1968) that the random earthquake magnitude, m, in the range of $m_{min} \le m \le m_{max}$, is distributed according to the doubly truncated Gutenberg-Richter relation given in (2.1) above (See Figure 2.5.2 (i) below).

Acceptance of the classical frequency-magnitude Gutenberg-Richter relation is equivalent to the assumption that the cumulative distribution function (CDF) of earthquake magnitude is of the form given in (2.10) as

$$F_M(m) = \frac{\exp(-\beta m_{\min}) - \exp(-\beta m)}{\exp(-\beta m_{\min}) - \exp(-\beta m_{\max})}$$

In this case it is bounded above and below. In Figure 2.3 and equation (1.10), $m_{\min}$ is the minimum earthquake magnitude corresponding to acceleration $PGA_{\min}$, which is the minimum value of PGA of engineering interest at the site, m_{max} is the maximum credible (maximum possible) earthquake magnitude and $\beta = b \ln(10)$, where b is the parameter of the Gutenberg-Richter magnitude-frequency relation. Parameter b indicates the relative frequency of occurrence of earthquakes of different magnitudes and it is the slope of the Gutenberg-Richter recurrence relationship (2.1).

It can be shown (Kijko and Graham, 1999) that choosing equation (2.32) as a model for attenuation of PGA and equation (2.2) as a distribution of earthquake magnitude, is equivalent to the assumption that

$$\log N(x) = c - d \cdot x, \tag{2.33}$$

where $N(x)$ is the number of earthquakes recorded at the site, with PGA equal to or exceeding $x = \ln(PGA)$, c and d are parameters and $d=b/c_2$, where c_2 is the coefficient related to the attenuation formula (2.32). Equation (2.33) is illustrated schematically in Figure 2.5.2 (i).

From equation (2.33) it follows that CDF of the logarithm of PGA, denoted as x, is of the form,

$$F_X(x) = \frac{\exp(-\gamma x_{\min}) - \exp(-\gamma x)}{\exp(-\gamma x_{\min}) - \exp(-\gamma x_{\max})}, \tag{2.34}$$

where, $x_{min} = \ln(PGA_{min})$, $x_{max} = \ln(PGA_{max})$, PGA_{max} is the maximum possible PGA at the site, $\gamma = \beta/c_2$ and $\beta = b \ln(10)$.

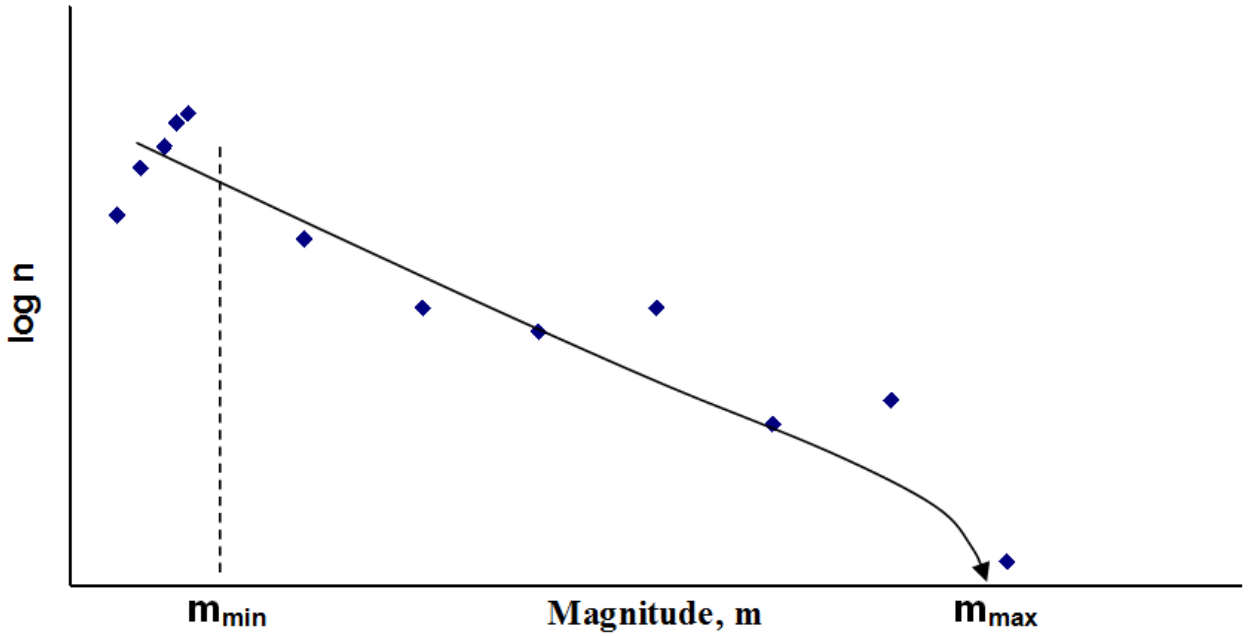

Figure 2.5.2 (i): Schematic illustration of the doubly truncated frequency-magnitude Gutenberg-Richter relation

The slope of the curve is described by parameter b, known as b-value of the Gutenberg-Richter relation. Value m_{min} is the minimum earthquake magnitude corresponding to peak ground acceleration PGA_{min}, which is the minimum value of PGA of engineering interest and m_{max} is the regional characteristic, maximum credible earthquake magnitude.

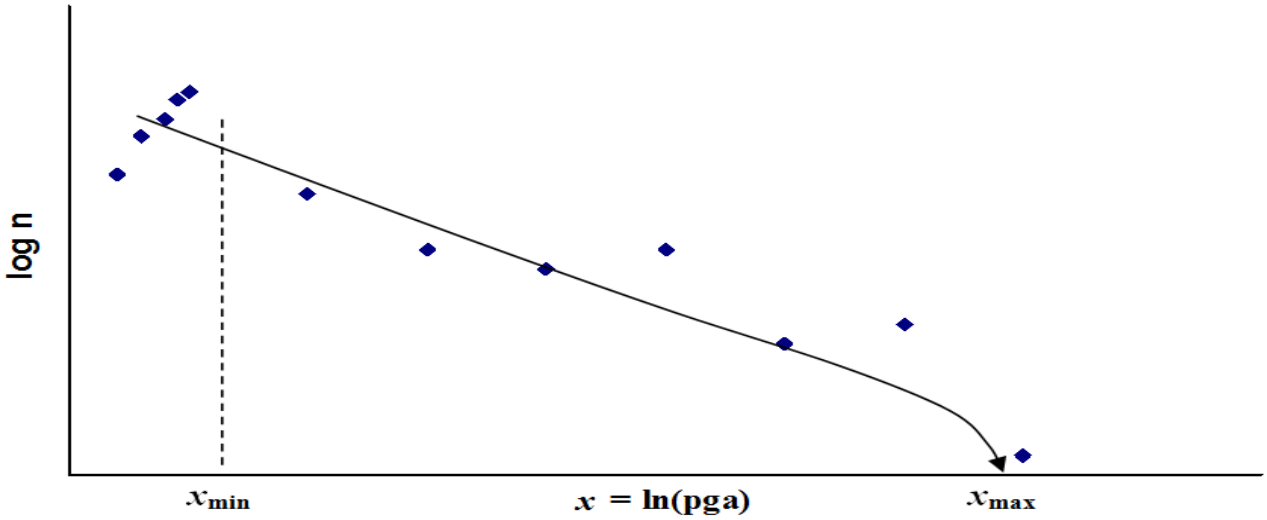

Figure2.5.2 (ii): Schematic illustration of the distribution of the PGA

If earthquake magnitude follow a doubly truncated Gutenberg-Richter relation, the logarithm of the PGA, at a given site follows the same type of distribution as the earthquake magnitude (2.2), i.e. doubly truncated negative exponential – the form of the Gutenberg-Richter distribution in equation (2.2). The two distributions differ only in the value of their parameters. If the *b*-value indicates the slope of the Gutenberg-Richter frequency-magnitude relationship, the parameter *d* characterizing the slope of the distribution of *x = ln (PGA)* is equal to $\boldsymbol{b}/\boldsymbol{c_2}$.

From formula (2.34) it follows that the logarithm of the PGA at a given site follows the same type of distribution as the earthquake magnitude, i.e. doubly truncated negative exponential – the form of the Gutenberg-Richter distribution. The two distributions differ only in the value of their parameters. If the parameter describing the slope of the magnitude distribution is equal to *b*, the slope of the distribution of *x = ln (PGA)* is equal to $d = b/c_2$. One should note that CDF (2.34) was derived under the condition that no matter how diverse the spatial distribution of seismicity within the area surrounding the specified site is, the distribution of earthquake magnitudes, described by parameters m_{max} and *b*, remain the same.

Probabilistic seismic hazard is defined as the probability of a given value of PGA (equal to, or greater than, the chosen threshold value, PGA_{min}) being exceeded at least once at the site during a specified time interval *t*. Such a probability can be written as

$$H(x \,/\, t) = 1 - \exp\{-\lambda t[1 - F_X(x)]\}, \tag{2.35}$$

where λ is the site-specific activity rate of earthquakes that cause a PGA value, at the site, exceeding the threshold value PGA_{min}. Clearly, a hazard curve so defined is doubly truncated: from below, by $x_{min} = \ln(PGA_{min})$, and from above, by $x_{max} = \ln(PGA_{max})$. The distribution in equation (2.35) was derived under the assumption that the earthquakes that cause a PGA $\geq PGA_{min}$, at the site, follow the Poisson process with mean activity rate $\lambda(x) = \lambda[1 - F_X(x)]$, with $x = \ln$ (PGA).

For a given value of x_{max} (or equivalently, the maximum possible PGA at the site), the maximum likelihood procedure is used to determine the parameters λ and γ. However, this procedure for the estimation of unknown hazard parameters is used only when the *b* parameter of the Gutenberg-Richter frequency-magnitude relationship is not known. When the *b*-value is known, parameter γ is calculated as β/c_2 and the maximum likelihood computation reduces to the estimation of the site-specific mean seismic activity rate λ. In addition, in all calculations, uncertainty of the employed seismicity models has been incorporated, by application of the Bayesian formalism.

In cases where there is difficulty in assessing seismic parameters reliably, the procedure can be modified to incorporate geological and geophysical information. This feature is particularly useful in cases of low seismicity, low probabilities of exceedance or when there is not sufficient information in the historical part of the catalogue to accurately calculate seismic parameters. This additional data is incorporated as *a priori* information using Bayesian formalism.

2.6 Contentious aspects of PSHA

Over the years since its introduction by Cornell (1968) there have been aspects of PSHA that have been disputed. These have centred on treatment of uncertainty, as well as, some arguments about the mathematical foundations of the methodology itself. Wang and Zhou (2007) outline some of these issues. Amongst other matters they argue that PSHA is not based on a valid earthquake source model.

Wang and Zhou (2007) state that PSHA is based on a point source model though at present an earthquake is now considered as a finite fault rapture which together with one single distance R_{RUB} and R_{JB} (Figure 2.6) are considered in a GMPE. This then means that the distance *R* in the probability density function is different from the distance in the GMPE. Furthermore, the distribution of ground motion parameters are distributed log normally but log normal distributions are not bounded at the top which in theory means that it is possible to have unrealistic high values of ground motion parameters. This is not physically possible as there has to be a cut-off value for quantities like velocity or acceleration due to the material properties (e.g. rock strength) of the medium.

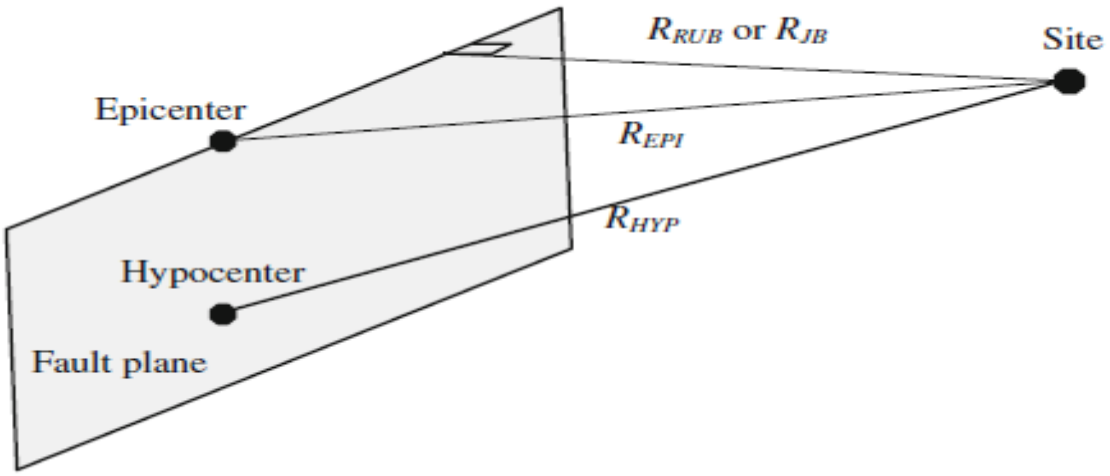

Figure 2.6: Schematic geometry of earthquake fault and source-to-site distances (Wang, 2010)

The uncertainty σ (which contributes the largest uncertainty in PSHA) in the GMPE is dependent on earthquake magnitude and distance and characterizes spatial not temporal uncertainty at a point in the

equation. However in PSHA these three quantities are taken to be independent of each other. This leads to violation of ergodic assumption (Anderson and Brune, 1999) and has been known to lead to overestimation of hazard at short distances (Bommer and Abrahamson, 2006). Another argument in PSHA is the use of logic tree formalism e.g. Castanos and Lomnitz (2002) describe its use as a misconception of statistics as it is wrong to put the same value on expert opinions and hard earthquake data.

Chapter 3

General Seismotectonics of Zimbabwe

3.1 Seismicity and clusters

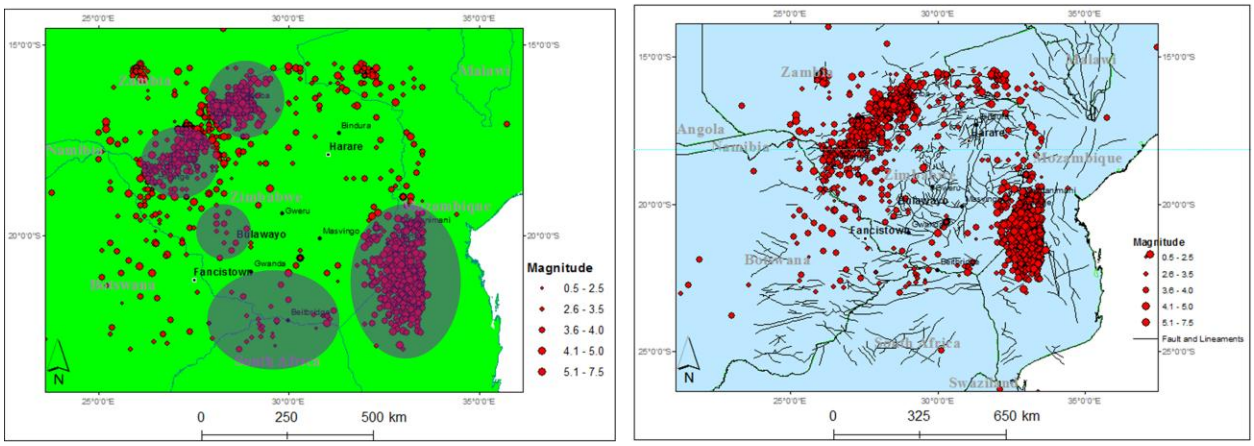

Figure 3.1(i): Map showing seismicity clusters (left) and seismicity of Zimbabwe superimposed on broad scale lineaments and fault map (right)

i. Lake Kariba Cluster (mid-Zambezi basin)

This area lies under the Lake Kariba water table and is part of the East African Rift System of the Mid-Zambezi Valley (EARS-MZV) which is generally associated with a network of faults. It has been experiencing moderate earthquakes spanning from the time the Kariba dam was constructed in December 1958. The largest event that has been recorded in the area so far was one which occurred on 2 September 1963 having a magnitude of 6.3 on the Richter scale. This event was recorded by many seismic stations around the world. This earthquake is believed to have been caused by changes in water levels in the Kariba dam and falls under the category of reservoir induced earthquakes as suggested by (Gough and Gough, 1970; Gough 1978).

Seismic activity in the area is related to the extra water pressures created in micro cracks and fissures in the ground under and near the reservoir. When the pore pressure of the rock increases it acts as if to lubricate the faults which are already under tectonic strain but are prevented from slipping by the friction of the rock surfaces. This movement of the ground is what is observed as an earthquake. This explanation

can also be extended to the recent event that occurred on the 31 August 2010 having a magnitude of $M_w = 5$.

The area also shows evidence of volcanism in its past history and is characterized by the presence of very porous rocks. Pore pressure hence plays a significant role (Gupta *et al.*, 1972).There is also an element of plate tectonic activity within the region as suggested by Scholz *et al.* (1976), especially further north of the lake. Ambraseys and Adams (1991) have given a description of an earthquake of surface-wave magnitude 6.0 occurring in the area on the 28th of May 1910.This evidence clearly indicates that a region of high seismic activity exists and indicates that the lake covers an area of numerous faults which was not pre-stressed but also already seismic.

ii. Deka fault zone (Hwange area)

The Deka fault zone lies to the south west of the Lake Kariba area and includes the Victoria Falls (Hlatywayo, 1995). Seismic activity occurring in the Hwange area is associated with this fault which is responsible for seismicity in the region. Migratory rift faulting is thought to have been the controlling dynamic influence the thick Karoo belt that covers this area.

McKenzie *et al.* (1922) have treated the East African Rift System as a plate boundary. No evidence has however been put forward to suggest that the East African Rift System connects with the mid-Indian Ocean ridge to the south. All indications from studies of the seismicity of Southern Africa point towards the southern tip of the western arm of the East African Rift System, terminating on the continental, perhaps into three sub-branches (Scholz *et al.*, 1976).

Accretion of new crustal material over the area does not exist and the lithosphere has been found to still be continuous. This area therefore represents some mode of break-up which has not started, yet it is visible in the guise of a sub-plate boundary. Scholz *et al.* (1976) found concentrations of epicentres of earthquakes trending along a north easterly direction from Botswana into the Deka fault zone-Zambezi valley suggesting a branch of the East African Rift System beginning from just north of Malawi. The Southern African region is under a northwest-southeast extension normal to the direction of the main lineaments. Maasha and Molna (1972) found the directions of the principal stresses in this region similar to those that existed in the East African Rift system from the Miocene period.

iii. South-Eastern border of Zimbabwe and Mozambique

This zone has become highly seismic in recent times. It falls on the seismic tip of the southern extremity of the East African rift system which is Africa's most pronounced tectonic feature. The south-eastern border area forms the western flank of the rift extension from Lake Malawi. Along the Zimbabwe border, extending from Nyanga in the north to Chipinge in the south, the area is comprised of highly folded and sheared quartzite separated from neighbouring formations by numerous faults (Hlatywayo, 1995).

A major earthquake of magnitude $M_L = 7$ occurred on 22 February 2006 in Mozambique is attributed to the presence of the East African Rift System. It spans more than half of the length of African continent from the Gulf of Aden in the north to Malawi in the south. Zimbabwe is on the southern tip of this East African Rift System which is responsible for seismic activity in this region. Studies on the incipient rifting in the region seem to confirm tectonic activity to be the cause of the Mozambique earthquake (Fairhead & Girlder, 1969: Fairhead and Henderson, 1977). This earthquake was observed in the whole of Zimbabwe and resulted in the death of four people and caused major destruction in the Chipinge area.

iv. Save-Limpopo mobile belt

Along the Save-Limpopo mobile belt there is not much activity though an event of magnitude 6 on the Richter scale occurred in 1940. Since that time there has not been any noticeable activity in the region that could suggest the area becoming a zone of high seismic activity (Hlatywayo 1995), only vents of a small magnitude have occurred since then. This area forms the boundary between the Zimbabwe craton and the Kaapvaal craton.

v. Nyamandlovu aquifer

Though this area is displays the lowest seismicity relative to the other seismic active areas, in 2008 an earthquake of body-wave magnitude 4.3 occurred in the area. The activity in the area is generally attributed to changes in pore pressure in the underlying rock formation .Local authorities have drilled boreholes in this area to augment water supplies in neighbouring city of Bulawayo. Hlatywayo and Midzi (2005) concluded that there is a possibility that excessive pore pressure build up by slow pressure changes is the driving mechanism and causes instability in small low permeable creeping joints in the underlying rock formation resulting in seismic activity.

3.2 Geology of Zimbabwe

The southeast (Save-Limpopo basin) and the northwest (Hwange-Zambezi basin) areas of the country are covered by Karoo sediments which thin out towards the centre of the country. The geology of Zimbabwe is dominated by a largely aseismic craton which is an assemblage of crystalline basement rocks. It is an example of early Archaean lithology dating back to 3.46 Ga. Figure 3.2 below shows the distribution of geological units in Zimbabwe.

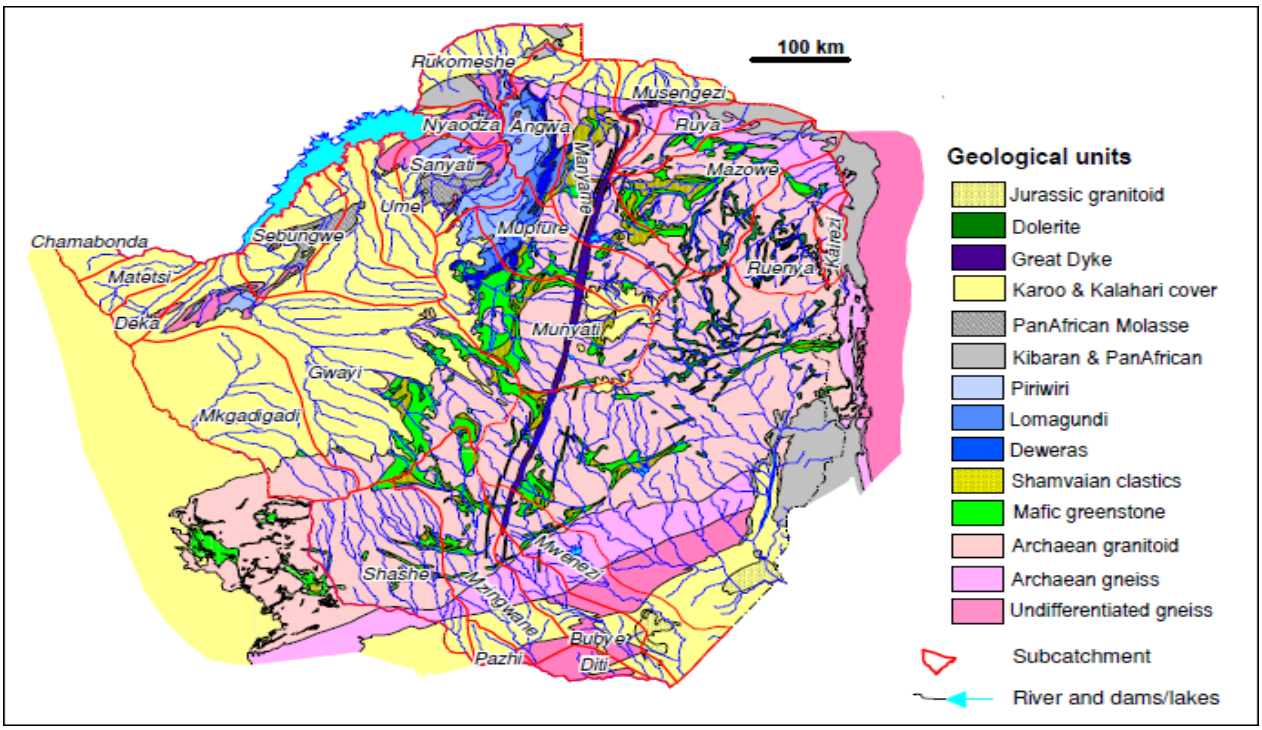

Figure 3.2 (i): Distribution and extent of different geological units of Zimbabwe

(Source Geological Survey of Zimbabwe – http://www.mining.wits.ac.za)

The Archaean core, consisting of the Kaapvaal craton, Zimbabwe craton and the Limpopo mobile belt (Fig. 3.2), has formed a stable unit for the past 2.3 billion years (McElhinny and McWilliams, 1977). It is intruded by the Great Dyke hosting the world's largest reserve of chrome and platinoids (Mekonnen, 2004). The main geology of the craton comprises igneous rocks that include granites and rhyolites and basic rocks such as dolerites, basalts and andesites. Karoo sediments covering the rift zones comprise mainly sedimentary rocks composed of undifferentiated sediments of mixed minerals of igneous origin

and/or differentiated sediments of mixed sediments such as sandstones, quartzites, shales, slates, coal, limestones and dolomites.

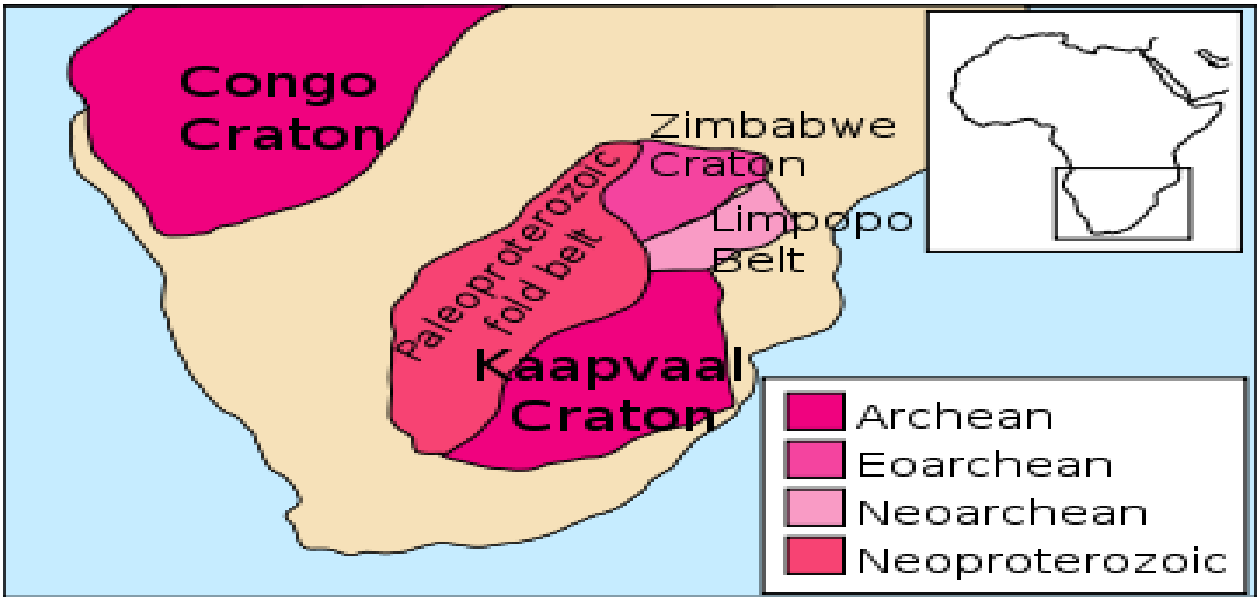

Figure 3.2 (ii): Achaean core, consisting of Zimbabwe and Kaapvaal craton and Limpopo belt

The sandstones, quartzites, shales, slates, coal, limestones and dolomites form consolidated sediments in most areas of the Karoo zones. Fault-plane solutions of earthquakes in the region are associated with rifting and show normal faulting with tensile axes directed to the southeast, confirming the extent of the east Africa rift this far south (Sykes 1967; Scholz, Koczynski and Hutchins 1976; Shudofsky 1985; Hlatywayo 1995). Subsequent tectonic evolution was characterized by repeated cycles of extensional basin development around the margins of the craton, and their compression and thrusting onto the craton. This resulted in reactivation of some pre-existing fractures and associated seismic activity on the craton. Also some of the sparse seismic events in this area can be attributed to induced seismicity as a result of the many mining ventures taking place along this area but at this point, it is difficult to distinguish between mining related events and those of pure tectonic origin because there are no seismometers which are in the vicinity of this area to monitor tremors which may be due to mining activities.

The Limpopo mobile belt (Figure 3.2 (ii)) separates the Zimbabwe craton and the Kaapvaal craton and some workers (Cox *et al*., 1965) have subdivided it into three zones: the northern and southern Marginal Zones and the Central Zone. The Northern Marginal Zone (NMZ) lies within Zimbabwe with structural fabric trending east-northeast to west-southwest (Mkweli *et al*., 1995). Rocks of the NMZ consist of high-

grade metamorphic equivalents of the flanking Archaean granite-greenstones of the Zimbabwe craton (Rollinson, 1993; Rollinson and Blenkinsopp, 1995). The NMZ has been subdivided by some workers into the Transition Zone and the Triangle shear zone (Rollinson and Blenkinsopp, 1995).

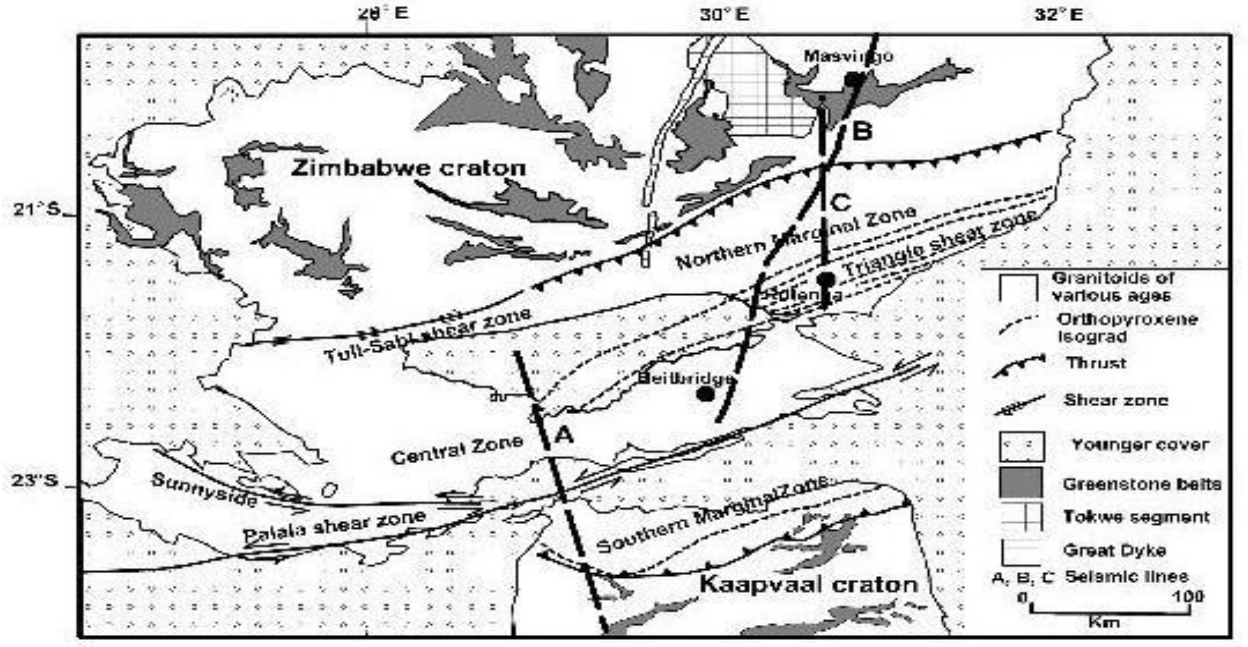

Figure 3.2 (iii): Geological map of the Limpopo Belt (Rollinson, 1993)

The Triangle shear zone, which defines the boundary between the NMZ and the Central Zone (CZ), is related to the Tuli-Sabi shear zone (Mkweli *et al*., 1995). The Southern Marginal Zone (SMZ) lies within South Africa and comprises high-grade metamorphic equivalents of the flanking Archaean granite-greenstone terrains (Du Toit *et al.*, 1983; Kreissig *et al*., 2000) of the Kaapvaal Craton. The Sunnyside-Palala shear zone forms the boundary between the SMZ and the CZ.

The CZ is situated between the two marginal zones, with folds that trend almost northerly (Watkeys, 1983). The CZ is bounded to the north by the Triangle shear zone and in the south by the Palala shear zone. Rocks in the CZ are dominated by high-grade paragneisses and meta-sediments as well as layered igneous complexes with rare intrusive granites (Watkeys *et al*., 1983). A possible explanation to the origin of the high-pressure grade rocks is that the crust of the CZ was thickened down to depths of 60 to 70 km at about 2.7 Ga as a result of continent-continent collision (Van Reenen *et al*., 1987). It then had 20 to 30 km of its upper crust exhumed, as indicated by relict kyanite inclusions in garnets, leaving high pressure metamorphic assemblages at the surface (Van Reenen *et al*., 1987).

Along the Zimbabwe eastern border, the area comprises highly folded and sheared quartzites separated from neighbouring formations by numerous faults. The main lineaments trend in an east-north-east direction. This region falls on the southern tip of the East Africa Rift System. The south-eastern Zimbabwe area along the border with Mozambique forms the western flanks of the rift extension through Lake Malawi. This area shows significant seismic activity which is of pure tectonic origin.

Lineaments in the Deka fault zone mid-Zambezi basin to the north-west of Zimbabwe trend in a north-easterly direction extending further north into the Luangwa rift in eastern Zambia (Hlatywayo, 2001). The surface is covered with thick Karoo sediments of Mesozoic and Paleozoic ages. The Karoo sediments of the mid-Zambezi basin extend south-westwards through the Deka fault zone into Botswana. The general geology is white and red sandstones overlain by basaltic lavas (Maufe, 1924; Vail, 1967; Reeves and Hutchins, 1975).

3.3 Geophysical observations in Zimbabwe

Information inferred from geophysical studies such as magnetics and gravity gives a better understanding of subsurface geology. Gravity data provides information about densities of rocks underground and generally gravity anomalies indicate the presence of rocks which are of high densities whereas magnetic anomalies are normally an indication of rocks that contain magnetic minerals in them such as magnetite and hematite. Very high-intensity anomalies (more than 50 milligals) typify major changes in rock type, usually in basement rocks.

The depth to which magnetic minerals can be mapped depends on their dimensions, shape as well as the magnetic properties of the rock. Sedimentary rocks are not usually magnetic with the exception of banded ironstones and so they have little effect in variation of the magnetic pattern whereas the same cannot be said of igneous and metamorphic rocks and this makes them useful when exploring the geology of the bedrock that may be hidden.

Mekonnen (2004) studied the mafic dykes of Zimbabwe and Mozambique and these normally give rise to magnetic anomalies that are prominent on an aeromagnetic map as shown in figure 3.3 (a) and (b) below and give rise to well defined topographic features. The occurrence of dykes provides information on the evolution of the continental crust into which dykes were intruded as well as stress patterns through time,

and may relate to past plate configurations and help discover their implication for tectonic events which need to be answered.

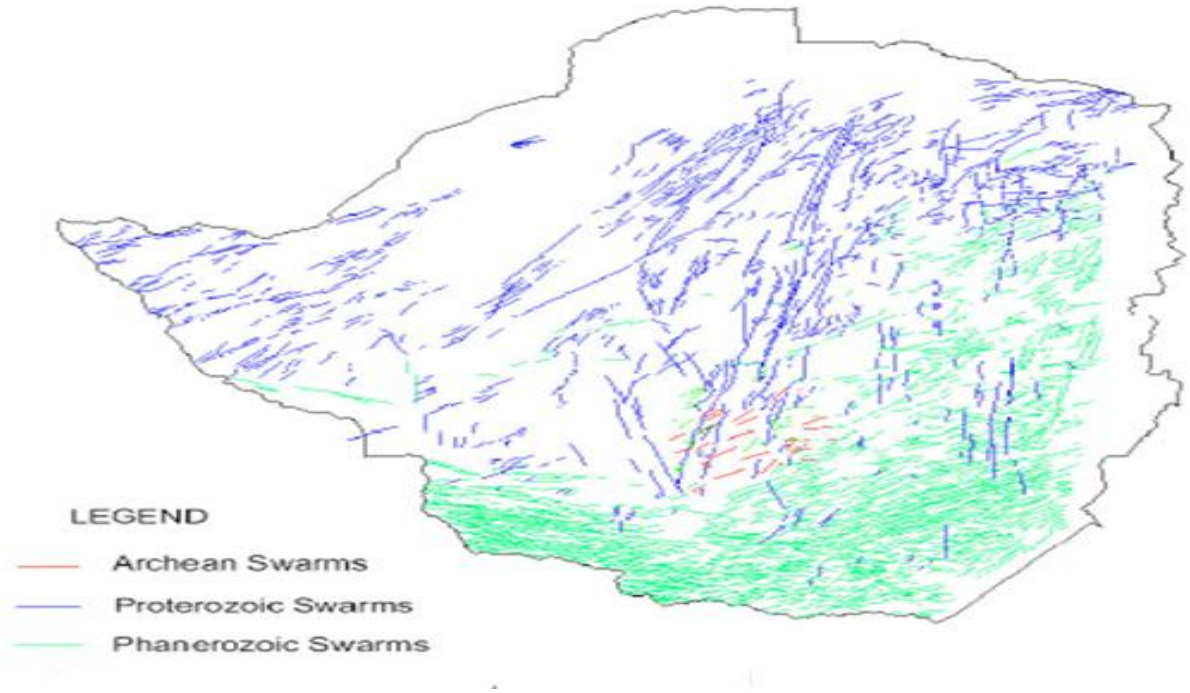

Figure 3.3 (i): Mafic dyke swarms in Zimbabwe (Mekonnen, 2004)

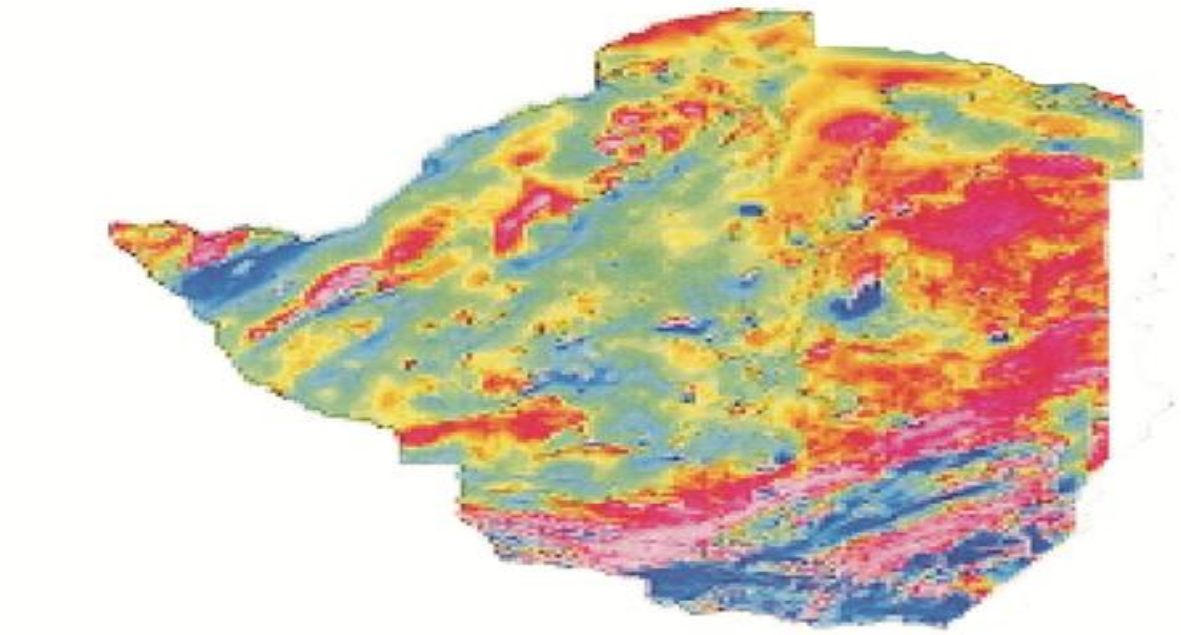

Figure 3.3 (ii): Aeromagnetic map of Zimbabwe (Mekonnen, 2004)

From the two maps above it can be seen that the Save-Limpopo and the Deka Fault Zone lie on or are close to magnetic lineaments and mafic dyke swarms. The Lake Kariba and Nyamandlovu areas are not as close to areas that show anomalies as compared to the Save-Limpopo and the Deka Fault Zone as the seismic activity in those areas is largely reservoir induced as well as due to changes in pore pressure in the underlying rock formation respectively and not of a tectonic nature. We cannot make a conclusive correlation on earthquakes that have occurred on the Zimbabwe-Mozambique border as the area was excluded from aeromagnetic surveys when the rest of the country was flown due to the war at that time.

Chapter 4

Cornell-McGuire and Parametric-Historic procedure applied on Zimbabwe

4.1 Introduction

The first step to assessing the seismic hazard for any site is to develop a seismotectonic model, whereby the area under investigation is divided into smaller zones of similar tectonic and seismic potential setting (Cornell 1968). In order to do this, a study of available seismological, geological and geophysical information is undertaken in order to identify seismic sources and describe the quaternary tectonic regime as well as using any other data which would better define the seismotectonic regions.

4.2 Earthquake Catalogue and unification of magnitudes

Earthquake records spanning a period of 100 years from 1910-2010 were use. This catalogue was compiled from various bulletins which include databases from the International Seismological Centre (ISC) and Bulawayo (BUL). The epicenter map for this catalogue is shown below in Figure 4.2.

The events in these databases were reported in different magnitude scales namely M_l, M_s and M_b . These display various levels of saturation effects at different magnitudes; therefore it was necessary for a suitable scale to be chosen and to harmonise our catalogue to it. In this case the moment magnitude M_w which is controlled by fault size and dislocation was chosen. Some of the advantages of using moment magnitude are that it is directly proportional to the logarithm of seismic moment, it is based on spectral amplitudes which makes it have a uniform behaviour at all magnitude ranges (Joyner, 1984; Scordilis, 2006), it can be estimated from paleoseismological studies and it is the variable of choice for empirically as well as theoretically based equations for the prediction of ground motions (Boore, 2003).

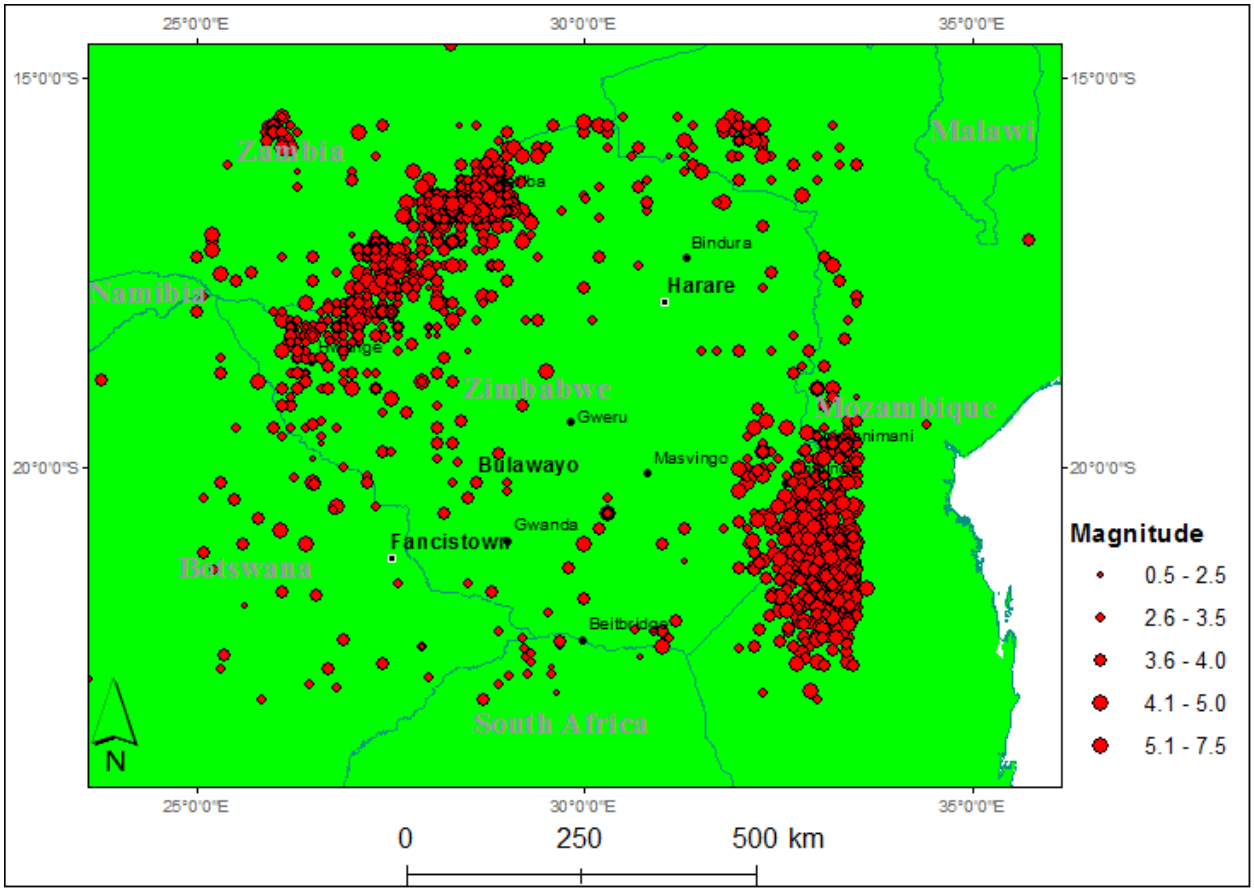

Figure 4.2: Epicenter map of events in Zimbabwe from 1910-2011

The various relations given below were used to convert different magnitudes to M_w. Singh *et al.* (1990) concluded that for small events magnitude M_L is a reliable measure of event size while Hanks and Kanamori (1979) showed that surface wave magnitude M_s when converted to moment magnitude has a similar relation to M_L . The relations used to convert M_L and M_S to moment magnitude via seismic moment M_0 are

$$Log_{10}\, M_o = 1.5\, M_S + 16.1 \pm 0.1 \qquad (4.1)$$

$$Log_{10}\, M_o = 1.5\, M_L + 16.1 \pm 0.1 \qquad (4.2)$$

$$M_w = {}^{2}/_{3}\, log_{10}\, M_o - 10.7 \qquad (4.3)$$

M_o is the seismic moment given in dyne-cm. These conversion relations are valid for the range $3 \leq M_L \leq 7$ and $5 \leq$ Ms $7 \leq .5$. A theoretical relationship determined by Marshall (1970) was used to convert M_b to Ms:

$$M_S = 2.08\, M_b - 5.65 \tag{4.4}$$

To convert M_L to M_b, the relationship of Richter (1958) was applied:

$$M_b = 1.7 + 0.8\, M_L - 0.01 M_L^{\,2} \tag{4.5}$$

The BUL magnitudes were converted to the ISC magnitude using the least squares regression relations of Hlatywayo (1995):

$$M_b \text{ (ISC)} = 0.59 \pm 0.08 M_b \text{ (BUL)} + 1.97 \pm 0.26 \tag{4.6}$$

4.3 The parametric-Historic approach applied to Zimbabwe

The major difference between the Cornell-McGuire approach and the parametric-historic approach is that the latter approach does not require the delineation of seismic active zones which is a subjective matter since the causes of seismicity are not fully understood and delineation of zones is normally based on the distribution of earthquakes in space. At the depths at which most earthquakes occur, except for simple vertical strike-slip faults, the usual techniques for mapping faults may sometimes prove unreliable in the location of the faults.

A common challenge with seismic records is the fact that on most occasions they are incomplete, the earthquake location and magnitude is not always accurate and this leads to errors in the evaluation of seismic hazards for a given area. The parametric-historic approach is capable of taking account of incomplete seismic records together with inaccurate earthquake location and magnitude. This method will accept data of two types, one containing incomplete historical events of large magnitudes whereas the other contains recent instrumental events divided into sub-catalogues with various levels of completeness which could be due to various factors such as downtime of a seismic network.

In this study the seismic hazard of Zimbabwe was calculated in the form of a matrix with a grid spacing of 0.25˚ in both latitude and longitude. The area covered lies within latitude 24 to14˚S and longitude 22 to 36˚E and the procedure is applied to an arbitrarily chosen hypo-central distance of 450km. The seismic catalogue was divided into two sections, an incomplete historic part containing the largest historic events as well as a section containing recent instrumental events which is itself divided into four sub-catalogues with varying levels of completeness.

The historical catalogue starts from the year 1910 up to the end of 1974 with a level of completeness of m_{min} = 4 and standard error of magnitude determination of 0.3. The first of four catalogues for recent instrumental events starts from 1 January 1975 to 31 December1988 with m_{min} = 3.3 level completeness and standard error in magnitude determination of 0.3. The second sub-catalogue starts from 1 January 1989 to 1 December 1995 with a level of completeness of m_{min}= 4 and standard error in magnitude determination of 0.2. The third sub-catalogue starts from 1 January 1996 to 31 December 2004 with m_{min} = 4.5 and standard error in magnitude determination of 0.2. The fourth and final sub-catalogue starts from 1 January 2005 to 28 February 2011 with m_{min} = 5.5 and standard error in magnitude determination of 0.2.

The method for evaluating the maximum earthquake magnitude m_{max} is based on Kijko and Sellevoll (1989, 1992) Kijko and Graham (1998, 1999). It was chosen for its suitability to data that contains historical events of large magnitudes, recent data with varying levels of completeness in various parts of the catalogue which may contain "gaps" and is extended for cases with uncertain magnitude determination. It requires the application of maximum likelihood procedures on seismological data.

The procedure does this by applying a compound Poisson-Gamma distribution as a model of earthquake occurrence in time and a compound Exponential-Gamma distribution as a model of earthquake magnitude. These models then make it possible to incorporate the uncertainty associated with randomly, time-varying seismicity which is appropriate for the catalogue of Zimbabwe used for this study.

The maximum observed event in the catalogue had a magnitude of 7.2 and occurred on 14 August 1962 in Kariba, its standard deviation was assumed to be 0.25. The b-value was taken to be 0.96 ± 0.11 equivalent

to neighbouring South Africa which is of similar tectonic setting. Then by maximizing the likelihood function (2.31) and applying the Kijko-Sellevoll-Bayes (K-S-B) estimator which performs better on deviations from a Gutenberg-Richter deviation model m_{max} = 7.6 ± 0.47. The approach follows the common assumptions of engineering seismology, that is, earthquake occurrence follows a Poisson process with activity rate λ and that earthquake magnitudes follow a Gutenberg- Richter doubly truncated distribution. In order to find the solution from these equations it is clear that we require the value of the mean seismic activity rate λ as well. These parameters are solved simultaneously by the application of an iterative scheme. Using the values of these parameters the probability density function PDF of distance to a site is the calculated.

At this point an appropriate attenuation relationship is then applied to compute the cumulative distribution function CDF so as to express seismic hazard in terms of PGA. In this study four ground motion prediction equations were applied and these are Atkinson and Boore (1995, 1997), Twesigomwe (1996), Jonathan (1996) and Ambraseys *et al*. (1996).

The GMPEs mentioned above were chosen for a various reasons. Atkinson and Boore (1995, 1997) model describe ground motion for stable continental regions. They were developed as predictive ground motion relations for Eastern North America which is similar to Zimbabwe. Twesigomwe (1996) and Jonathan (1996) were used because they are the only available GMPEs in the region. The Ambraseys *et al*. (1996) attenuation model was derived using a dataset of shallow earthquakes representative of Europe which is meant to be used in the construction of hazard-consistent design spectra in Europe and the Middle East. This model is suitable for shallow earthquakes which are comparable to Zimbabwe. These ground motion relations are in the form

$$\ln(a) = c_1 + c_2 m + c_3 R + c_4 lnR + \sigma$$

where a is PGA in units of gravitational acceleration g while $c_1, c_{2,} c_{3,} c_4$ are empirical constants, m is earthquake moment magnitude, R is the earthquake hypocentral distance in kilometres and σ denotes a randomly distributed random error. These relations were chosen since they are for hard rock conditions that are comparable to Zimbabwe. Also our region has little strong motion data, therefore as suggested in

Douglas (2007) it is preferable to use well-constrained models based on data from another regions with similar characteristics.

The acceleration, magnitude and distance in the ground motion prediction relations are taken to be log-normally distributed. The quantity σ is a constant independent of earthquake magnitude and distance representing the uncertainty in the attenuation relation. In addition to uncertainty contributed by the GMPE there are also errors from the determination of earthquake magnitude and location σ_m *and* σ_R respectively.

To treat these errors, they were also taken to be log normally distributed with mean zero following Tinti and Mulargia (1985a, b). By determination of approximate distribution of functions (e.g. Benjamin and Cornell, 1970) the total standard deviation is

$$\sigma_{TOTAL} = \sqrt{\{\sigma^2_{In\,(PGA)} + c_2^2\sigma_M^2 + \sigma_R^2(c_3 + \frac{c_4}{r})^2\}} \quad (4.7)$$

This error term is significant and was incorporated in hazard calculations. For an earthquake of apparent magnitude *m*, the probability of it having a PGA greater than or equal to *a* will be

$$\Pr\,[\text{PGA} \geq \text{a}] = 1 - \Phi\,(\frac{In(a) - In(a_{median})}{\sigma_{TOTAL}}) \quad (4.8)$$

This equation was used to assess the required value of maximum acceleration a_{max} (the PGA calculated from ground-motion attenuation formulae by assuming the occurrence of the strongest possible earthquake ($\hat{m}_{max}$) at a site together with its uncertainty. This approach by (Kijko and Graham, 1999) was used to calculate 10% probability of exceedance at least once in 50 years.

4.4 The Cornell-McGuire approach applied to Zimbabwe

The procedure applied is based on Cornell (1968), McGuire (1976), Merz and Cornell (1973) and accounts for ground motion variability by integrating across the scatter in the attenuation relationship. It also accounts for spatially varying seismicity parameters as well as deaggregation of PSHA. This procedure was in a MATLAB code which requires information about the seismic source. This

information includes latitude, longitude, mean seismic activity rate λ, b-value of the frequency-magnitude Gutenberg-Richter distribution, minimum earthquake magnitude m_{min} and the characteristic maximum earthquake magnitude m_{max} of the seismic source.

Since information that could be used as a firm basis for delineating source zones such as a map of heterogeneity of the lithosphere and fault pattern, derived from geological evidence of large earthquakes in the past, and no coda wave attenuation were available the procedure has relied purely on statistical tools applied on seismic data. The area under consideration was divided into small grids with a grid separation of 0.25˚ in latitude and longitude. These small divisions were treated as "source zones" then the seismic parameters Gutenberg-Richter b-value, mean seismic activity rate λ and the maximum earthquake magnitude are calculated as weighted averages of respective parameters from grid points. The resulting hazard parameters are maximum likelihood estimators based on the available seismic catalogue.

The catalogue was divided into two sections, one containing historical events of large magnitudes and the other containing recent events which are further divided into four sub-catalogues with varying levels of completeness m_{min}. The historical catalogue starts from the year 1910 up to the end of 1974 with a level of completeness of m_{min}=4 and standard error of magnitude determination of 0.3. The first of four catalogues for recent instrumental events starts from the beginning of 1975 to the end of 1988 with m_{min}=3.3 level completeness and standard error of magnitude determination of 0.3. The second sub-catalogue starts from the beginning of the year beginning of 1989 to the end of 1995 with a level of completeness of m_{min}=4 and standard error of magnitude determination of 0.2. The third sub-catalogue starts from the beginning of 1996 to the end of 2004 with m_{min}= 4.5 and standard error of magnitude determination of 0.2. The fourth and final sub-catalogue starts from the beginning of 2005 to the end of February 2011 with m_{min}= 5.5 and standard error of magnitude determination of 0.2.

The level of completeness of the catalogues was computed based on information based on the catalogue and takes the Gutenberg-Richter relation to be valid while m_{min} is said to be defined as the minimum magnitude at which the (complementary) cumulative frequency magnitude distribution (FMD) departs from the exponential decay after Wiemer and Wyss (2000) by making plots of cumulative number of events against earthquake magnitude. The calculation of the seismic parameters is calculated using the same methodology outlined for the parametric-historic approach outlined above, using the Kijko-Sellevoll (1989, 1992) procedures based on the equation derived by Cooke (1979) which then followed by the calculation of the probability density function.

As stated earlier, the grid spacing, was 0.25˚ in both latitude and longitude and the result of the peak ground acceleration (PGA) which is contained in a matrix is then smoothed using a 2- D Gaussian smoothing operator of the form,

$$G(x,y) = \frac{1}{2\pi\sigma^2} e^{-\frac{x^2+y^2}{2\sigma^2}} \tag{4.7}$$

where σ is the standard deviation of the distribution while *x* and *y* are coordinates.

Chapter 5

Results and Discussion

5.1 Introduction

The results of PSHA for Zimbabwe are displayed as maps which show median values of PGA in units of *g* with a 10% probability of exceedance in 50 years. The accelerations range from 0.001g up to 0.2g with different shades of green, yellow, red and dark red indicating levels of seismic hazard which range from very low, moderate, high to very high. Figure 5.1 (i) shows results based on the Cornell- McGuire (1968, 1976) procedure whereas Figure 5.2 (ii) shows results based on the parametric-historic procedure using the modified Atkinson and Boore (1995, 1997).

For the Cornell-McGuire approach the central part of the country stretching towards the south-eastern border of Zimbabwe and Mozambique as well as along the vicinity of the Save-Limpopo mobile belt near

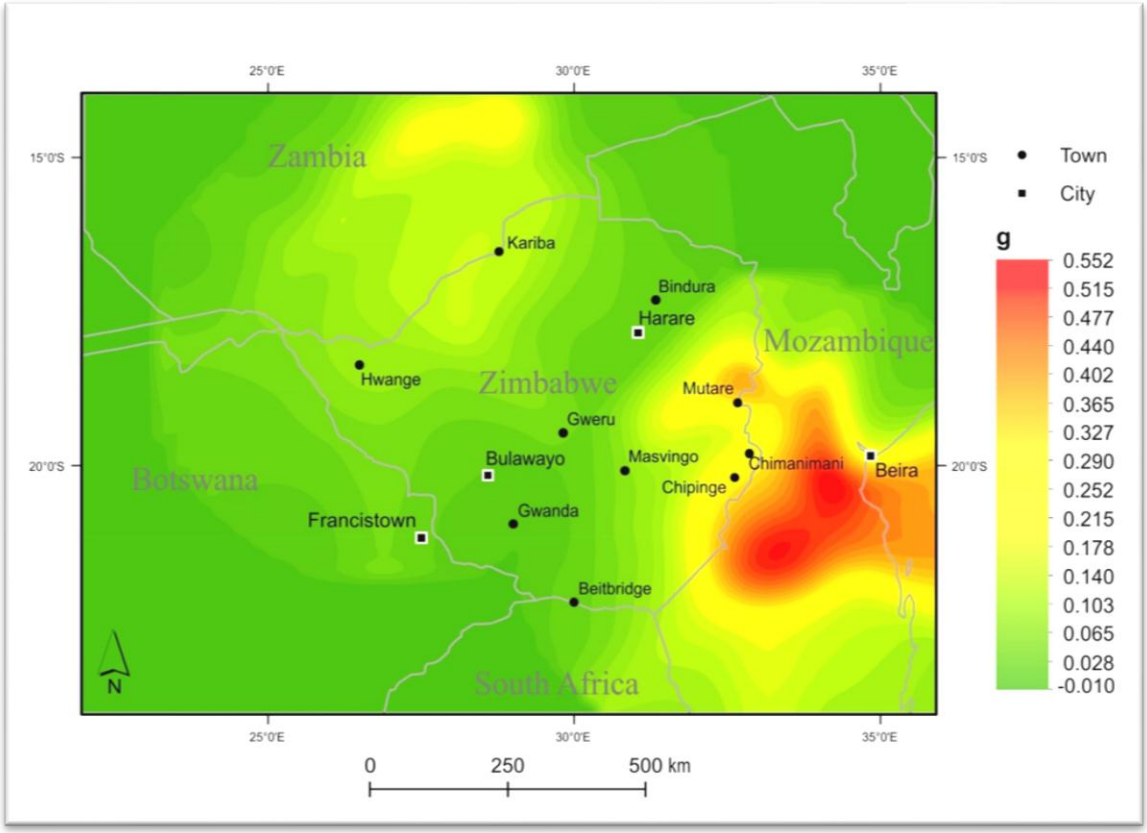

Figure 5.1 (i): Map of the expected PGA with a 10 % probability of being exceeded at least once in a 50 year period according to the classic Cornell-McGuire procedure using the ground motion prediction equation by Atkinson and Boore (1995, 1997)

Masvingo showed the highest values of PGA. These areas show PGA values of up to 0.173g which is shown as a dark red colour. The hazard levels in the Zambezi basin is seen to have values of approximately 0.1 g. The cities of Harare and Bulawayo are in the light orange region of the map with moderate levels of PGA.

.

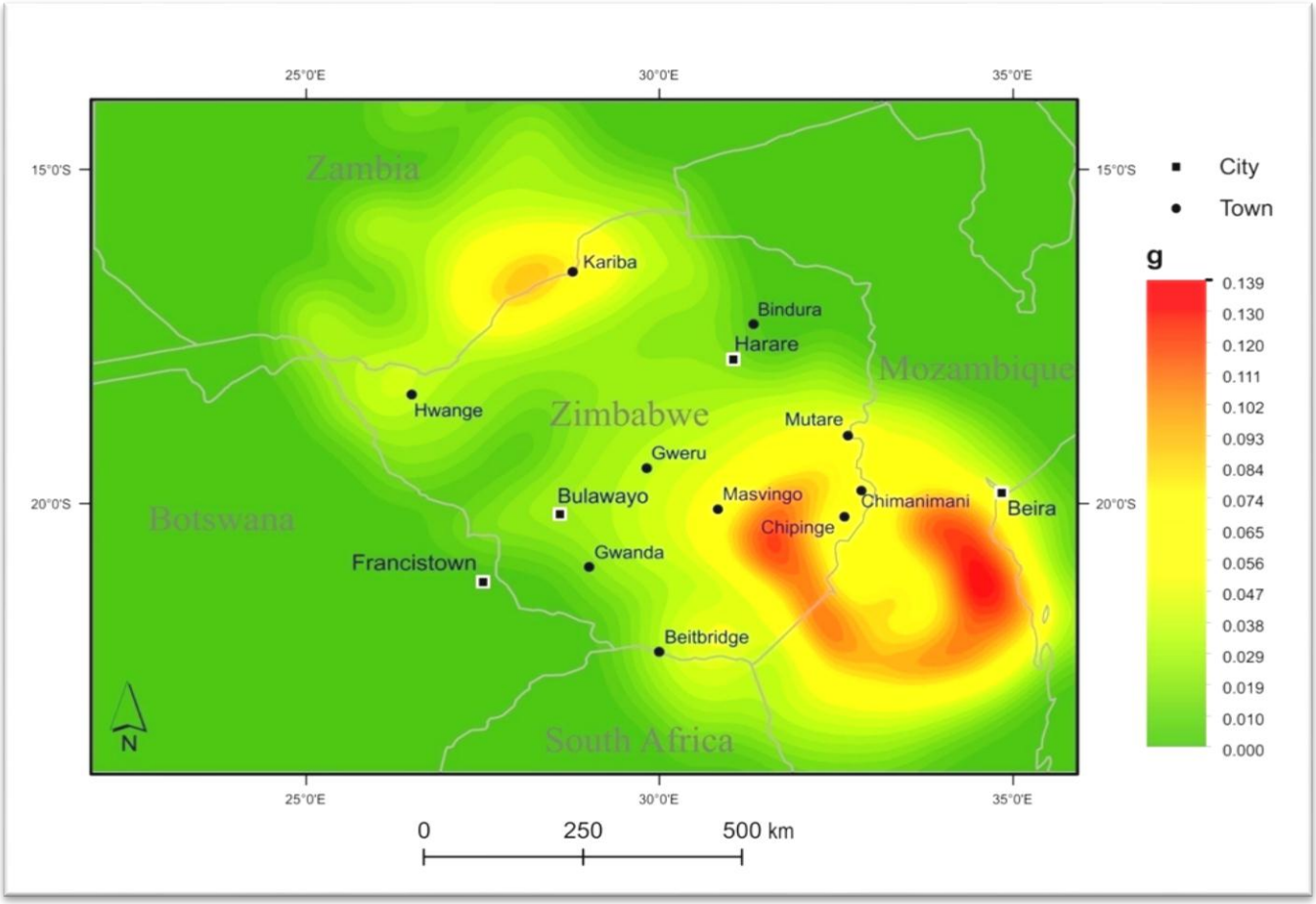

Figure 5.1 (ii): Map of the expected PGA with a 10 % probability of being exceeded at least once in a 50 year period according to the parametric-historic procedure using the ground motion prediction equation by Atkinson and Boore (1995, 1997)

Results for the parametric-historic approach show the highest hazard to be on the south-eastern region of Zimbabwe between Chipinge and Masvingo stretching towards the border with Mozambique with a PGA of up to 0.14g. The second region is the Zambezi basin in Kariba with PGAs of approximately 0.1g shown as a light red colour and of comparable magnitude with the values obtained using the Cornell-McGuire procedure in Figure 5.1 (ii): for the same area. This is followed by the area at the boundary of the Save-Limpopo belt which has moderate levels of PGA of up to 0.06g shown in a light yellow shade.

The effect of using other available attenuation relationships for both methodologies was also tested to see how the results compared. The resulting hazard maps are displayed below. It is interesting to note that the map for the Cornell- McGuire approach using the Jonathan (1996) attenuation relationship closely resembles the one where the modified Atkinson and Boore (1995, 1997) relationship was applied only that the values of PGA of the latter are higher.

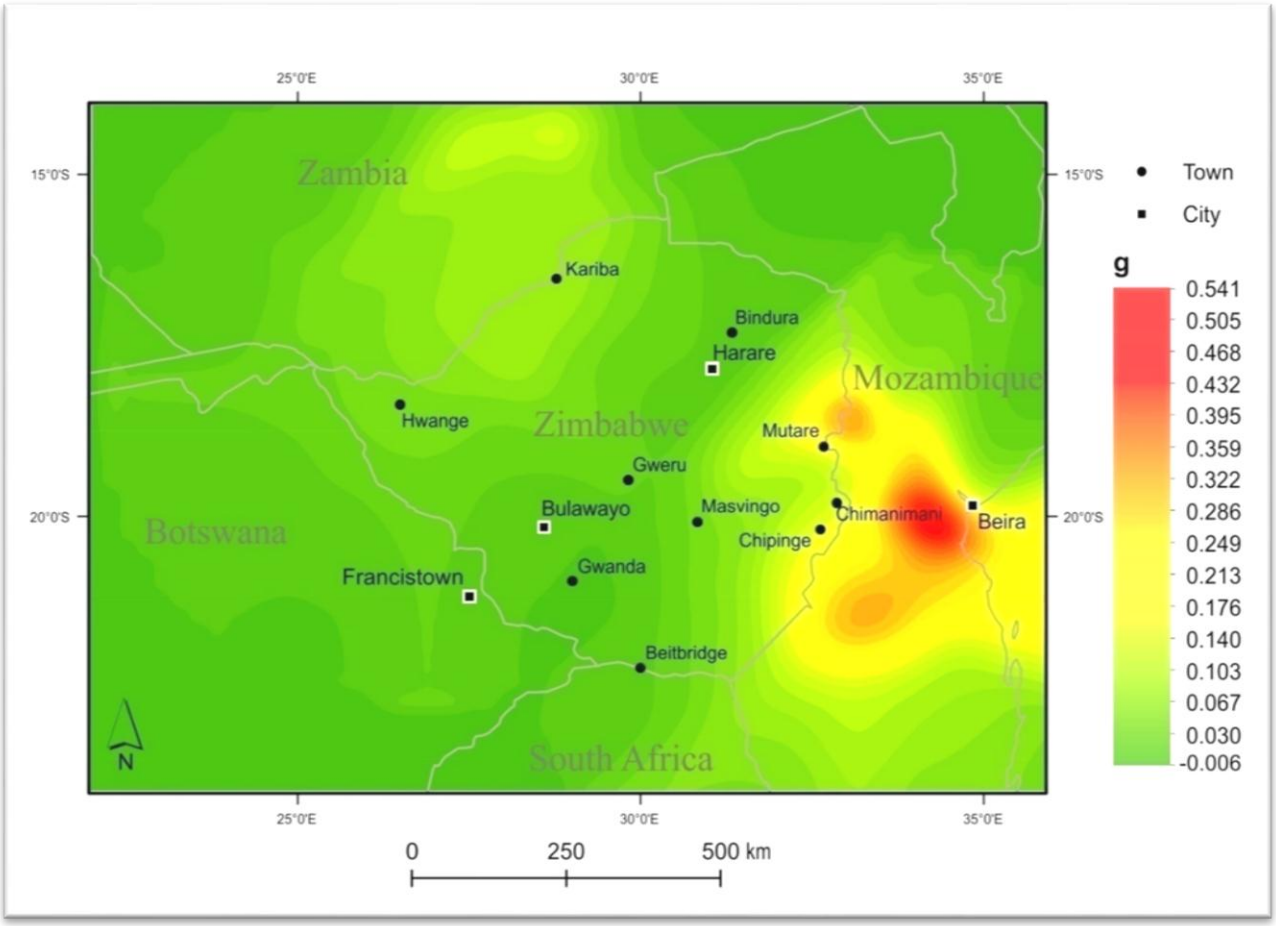

Figure 5.2 (iii): Map of the expected PGA with a 10 % probability of being exceeded at least once in a 50 year period according to the classic Cornell-McGuire procedure using the ground motion prediction equation by Jonathan (1996)

The parametric-historic approach gives the highest values in a smaller geographical area of the Eastern highlands in comparison to the previous scenarios and with almost comparable values to the parametric-historic procedure using the Atkinson and Boore (1995, 1997) of up to 0.19g which is indicated by a very dark shade of red on the map and decreases in a radial manner going outwards. The mid-Zambezi basin has the second highest values of PGA indicated by a shade of blue on the map indicating values of up to 0.15g

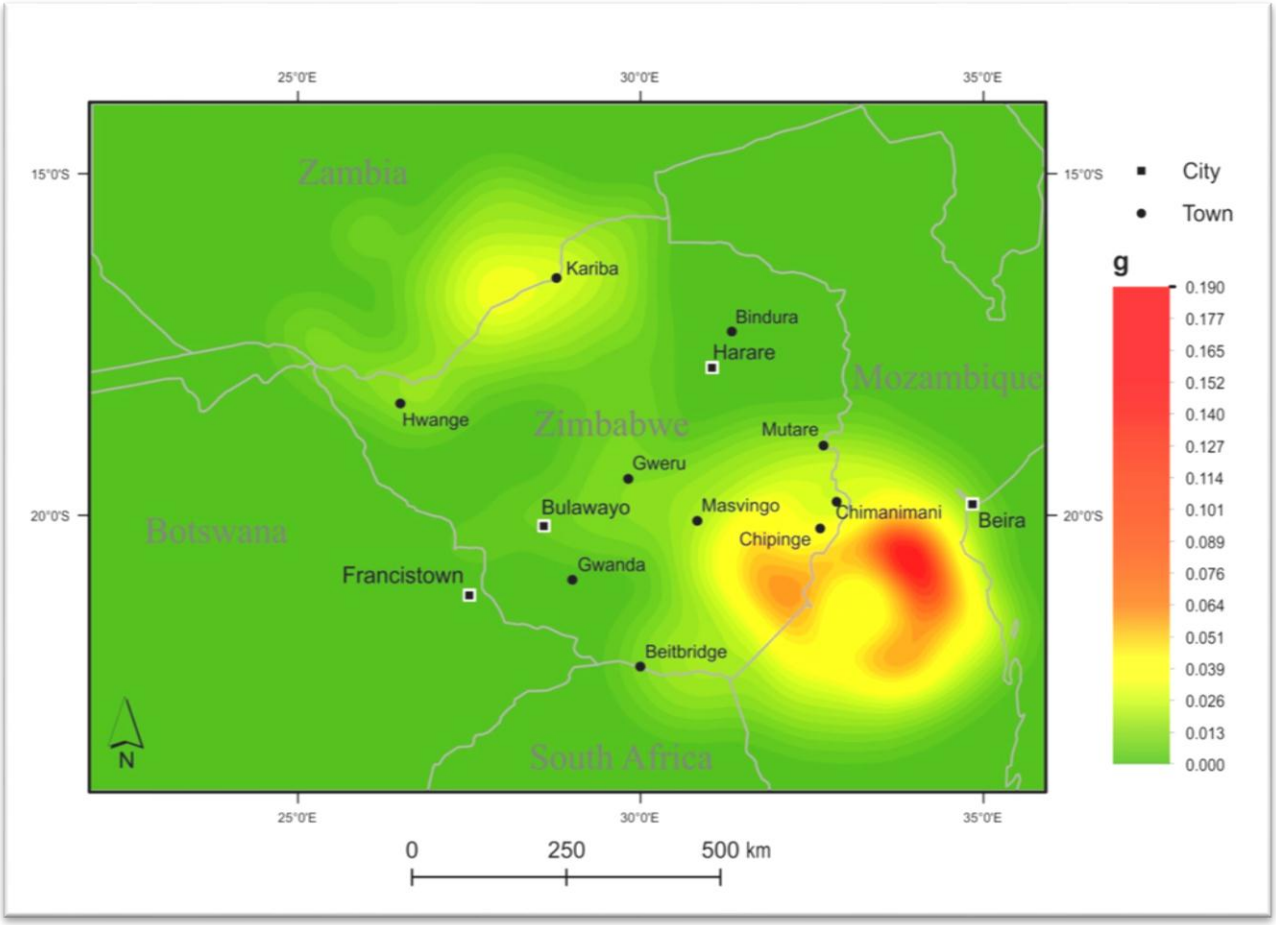

Figure 5.2 (iv): Map of the expected PGA with a 10 % probability of being exceeded at least once in a 50 year period according to the parametric-historic procedure using the ground motion prediction equation by Jonathan (1996)

The maps resulting from the Ambraseys *et al*. (1996) attenuation relation using the Cornell-McGuire and the parametric-historic approach are shown in figure 5.2 (v) and 5.2 (vi) respectively. The map for the Cornell-McGuire approach shows the greatest hazard to be in the south-eastern part of the country with PGA values of up to 0.08g which is represented a dark shade of red on the map. This belt of hazard extends northwards in the region of Mutare, Beira and Tete. The central part of the country also shows significant levels of hazard which decreases radially towards the Zambezi basin which has PGA values of up to 0.05g shown as a light shade of red on the map going all the way down towards the Deka fault zone and these values are similar to what was obtained using the Cornell-McGuire procedure for the same region.

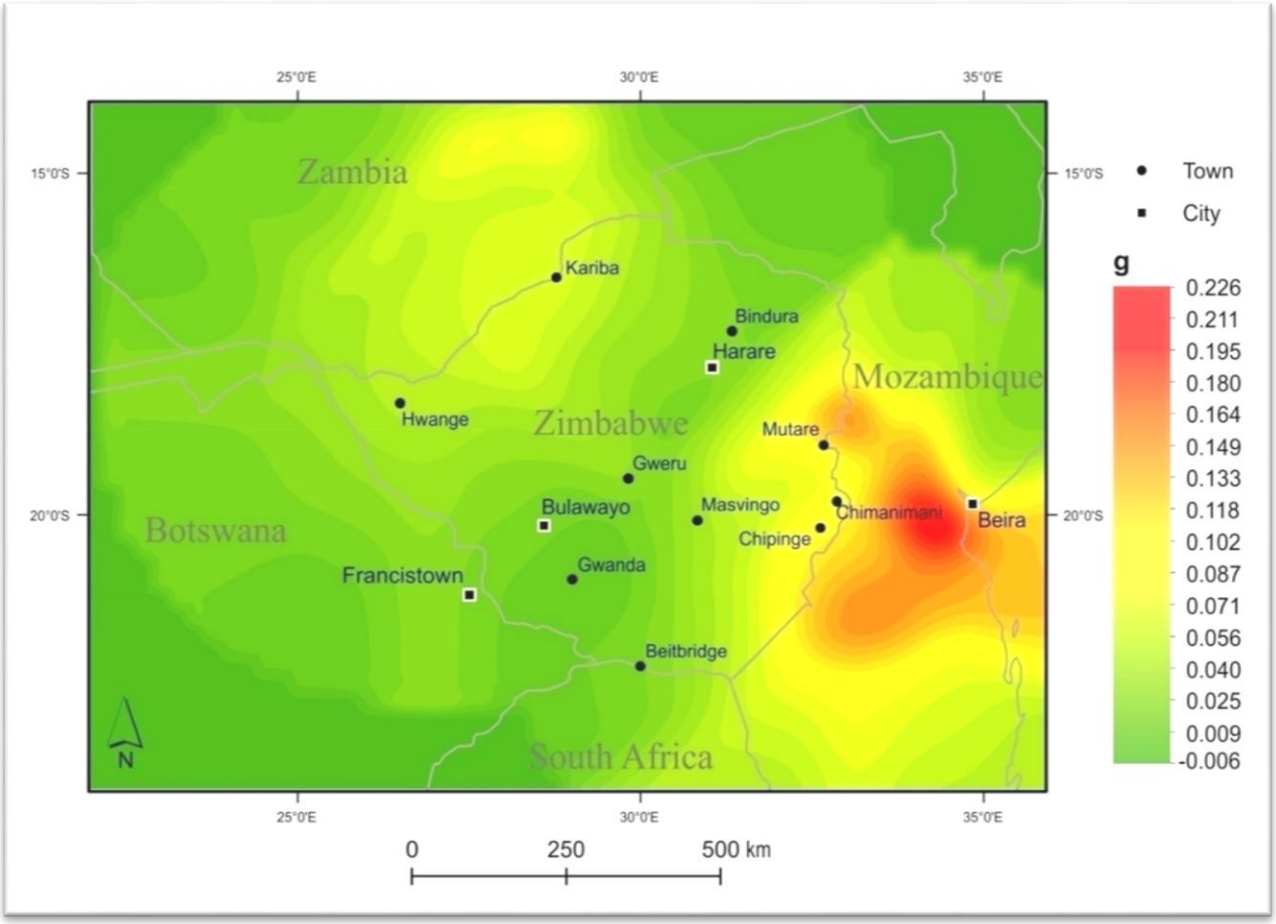

Figure 5.2 (v): Map of the expected PGA with a 10 % probability of being exceeded at least once in a 50 year period according to the classic Cornell-McGuire procedure using the ground motion prediction equation by Ambraseys *et al*. (1996)

The parametric-historic approach map (Figure 5.2 (vi)) displays more defined variation in the hazard pattern. The highest levels of PGA are in eastern part of the country towards Mutare 0.044g shown as a dark red colour on the map. The level of hazard reduces in a radial pattern which is shown in a yellow colour for moderate values of PGA to light green for lower PGA levels. The Zambezi basin has PGA values of up to 0.04g shown as a light shade of red. The Save-Limpopo mobile belt has the third highest values of PGA which reach as much as 0.03g shown as a shade of yellow-green. Interestingly the map shows a region of moderate hazard levels between the towns of Masvingo and Mutare which is shown in orange on the map with PGA values of 0.04g.

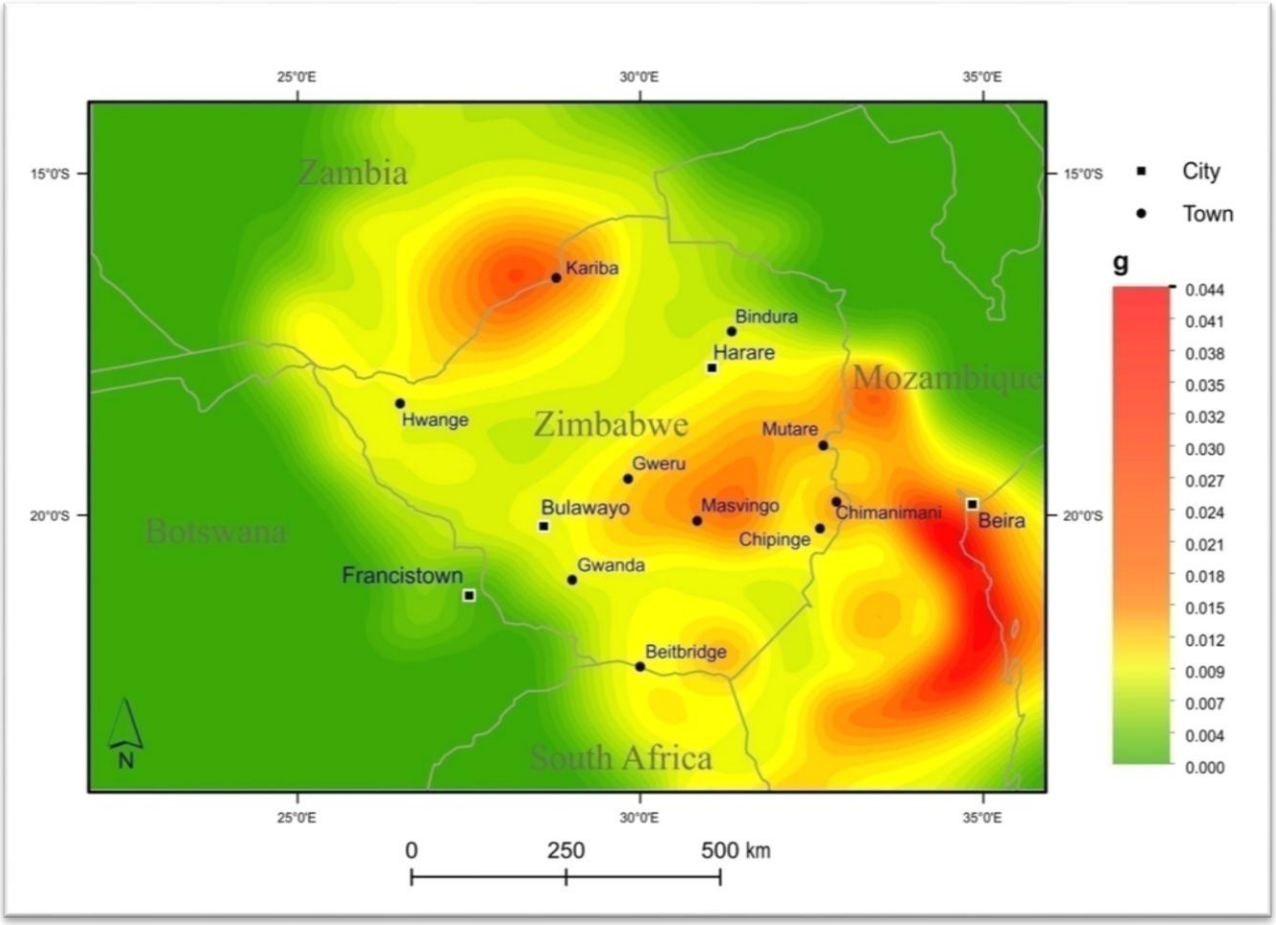

Figure 5.2 (vi): Map of the expected PGA with a 10 % probability of being exceeded at least once in a 50 year period according to the parametric-historic procedure using the ground motion prediction equation by Ambraseys *et al*. (1996)

Figure 5.2 (vii) and 5.2 (viii) above show the maps resulting from the Twesigomwe (1997) attenuation relationship using the Cornell-McGuire and the parametric-historic approach respectively. The highest levels of hazard using the Cornell-McGuire approach are found in the south eastern region of the country largely influence by the East African Rift Valley with PGA values of up to 0.08g indicated by a dark red colour on the map.

This belt of hazard stretches from Tete going south through Beira. The central region of the country also shows marked levels of hazard. This is shown in a dark red colour with hazard levels of up to 0.07g. It decreases in a radial pattern and affects the major cities of Harare, Bulawayo and Gweru which lie within this zone. The hazard levels in the vicinity of the Save-Limpopo mobile belt are shown in a light red

shade indicating PGA values of up to 0.06g. The Zambezi basin is shown as a shade of light yellow-green indicating a PGA of up to 0.04 g.

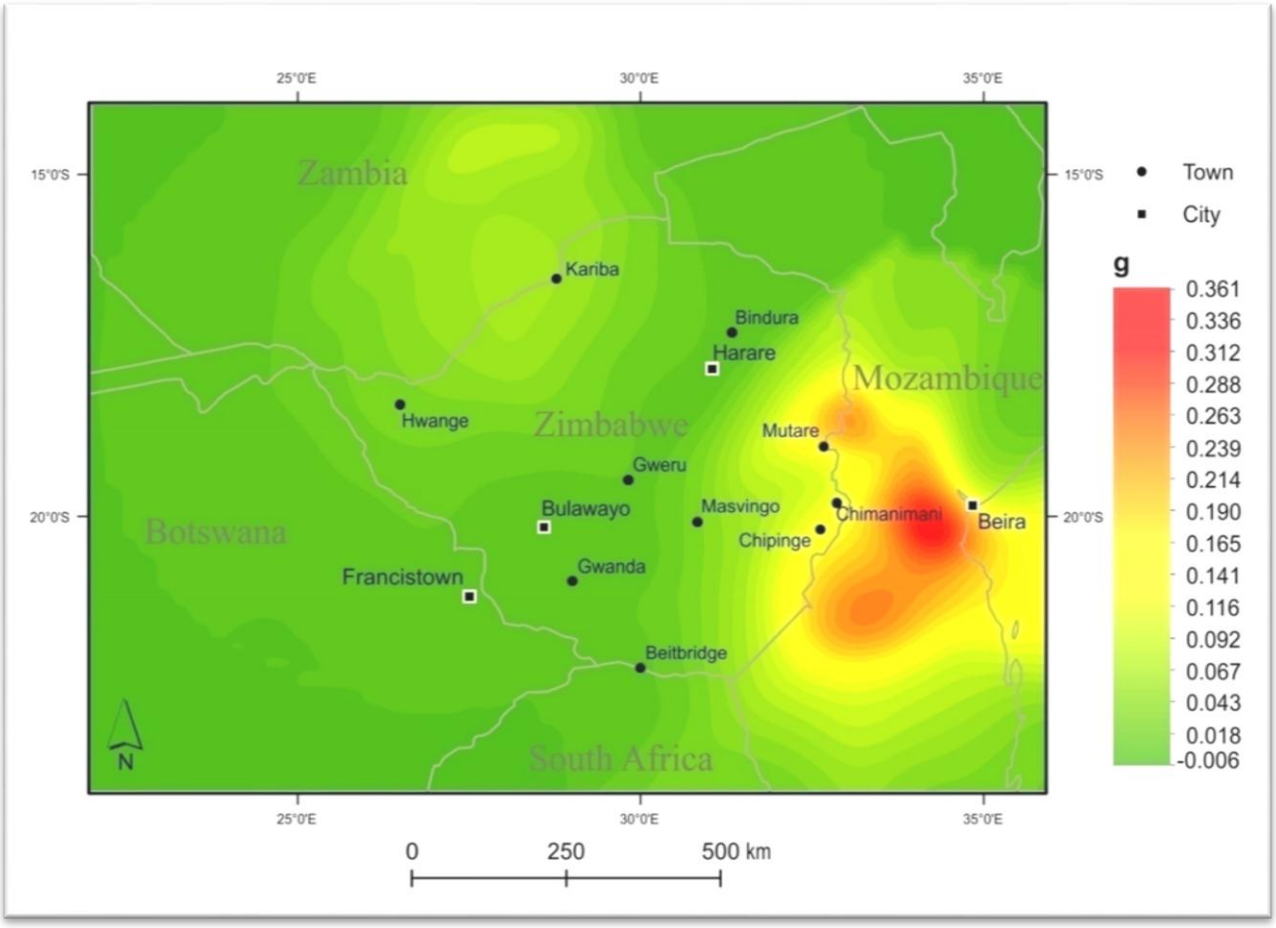

Figure 5.2 (vii): Map of the expected PGA with a 10 % probability of being exceeded at least once in a 50 year period according to the classic Cornell-McGuire procedure using the ground motion prediction equation by Twesigomwe (1997)

The highest levels of hazard for the parametric-historic approach are in the eastern part of the country with a maximum PGA value of 0.16g which is indicated on the map as a shade of dark red colour. This is then followed by the Zambezi basin with moderate hazard with PGA values of up to 0.06g. This decreases in a radial pattern with key towns such as Hwange having moderate levels of hazard shown as a light shade of yellow indicating PGA of up to 0.03g.

The region in the vicinity of Masvingo has significant levels of hazard shown as a red colour shown indicating hazard levels of 0.08g. It is interesting to note that these values are comparable to the ones obtained using the Cornell-McGuire procedure using the same ground motion prediction equation.

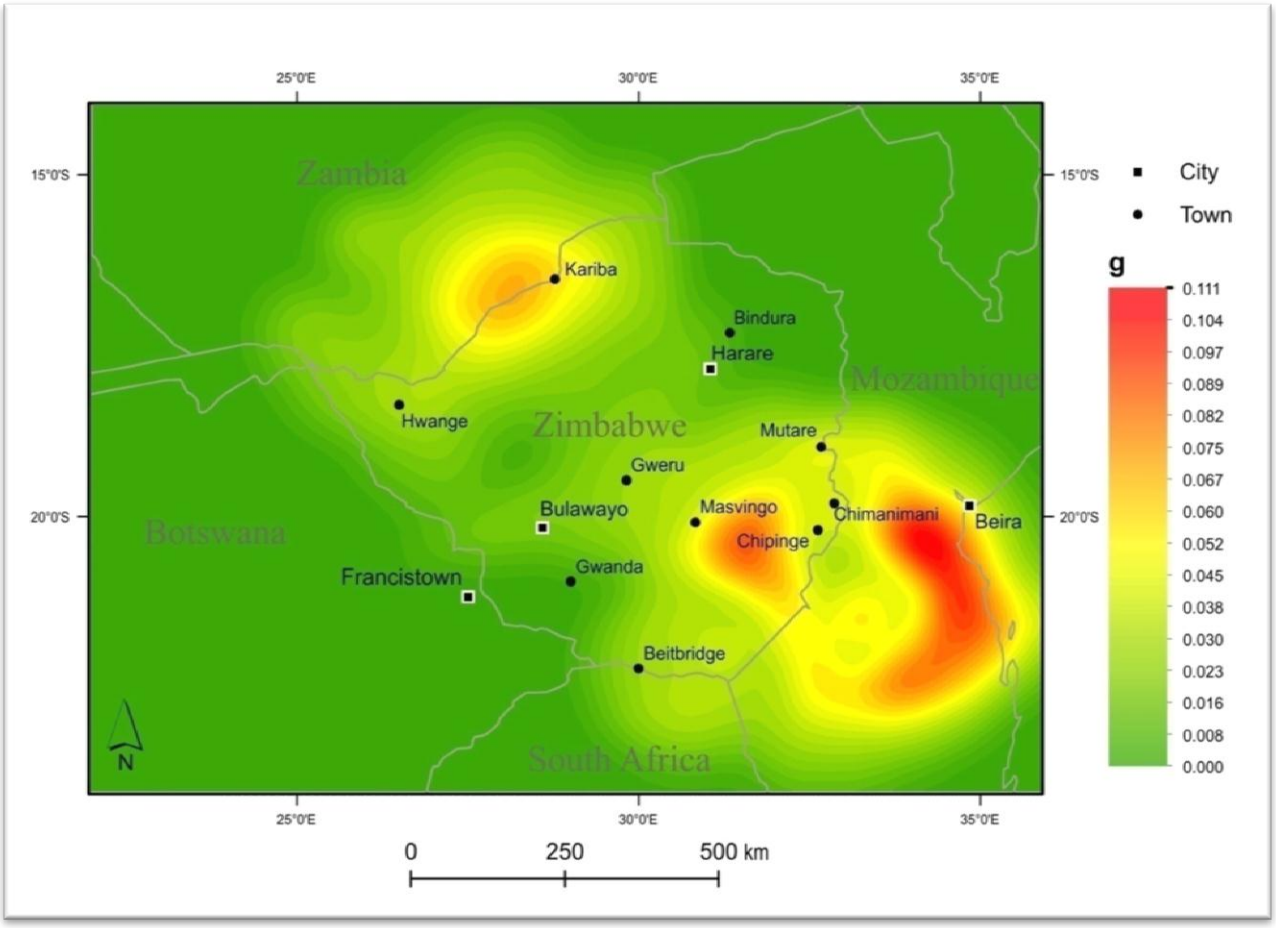

Figure 5.2 (viii): Map of the expected PGA with a 10 % probability of being exceeded at least once in a 50 year period according to parametric-historic procedure using the ground motion prediction equation by Twesigomwe (1997).

The Save-Limpopo mobile belt region has less levels of hazard shown displayed as a light shade of yellow-green indicating a PGA value of up to 0.045g which is again comparable to the map obtained using the Cornell-McGuire procedure.

5.2 Logic tree results

There are a number of uncertainties entailed in seismic hazard analysis. Aleatory (random) uncertainties which are characteristic to the current model are readily integrated and accounted for in PSHA by means

of equation 2.20. Epistemic errors which are due to insufficient knowledge parameters are accounted for by use of logic tree formalism.

A logic tree consists of a sequence of nodes and branches for a diverse choice of hypotheses, each carrying a weighting of unity. Each node is assigned a subjective weighing based on engineering judgement (Kolathayar and Sitharam, 2012). In this case, three weightings of <0.75, 0.25>, <0.5, 0.5> and <0.25, 0.75> were considered for each of the Cornell-McGuire and parametric-historic procedures with each GMPE accounted for individually. The GMPEs are taken to have equal weighting since they were developed for different regions of the world that have similar tectonics settings to the study area and there is no criterion for assigning weights to them. The results from logic tree formalism are presented in the maps below and expected displayed merged outputs from the two procedures using assigned weightings.

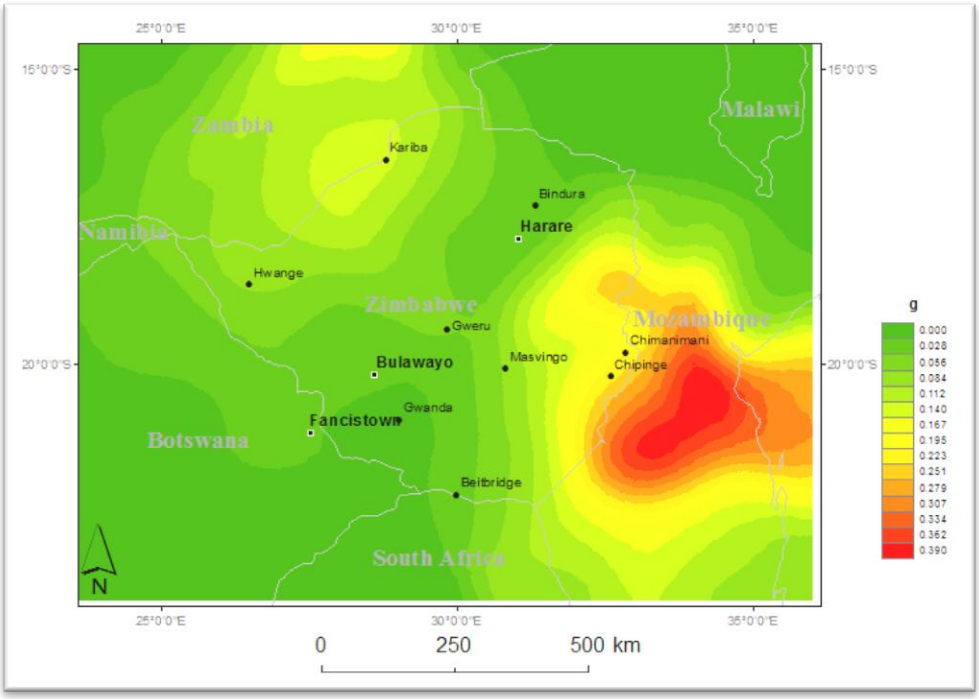

Figure 5.3 (i): Map of the expected PGA with a 10 % probability of being exceeded at least once in a 50 year period using logic tree with weightings of 0.25 for Cornell-McGuire and 0.75 for parametric-historic procedure using the ground motion prediction equation by Atkinson and Boore (1995, 1997).

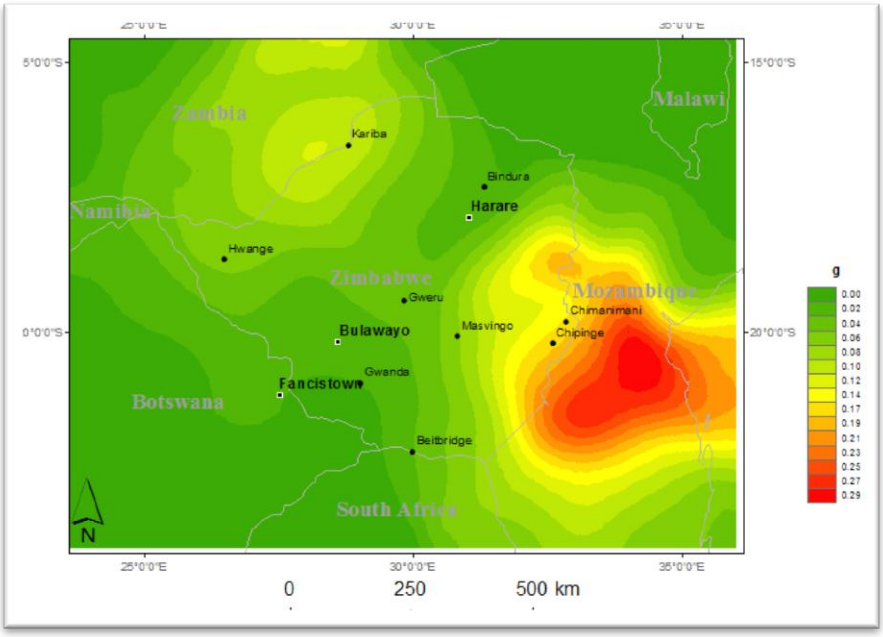

Figure 5.3 (ii): Map of the expected PGA with a 10 % probability of being exceeded at least once in a 50 year period using logic tree with weightings of 0.5 for Cornell-McGuire and 0.5 for parametric-historic procedure using the ground motion prediction equation by Atkinson and Boore (1995, 1997).

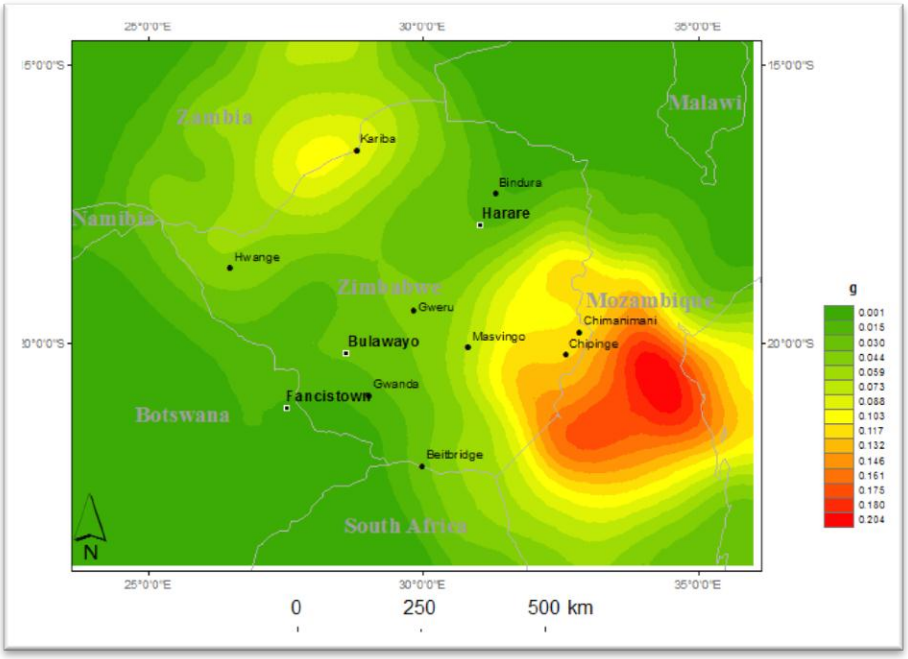

Figure 5.3 (iii): Map of the expected PGA with a 10 % probability of being exceeded at least once in a 50 year period using logic tree with weightings of 0.75 for Cornell-McGuire and 0.25 for parametric-historic procedure using the ground motion prediction equation by Atkinson and Boore (1995, 1997).

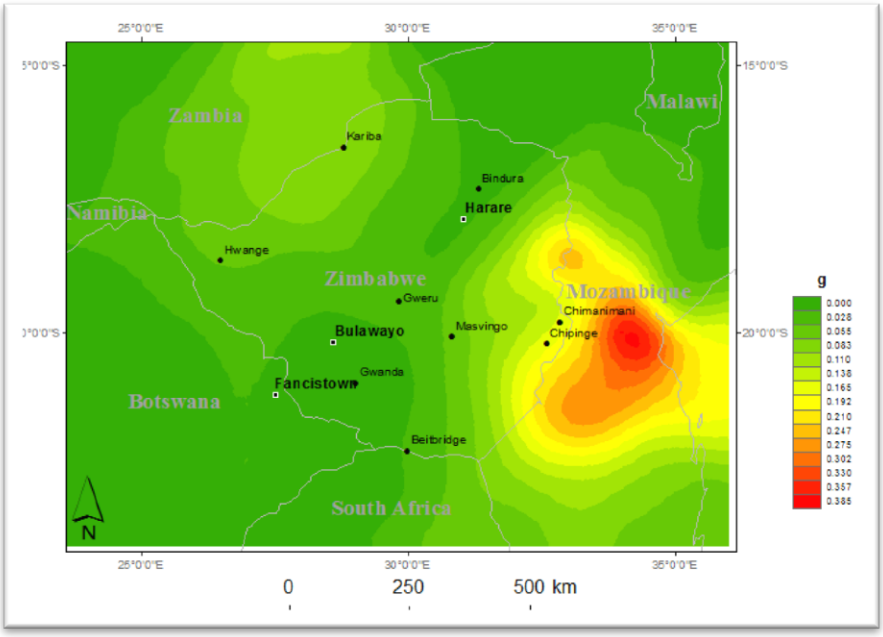

Figure 5.3 (iv): Map of the expected PGA with a 10 % probability of being exceeded at least once in a 50 year period using logic tree with weightings of 0.25 for Cornell-McGuire and 0.75 for parametric-historic procedure using the ground motion prediction equation by Jonathan (1996).

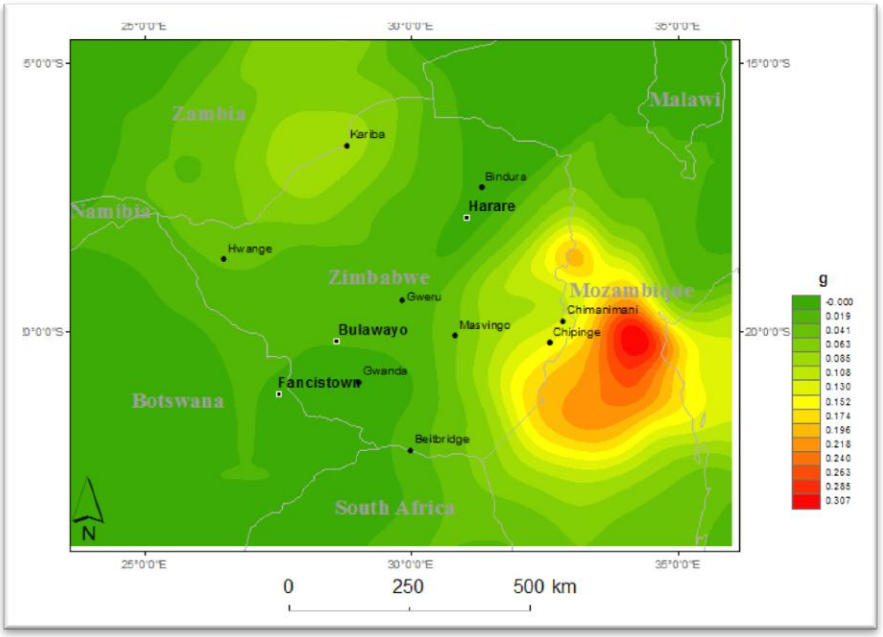

Figure 5.3 (v): Map of the expected PGA with a 10 % probability of being exceeded at least once in a 50 year period using logic tree with weightings of 0.5 for Cornell-McGuire and 0.5 for parametric-historic procedure using the ground motion prediction equation by Jonathan (1996).

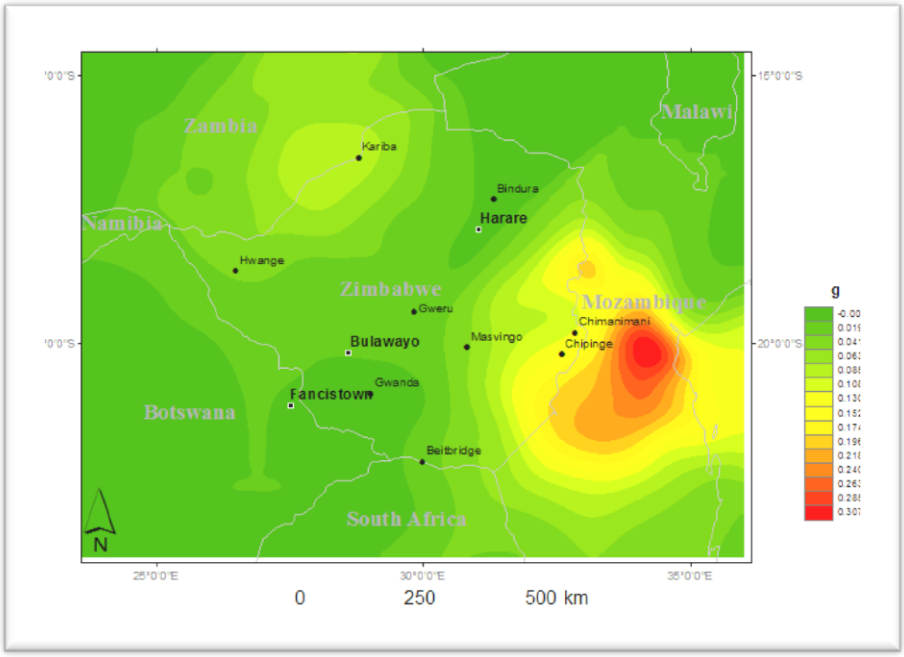

Figure 5.3 (vi): Map of the expected PGA with a 10 % probability of being exceeded at least once in a 50 year period using logic tree with weightings of 0.75 for Cornell-McGuire and 0.25 for parametric-historic procedure using the ground motion prediction equation by Jonathan (1996).

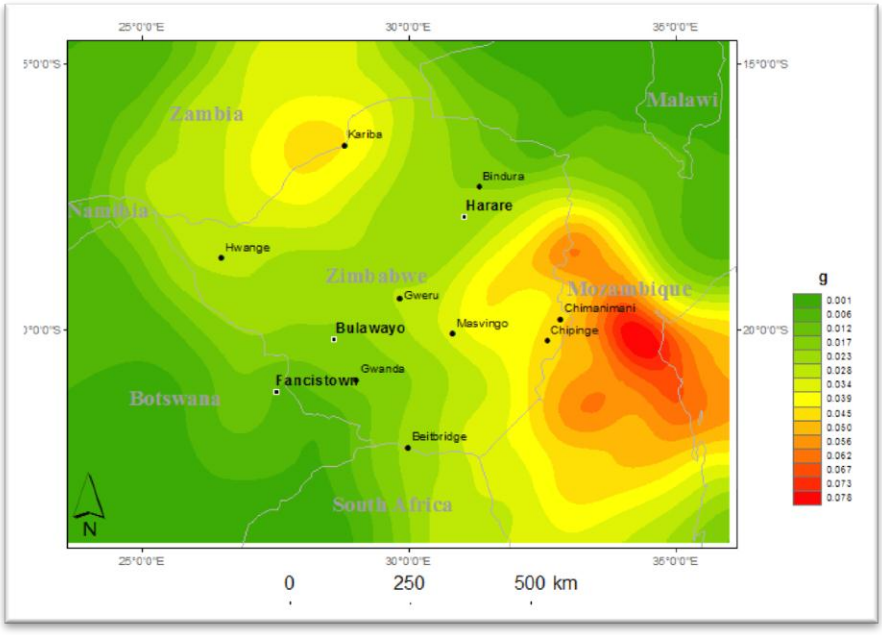

Figure 5.3 (vii): Map of the expected PGA with a 10 % probability of being exceeded at least once in a 50 year period using logic tree with weightings of 0.25 for Cornell-McGuire and 0.75 for parametric-historic procedure using the ground motion prediction equation by Ambraseys *et. al* (1996).

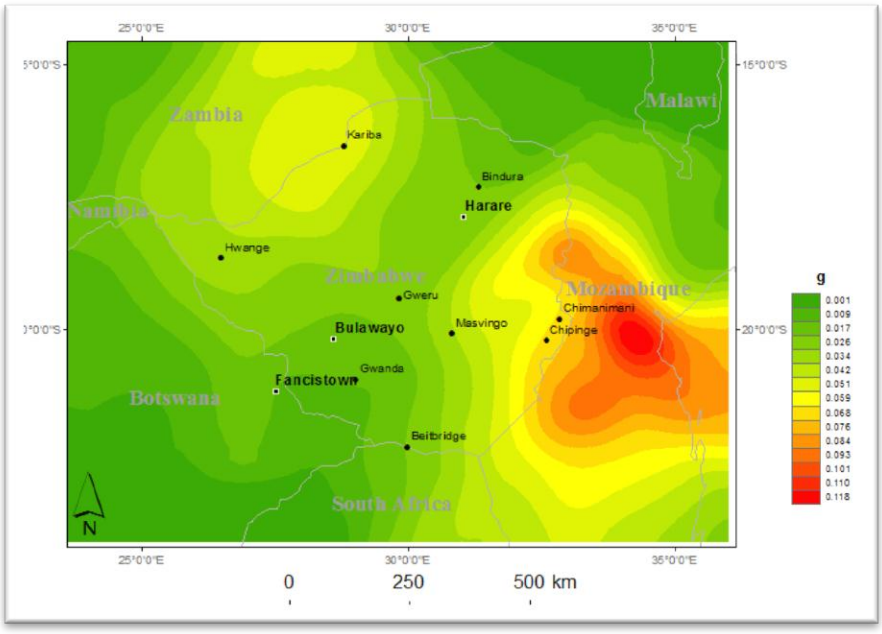

Figure 5.3 (viii): Map of the expected PGA with a 10 % probability of being exceeded at least once in a 50 year period using logic tree with weightings of 0.5 for Cornell-McGuire and 0.5 for parametric-historic procedure using the ground motion prediction equation by Ambraseys *et. al* (1996).

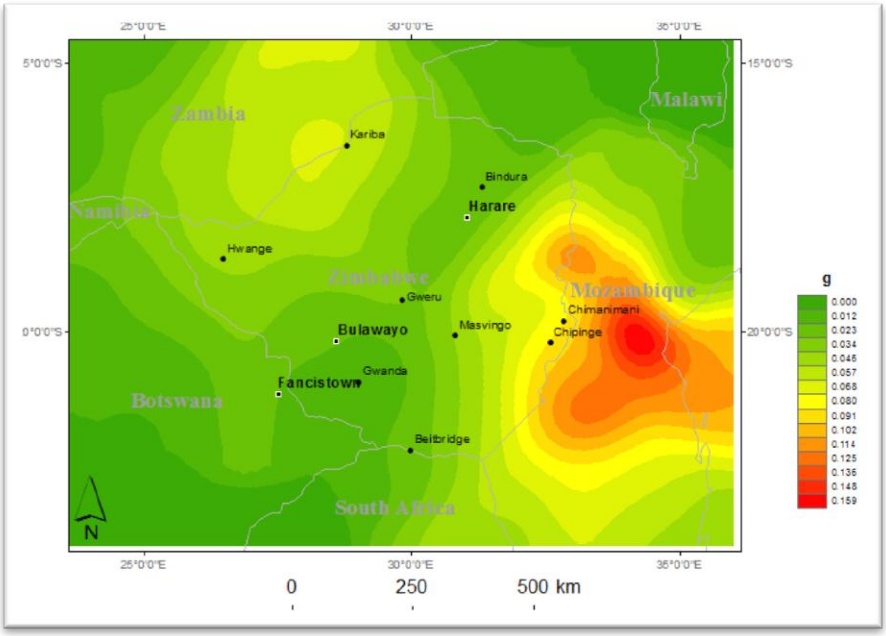

Figure 5.3 (ix): Map of the expected PGA with a 10 % probability of being exceeded at least once in a 50 year period using logic tree with weightings of 0.75 for Cornell-McGuire and 0.25 for parametric-historic procedure using the ground motion prediction equation by Ambraseys *et. al* (1996).

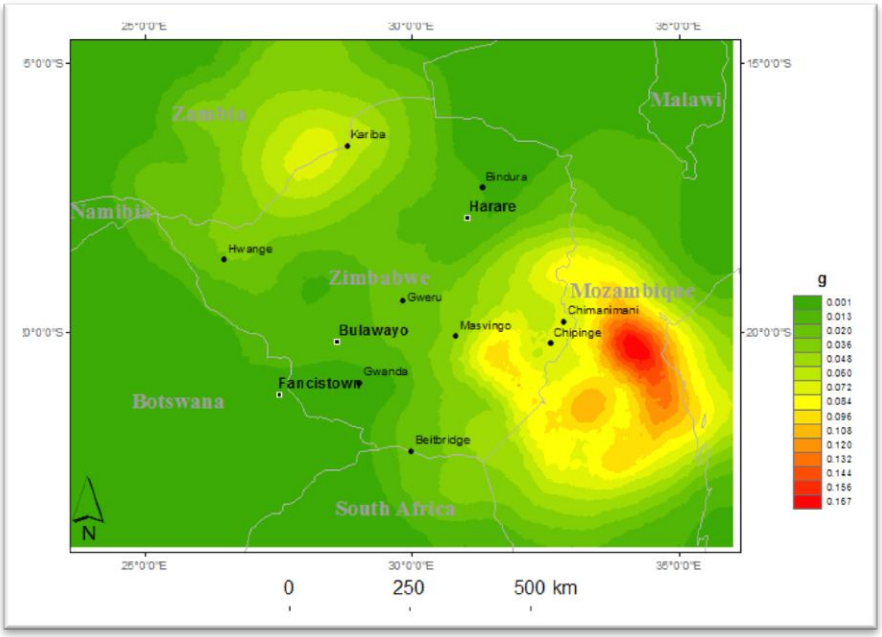

Figure 5.3 (x): Map of the expected PGA with a 10 % probability of being exceeded at least once in a 50 year period using logic tree with weightings of 0.25 for Cornell-McGuire and 0.75 for parametric-historic procedure using the ground motion prediction equation by Twesigomwe (1997).

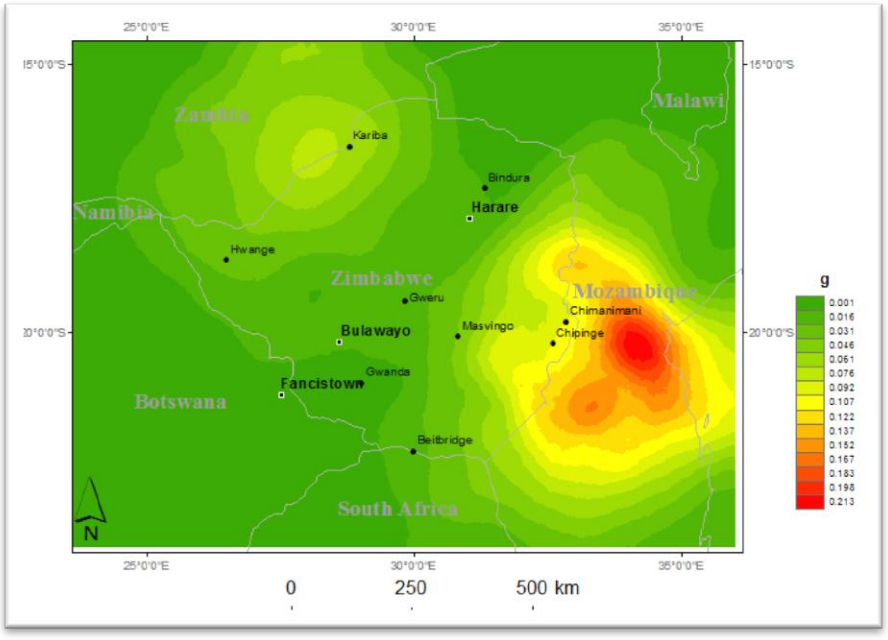

Figure 5.3 (xi): Map of the expected PGA with a 10 % probability of being exceeded at least once in a 50 year period using logic tree with weightings of 0.5 for Cornell-McGuire and 0.5 for parametric-historic procedure using the ground motion prediction equation by Twesigomwe (1997).

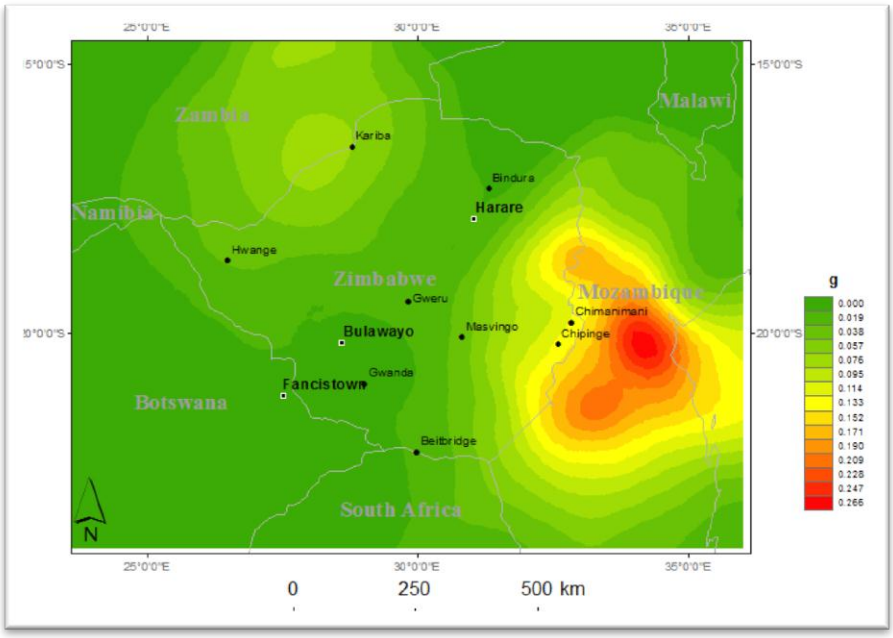

Figure 5.3 (xii): Map of the expected PGA with a 10 % probability of being exceeded at least once in a 50 year period using logic tree with weightings of 0.75 for Cornell-McGuire and 0.25 for parametric-historic procedure using the ground motion prediction equation by Twesigomwe (1997).

Chapter 6

Conclusion

6.1 Introduction

The general observation that can be concluded from all the results is that greatest levels of hazard lie in three major areas. These include a belt in the south-east part of the country, along the border with Mozambique covering the Chimanimani-Inyangani eastern highlands, the Zambezi basin extending from Lake Kariba up to the Deka-fault and finally the Save-Limpopo mobile belt area. Moderate levels of hazard can be observed in the vicinity of Nyamandlovu depending on the attenuation relationship and methodology used.

The high PGA values obtained in the eastern highlands can be attributed to high seismicity in the area which is mainly influenced by the East African Rift System as this area is an extension of the southern tip of the western arm of the system. High PGA values in the Zambezi basin are due to high seismicity resulting from reservoir induced seismicity caused by the Lake Kariba dam as well as natural tectonic activity supported by the occurrence of M_w=6.6 on 28 May 1910, long before the construction of the dam.

The area in the vicinity of the Save-Limpopo mobile belt levels of hazard are moderate and seismicity is sparse except for the notable event of $M_L = 6$ that occurred in 1940. The area forms the region that separates the Kaapvaal and Zimbabwe craton. Nyamandlovu has the lowest levels of hazard compared to the other areas and seismic activity in the area is sparse though events of notable magnitude have occurred in the area as a result of changes in pore pressure in the underlying rock formations (Hlatywayo and Midzi, 2005).

6.2 Comparison of Cornell-McGuire and parametric-historic results

Each of the two procedures followed in this study maintains the same general pattern for each of the four ground motion prediction equations applied. The major difference between the Cornell-McGuire and parametric-historic approach is the fact that the latter places an emphasis on areas where events of high magnitude take place whereas the former accounts for the entire catalogue. This is the major reason that

causes a marked difference in results for these procedures even when similar attenuation relationships are used.

Maps obtained using the parametric-historic approach show a lot more detail in delineating the hazard over the whole country and show better correlation to the seismicity pattern of Zimbabwe and more often than not it was observed that they have comparable values of PGA in comparison to the Cornell-McGuire approach. The Cornell-McGuire approach seems to "average out" the hazard of a region as the seismic parameters are assumed to be similar for every point in a seismic source zone that would have been delineated. This clearly shows that the parametric-historic procedure gives a result that is a mirror of the seismicity pattern whereas the Cornell-McGuire approach gives a mirror of the chosen zones (see Hlatywayo, 1997).

For a typical region in most parts of the world especially in the African context it would seem the parametric-historic approach would be ideal in the evaluation of seismic hazard for two major reasons. The first one is the fact that most seismic catalogues are incomplete and the parametric-historic approach has the ability of taking that into account whereas for the Cornell-McGuire approach the assessment of seismic parameters cannot be done in a reliable manner when faced with an incomplete seismic history which unfortunately will almost always be the case in most parts of the world. The second reason is the requirement of the Cornell-McGuire to delineate seismic source zones. As previously stated, this is a subjective matter.

The Cornell-McGuire approach has the major advantage of being able to incorporate geological and geophysical data in the assessment of hazard at a site. This is critical in understanding the underlying causes of seismic activity of a region so as to develop a seismotectonic model. It is worth noting that the procedure will also account for seismic gaps, migration in seismicity and cyclical strain release. This procedure is reliable at lower probabilities as it takes into account the whole catalogue unlike the parametric-historic procedure which places emphasis on the largest events as can be observed from the resulting maps.

This study is based on the application of statistical procedures on seismological data. An earthquake catalogue with events spanning a period of just over 101 years is not considered long enough to give highly accurate results. The catalogue showed unusual inconsistencies such as having gaps and incomplete data in recent times, for example, from the mid-90s up to 2003. This could be attributed to downtime of the Zimbabwean seismic network which was as a result of the economic challenges bedevilling the country during this phase. Since an assumption has to be made that the data is complete this results in inaccurate evaluation of seismic parameters which in turn affects the accuracy of PGA values calculate thus the results of this study only serve to provide average estimates of hazard calculations.

The two procedures are of a parametric nature with reasonably established theoretical basis that represent our best efforts as seismologists so far to quantify seismic hazard. Compared to other fields of science they are still fairly young concepts with the Cornell-McGuire approach having been around for just under 50 years and the parametric-historic still less than 15 years. The two would be best used in such a manner that they are complementary to each other as suggested by SSHAC (1997), depending on available data as they are progressively improved. In the words of Atkinson (2004) “The same lack of knowledge that causes our uncertainty of the hazard also prevents us from accurately quantifying that uncertainty” such that more effort should be directed towards understanding and quantifying inputs (with minimal uncertainty) of earthquake characteristics and causes together with ground motion prediction relations.

In the parametric-historic procedure a necessary improvement would be in the assessment of the b-value and seismic activity rate λ. Instead of taking one average b-value for the whole region, the reliability of the results would improve markedly by incorporating the Kijko and Sellevoll (1992) procedure used in the assessment of earthquake parameters for incomplete data sets to calculate these parameters at each grid point.

In the Cornell-McGuire procedure, areas of attention include the absence of an upper limit in the evaluation of a chosen ground motion such as PGA which leads to unrealistically high values of ground motion parameters such as PGA=20g, obtained for a nuclear-waste repository at Yucca Mountain in the USA (Corradini, 2003). Another concern is in the treatment of uncertainties in GMPE residual δ. Wang and Zhou (2007) amongst other factors highlight the flaw of treating this quantity as an independent variable yet by definition it is dependent on earthquake magnitude M and distance R.

The results clearly show different values of PGA when the attenuation relation applied is changed though the general pattern of hazard remains similar in general. This variation in PGA values is not ideal seeing that this is a parameter that is of direct engineering application for the purposes of town planning, construction of high rise buildings as well as nuclear plants and water reservoirs. It is therefore critical that more research be directed toward the development of regional attenuation and scaling characteristics of the various strong motion parameters with distance, earthquake size and the local geological conditions. Also in this study local site effects were not accounted for, therefore it will be necessary that future detailed studies take these into account when performing realistic hazard studies.

6.3 Use of logic formalism

Use of logic trees is a widely accepted procedure in seismic hazard assessment that is recommended by Senior Seismic Hazard Analysis Committee (SSHAC) frame work (Budnitz *et al*., 1997). It accounts for uncertainties thereby allowing for a consensus estimate from differing views and neutralises dissenting views. The maps resulting from logic tree formalism displayed in the previous chapter can be seen as a merging of the two methodologies according to assigned weightings. There is an ongoing line of questioning related to the interpretation of branch weights in a logic-tree and whether they are probability or simply subjective indications that cannot be “admitted at the same level as hard earthquake evidence” (Castanoz and Lomnitz, 2002).

References

Ambraseys, N. N., & Adams, R. D. (1991). Reappraisal of major African earthquakes, south of 20˚ N, 1900-1930. *Natural Hazards*, 4:389 – 419.

Ambraseys, N. N., Simpson, K. A. (1996). Prediction of vertical response spectra in Europe. *Earthquake Engineering and Structural Dynamics*, 25(4): 401–412.

Anderson, J.G. (1997). Benefits of scenario ground motion maps, *Engineering Geology*, 48 (1): 43-57

Anderson, G. A. & Brune, J. N. (1999). Probabilistic seismic hazard analysis without the ergodic assumption. *Seismological Research Letters*, 70: 19–28

Anderson, J. G, Brune, J.N, Anooshehpoor, R. & Ni, S. (2000). New ground motion data and concepts in seismic hazard analysis. *Current Science*. 79(9), 1278-1290.

Atkinson, G. & Boore, D. (1995). New ground motion relations for eastern North America, *Bulletin of the Seismological Society of America*,85:17–30.

Atkinson, G.M. & Boore, D.M. (1997). Some comparisons between recent ground motion relations. *Seismological Research Letters.*68, 24-40.

Atkinson, G.M. (2004). An overview of developments in seismic hazard analysis. 13th World Conference on Earthquake Engineering. Vancouver, B.C., Canada August 1-6. Paper No. 5001

Atkinson, G.M. & Boore, D.M. (2006). Earthquake ground motion prediction equations for Eastern North America. *Bulletin of the Seismological Society of America*, 96:2181–2205.

Benjamin, J. R. & Cornell, C. A. (1970*). Probability, Statistics, and Decision for Civil Engineers*. New York: McGraw-Hill.

Bommer, J. J. & Abrahamson, N. A. (2006). Why do modern probabilistic seismic-hazard analysis often lead to increased hazard estimates?. *Bulletin of Seismological Society of America*, 96:1976–1977.

Boore, D.M. (2003). Simulation of Ground Motion Using the Stochastic Method. *Pure and Applied Geophysics*, 160(3-4):635-676.

Bungum, H. A., Dahle, G. R., McGuire, R. K. amd Gudmestad, O. T. (1992). Ground motions from intraplate earthquakes, *Proceedings 10th World conference on earthquake engineering, Madrid.*

Bulajic, B. and Manic, M. (2006). Selection of the appropriate methodology for the deterministic seismic hazard assessment on the territory of the Republic of Serbia. *Architecture and Civil Engineering*, 4:41-50.

Cao, A. M., and Gao, S. S. (2002). Temporal variations of seismic *b*-values beneath north-eastern Japan island arc, *Geophysical Research Letters*. 29:1334. doi: 10.1029/2001GL013775

Castanos, H. and Lomnitz, C.(2002). PSHA: Is it Science?. *Engineering Geology*, 66(2002): 315–317

Cooke, P. (1979), Statistical inference for bounds of random variables. *Biometrika*, 66(2): 367-374, doi: 10.1093/biomet/66.2.367

Cornell, C. A. (1968). Engineering Seismic Risk Analysis. *Bulletin of the Seismological Society of America*, 58(5): 1583-1606.

Cornell, C. A. (1971). Bayesian Statistical Decision Theory and Reliability-Based Design, In Freudenthal, A. M. (Editor), Proceedings of the International Conference on Structural Safety and Reliability, April 9-11, 1969. Smithsonian Institute: Washington D.C.

Cornell, C. A. (1994). Statistical Analysis of Maximum Magnitudes. In Johnston, A. C., Coppersmith, K. J., Kanter, L. R., & Cornell, C. A. (Editors), The Earthquakes of Stable Continental Regions - Vol. 1. Assessment of Large Earthquake Potential. California, Electric Power Research Institute, Palo Alto, p. 5–1 - 5–27

Corradini, M. L. (2003). Letter from Chairman of the US Nuclear Waste Technical Review Board to the Director of the Office of Civilian Radioactive Waste Management; available from: http://www.nwtrb.gov/corr/mlc010.pdf

Cox, K.G, Johnson, R.L, Monkman, L.J, Stillman, C.J, Vail J.R. & Wood, D.N. (1965).The geology of the Nuanetsi igneous province. *Philosophical Transactions of the Royal Society of London*, 257 (1078): 71–218.

Cramér, H. (1961), Mathematical Methods of Statistics, 2nd Edition. Princeton University Press:Princeton.

Deif, A., Abed, A., Abdel- Rahman, K., & Abdel Moneim, E., (2011), Strong ground motion attenuation in Aswan area, Egypt. *Arab Journal of geophysics*, 4 (5):855-861.

Douglas, J. (2007). On the regional dependence of earthquake response spectra. *Journal of earthquake technology*, Paper No. 477, 44 (1):71-99.

Douglas, J. & Aochi, H. (2008). A survey of techniques for Predicting Earthquake Ground Motion for Engineering Purposes. *Survey in geophysics* 29(3): 187-220. doi: 10.1007/s10712-008-9046-y

Du Toit, M.C, Van Reenen, D.D. & Roering C. (1983),Some aspects of the geology, structure and metamorphism of the Southern Marginal Zone of the Limpopo metamorphic complex. *Special Publication of the Geological Society of South Africa*, 8:121–142

EERI Committee on Seismic Risk, (H. C. Shah, Chairman), (1984). Glossary of Terms for Probabilistic Seismic Risk and Hazard Analysis. *Earthquake Spectra*, 1: 33-36

EPRI, (1986), Seismic Hazard Methodology for the Central and Eastern United States, Report NP-4726.Volume 1-3, Revision 1. Electric Power Research Institute, Palo Alto, California

EPRI (1993), Guidelines for determining design basis ground motions, Early site permit demonstration program, Volume 1, RP3302, Electric Power Research Institute, Palo Alto, California.

Fairhead, D. J. & Girdler, R. W. (1969a). How far does the rift system extend through Africa? *Nature*, 221: 1018 – 1020.

Fairhead D. J. & Girdler, R. W. (1969b). Evolution of rifting in Africa. *Nature*, 224:1178 – 1182.

Fairhead D. J. & Henderson N. B. (1977). The seismicity of Southern Africa and incipient rifting. *Tectonophysics*, 41:T19 – T26

Frankel, A., Mueller, C., Barnhard, T., Perkins, D., Leyendecker, E.,N. Dickman, S. Hanson & Hopper, M. (1996). *National seismic hazard maps, June 1996*. (Open-file Report 96-532). U.S. Geological Survey.

Gough, D.I. & Gough, W. (1970). Load – induced earthquakes at Lake Kariba-II. *Geophysics Journal Research Society*, 21:79-101.

Gough, D. I. (1978). Induced Seismicity: The Assessment and Mitigation of Earthquakes. *Risk-UNESCO 1978*, 91-117

Gumper, F & Pomeroy, P.W. (1970), Seismic wave velocities and earth structure of the African continent. *Bulletin of Seismological Society of America*, 60(2):651-668.

Gupta, D. I. (2002). The State of the Art in Seismic Hazard Analysis. *ISET Journal of Earthquake Technology*, 39 (4):311-346.

Gupta, H (2011), Introduction to Probabilistic Seismic Hazard Analysis (Extended version of contribution by A. Kijko). Encyclopaedia of Solid Earth Geophysics, Harsh Gupta (Editor). *Springer*.

Gupta, K. H., Rastogi, B. K. & Narain, H. (1972a). Some discriminatory characteristics of earthquakes near the Kariba, Kremasta, and Koyna artificial lakes, *Bulletin of Seismological Society America*, 62 (2):493-507

Gupta, K. H., Rastogi, B. K. & Narain, H. (1972b), Common features of the Reservoir associated seismic activities, *Bulletin of Seismological Society of America*, 62 (2):481-492

Gutenberg, B. & Richter, C. F. (1944). Frequency of Earthquakes in California, *Bulletin of the Seismological Society of America*, 34 (4):185–188.

Habermann, R. E. (1987), Man-made changes of seismicity rates, *Bulletin Seismological Society America*, 77 (1): 141-159.

Hanks, T. & Kanamori, H. (1979). A moment magnitude scale, *Journal of Geophysical Research*, 84 (B5):2348–2350.

Hanks, T. C. & Johnston, A. C. (1992), Common features of the excitation and Propagation of strong ground motion for North American Earthquakes. *Bulletin Seismological Society America,* 82 (1): 1-23.

Hlatywayo, D. J. (1995). Fault-plane solutions of the Deka fault zone and mid-Zambezi basin, *Geophysics Journal International*, 120 (3): 567 - 576. doi:10.1111/j.1365-246X1995.tb01839.x

Hlatywayo D.J. (1996), *Seismicity of Zimbabwe during the period 1959-1990*. (Report 3-92). Institute of Geophysics, Seismological Department, University of Uppsala, Sweden.

Hlatywayo D. J., (1997), Seismic hazard estimates in central southern Africa, *Geophysics Journal International*. 130 (3):737 - 745.doi: 10.1111/j.1365-246X1997.tb01839.x

Hlatywayo D. J & Midzi V, (2005), *Report on the investigations into the location, causes and the effects of the 25th June 2004 Bulawayo-Nyamandlovu earthquake*, Harare: Government of Zimbabwe.

Ingleton, J. (Editor). (1999). *Natural disaster management: A presentation to commemorate the international decade for natural disaster reduction IDNDR 1990-2000*. Tudor Rose: Leicester.

Jonathan, F. (1996). *Some aspects of seismicity in Zimbabwe and eastern and southern Africa*. Unpublished MSc. Thesis, Institute of Solid Earth Physics, University of Bergen, Norway.

Joyner, B.W. (1984). A scaling law for the spectra of large earthquakes, *Bulletin of the Seismological Society of America*, 74 (4):1167–1188.

Kebede, F. & Van Eck, T. (1997). Probabilistic seismic hazard assessment for the horn of Africa based on seismotectonic regionalization. *Tectonophysics*, 270(3): 221–237.

Kijko, A & Graham G. (1998). Parametric-historic Procedure for Probabilistic Seismic H azard Analysis Part I: Estimation of Maximum Regional Magnitude m_{max}. *Pure and applied geophysics*. 152 (1998) 413–442

Kijko, A & Graham G. (1999). ‘‘Parametric-historic’’ Procedure for Probabilistic Seismic Hazard Analysis Part II: Assessment of Seismic Hazard at Specified Site Pure and applied geophysics 154 (1999). 1–22

Kijko, A., & Sellevoll, M. A. (1989). Estimation of Earthquake Hazard Parameters from Incomplete Data Files. Part I. Utilization of Extreme and Complete Catalogues with Different Threshold Magnitudes. *Bulletin of the Seismological Society of America*, 79 (3): 645-654

Kijko, A. & Sellevoll, M. A. (1992), Estimation of Earthquake Hazard Parameters From Incomplete Data Files, Part II, Incorporation of Magnitude Heterogeneity, *Bulletin of the Seismological Society of America*., 82 (1): 120-134.

Kijko, A. Retief, S. J. P. & Graham, G. (2002). Seismic Hazard and Risk Assessment for Tulbagh, South Africa: Part I – Assessment of Seismic Hazard, *Natural Hazards.* 26 (2)**:** 175–201.

Kijko, A. (2008), Data Driven Probabilistic Seismic Hazard Assessment Procedure for Regions with Uncertain Seismogenic Zones.In *Earthquake Monitoring and Seismic Hazard Mitigation in Balkan Countries*. Edited by Husebye, E. S. Available from: http:www.link.springer.com/chapter/10/1007%2F978-1-4020-6815-7_16#page-1

Kijko, A & Singh M. (2011). Statistical Tools for Maximum Possible Earthquake Magnitude Estimation. *Acta Geophysica*. 59(4): 674-700.

Kijko, A & Smit A. (2012). Extension of the Aki-Utsu *b*-Value Estimator for Incomplete Catalogs, *Bulletin of the Seismological Society of America*, 102(3):1283–1287.

Kolathayar, S and Sitharam T. G., Comprehensive Probabilistic Seismic Hazard Analysis of the Andaman-Nicobar Regions, *Bulletin of the Seismological Society of America*, 102(5):2063-2076.

Kramer, S. L. (1996). Geotechnical Earthquake Engineering. Englewood Cliffs: N.J. Prentice-Hall.

Kreissig, K. Nägler, T.F. Kramers, J.D. van Reenen, D.D. & Smit, C.A. (2000). An Isotopic and geochemical study of the northern Kaapvaal Craton and the Southern Marginal Zone of the Limpopo Belt: Are they juxtaposed terrains?. *Lithos*, 50 (1): 1–25.

Krinitzky, E. L., Chang, F. K. and Nutti, O. W. (1988). Magnitude-Related Earthquake ground motions. *Bulletin Association Engineers Geologists* XXV. 399-423.

Kulhanek O. (2005). Seminar on *b*-value; Department of Geophysics, Charles University, Prague, December 10-19.

Le Goff. B, Fitzenz, D. & Beauval, C. (2007). Towards a bayesian seismotectonic zoning for use in Probabilistic Seismic Hazard Assessment (PSHA), the Fundação para a Ciência e a Tecnologia report PTDC/CTEGIX/ 101852/2008.

Marsan, D. (2003). Triggering of seismicity at short timescales following Californian earthquakes. *Journal of Geophysical Research: Solid Earth*, 108 (B5):1978-2012. doi:10.1029/2002JB001946.

Marshall, P.D. (1970). Aspects of spectral differences between earthquakes and underground explosions, *Geophysical Journal of the Royal Astronomical Society*, 20(4): 397–416. doi: 10.1111/1365-246X.1970.tb06083.x.

Maufe, B. H. (1924). *An outline of the geology of Southern Rhodesia*. (Report No. 17). Southern Rhodesia:Geological Survey.

Mavonga, T. (2007). An estimate of the attenuation relationship for the strong ground motion in the Kivu Province, Western Rift Valley of Africa. *Physics of the Earth and Planetary Interiors*, 62 (1): 13–21.

McWilliams, M., and McElhinny and M. W., (1977), Precambrian geodynamics-A paleomagnetic view, Tectonophysics 40. 137-159.

McGuire, R. K. (1976). *FORTRAN computer program for seismic risk analysis*, U.S. Geological Survey Open-file Report 76: 1-67.

McGuire, R. M. (1993), Computation of Seismic Hazard, *Annali Di Geofisica*, 36 (3-4): 181–200.

McGuire, R.K. (1995). Probabilistic Seismic Hazard Analysis and Design Earthquakes: Closing the Loop. *Bulletin of the Seismological Society of America*, 85 (5): 1275-1284

McGuire, R. K. (2004). Seismic Hazard and Risk Analysis. Oakland: Earthquake Engineering Research Institute.

Mekonnen T.A.,(2004),*Interpretation and Geodatabase of Dykes Using Aeromagnetic Data of Zimbabwe and Mozambique*, Unpublished MSc Thesis in Geo-informatic Science and Earth Observation,

Department of Applied Geophysics., International Institute for Geo-information Science and Earth Observation.

Merz, H. A., and Cornell, C. A., (1973), Seismic Risk Based on Quadratic Magnitude Frequency Low. *Bulletin of the Seismological Society of America*, 63 (6-1): 1209-1214.

Midzi V. *et al*. (1999). Seismic Hazard assessment of East and southern Africa, *Annali Di Geofisica*, 42(6): 1067-1083.

Mkweli, S. Kamber, B & Berger M, (1995). Westward continuation of the craton-Limpopo Belt tectonic break in Zimbabwe and new age constraints on the timing of the thrusting, *Journal of the Geological Society of London*, 152:77-83.

Munich Reinsurance Company, (2000), Topics 2000. Natural Catastrophes - the current position. Special Millennium Issue. Munich, Munich Re Group.

Pisarenko, V.F. Lyubushin, A.A. Lysenko, V.B. & Golubieva, T. V. (1996). Statistical estimation of seismic hazard parameters: Maximum possible magnitude and related parameters, *Bulletin of the Seismological Society of America*, 86(3):691-700.

Reiter, L. (1990). *Earthquake Hazard Analysis: Issues and insights*. Columbia University press: New York.

Richter, C. F. (1958). *Elementary Seismology*, Freeman: San Francisco.

Rollinson, H.R. (1993). Aterrane interpretation of the Archaean Limpopo Belt, *Geological Magazine*, 130: 755–765.

Rollinson, H.R. & Blenkinsop, T. (1995). The magmatic, metamorphic and tectonic evolution of the Northern Marginal Zone of the Limpopo Belt in Zimbabwe, *Journal of the Geological Society of London*, 152(1):65–75. doi:10.1144/gsjgs.152.1.0065

Rydelek, P. A. & Sacks, I. S. (1989). Testing the completeness of earthquake catalogs and the hypothesis of self-similarity, *Nature*, 337(6204): 251– 253. doi: 10.1038/337251a0

Rydelek, P. A., & Sacks, I. S. (1992), Comment on "Seismicity and detection/ location threshold in the southern Great Basin seismic network" by Joan Gomberg. *Journal of Geophysics Research*, 97 (B11): 15361– 15362. doi: 10.1029/92JB00604.

Saman Yaghmaei-Sabegh., Anbazhagan, P. Neaz Sheikh, M. & Hing-Ho Tsang. (2010). A checking method for probabilistic seismic-hazard assessment: case studies on three cities. *Natural Hazards*, 58(1): 67-84. Available from http://hdl.handle.net/10722/145072

Sandi, H. *et. al*. (2007). S*eismic Vulnerability Assessment. Methodological elements and applications to the case of Romania*. International Symposium on Strong Vrancea Earthquakes and Risk Mitigation. Bucharest, Romania.

Sarma, S. K. (1994). 'Fortran program ATTEN'. *ESEE Internal Report.* Imperial College: London.

Scholtz, H. C. Kocynski, T. A. & Hutchins, D. G. (1976). Evidence for incipient rifting in Southern Africa, *Journal of Geophysical Research*, 44(1):135-144.

Scholz, C. H. (1968). The frequency magnitude relation of microfracturing in rocks and its relation to earthquakes, *Bulletin of the Seismological Society of America*, 58 (1), 399-415

Schorlemmer, D. Wiemer, S. & Wyss. M. (2005). Variations in earthquake size distribution across different stress regimes. *Nature*, 437(7058):539-542, doi: 10.1038/nature04094.

Senior Seismic Hazard Analysis Committee (SSHAC), Budnitz, R.J. (Chairman). Apostolakis, G.. Boore, D.M. Cluff, L.S. Coppersmith, K. J.Cornell, C. A. & Morris, P. A. (1997). Lawrence Livermore National Laboratory. Prepared for: U.S. Nuclear Regulatory Commission, U.S. Department of Energy and Electric Power Research Institute, NUREG/CR-6372, UCRL-ID-122160.

Sereno, T. J. Jr. & Bratt, S. R. (1989). Seismic detection capability at NORESS and implications for the detection threshold of a hypothetical network in the Soviet Union, *Journal of Geophysical Research*, 94 **(**B8):10397–10414.

Shudofsky, G. N., (1985), Source mechanisms and focal depths of East African earthquakes using Rayleigh-wave inversion and body-wave modelling, *Geophysics Research Journal*, 83, 563 –614.

Singh, K.S. Ordaz, M. Lindholm, C.D. & Havskov, J. (1990). Seismic hazard in southern Norway, *Bergen University Seismological Series*, 46:1-33

Somerville, P.G. Saikia, C. K. Wald, D. J. &. Graves, R. W. (1996). Implications of the Northridge earthquake for strong ground motions from thrust faults. *Bulletin of the Seismological Society of America*, 86(1B): S115-S125.

Somerville, P. Collins, N. Abrahamson, N. Graves, R. & Saikia, C. (2001). *Ground motion attenuation relations for the central and eastern United States*, (Report No 99HQR0098). United States of America: United States Geological Survey.

Sykes R. L. (1970). Seismicity of the Indian Ocean and a possible nascent Island arc between Ceylon and Australia, *Journal of Geophysical Research,* 75 (26): 5041 – 5055. doi: 10.1029/JB075i026p05041.

Theodorakatou, A. (2007). *Sensitivity analysis in probabilistic seismic hazard assessment*, Unpublished M.Sc. Thesis. European School for Advanced Studies in Reduction of Seismic Risk, Pavia: University of Pavia.

Tinti, S. & Mulargia, F. (1985a). Effects of Magnitude Uncertainties in the Gutenberg-Richter Frequency-magnitude Law. *Bulletin Seismological Society of America*, 75 (6): 1681–1697.

Tinti, S. & Mulargia, F. (1985b). Application of the extreme value approaches to the apparent magnitude distribution of the earthquakes, *Pure and applied geophysics* 123 (2): 199–220.

Trifunac, M.D. (1989).Threshold Magnitudes Which Cause Ground Motion Exceeding the Values Expected during the Next 50 Years in a Metropolitan Area, *Geofizika*, 6 (1):1-12.

Twesigomwe, E. M. (1997). Seismic hazards in Uganda, *Journal of African Earth Sciences*, 24 (1/2): 183–195.

Utsu, T. (1984). Estimation of parameters for recurrence models of earthquakes, *Bulletin of Earthquake Research Institute*, University of Tokyo. 59 (1): 53-66.

Vail J.R. (1967). The Southern extension of the East Africa rift system and related igneous activity. *Geological Rands*, 57 (1): 601-604.

Van Reenen D.D. McCourt, S. & Smit C.A. (1995). Are the Southern and Northern Marginal Zones of the Limpopo Belt related to a single continental collisional event?. *South African Journal of Geology*, 98 (4):498–504.

Veneziano, D. Cornell, C. A. & O'hara, T. (1984), *Historic Method for Seismic Hazard Analysis*, Electric Power Research Institute. (Report *NP*-3438). Palo Alto.

Wang, Z. & Zhou, M. (2007). Comment on ''Why do modern probabilistic seismic-hazard analysis often lead to increased hazard estimates?'' by Julian J. Bommer and Norman A. Abrahamson, *Bulletin of the Seismological Society of America* 97 (6): 2212–2214. doi: 10.1785/0120070004.

Wang, Z., (2010). Seismic Hazard Assessment: Issues and Alternatives. *Pure and Applied Geophysics*, 168(2011): 11–25. doi: 10.1007/s00024-010-0148-3.

Watkeys, M.K. (1983), Brief explanatory notes on the provisional geological map of the Limpopo Belt and environs, *Special Publication of the Geological Society of South Africa*, 8, 5–8.

Weichert, D. H. (1980). Estimation of the Earthquake Recurrence Parameters for Unequal Observation Periods for Different Magnitudes. *Bulletin of the Seismological Society of America*, 70 (4): 1337-1346

Weimer, S. & Wyss, M. (2000*).* Minimum magnitude of completeness in earthquake catalogs: Examples from Alaska, the Western US and Japan. *Bulletin of the Seismological Society of America*, 90 (4): 859 – 869.

Wheeler, R. L. (2009). *Methods of* M_{max} *Estimation East of Rocky Mountains*. (Open-File Report 2009-1018). USGS: United States of America.

Wiemer, S, & Katsumata, K. (1999). Spatial variability of seismicity parameters in aftershock zones. *Journal of Geophysical Research*, 104, (B6):13135–13151. doi 10.1029/1999JB900032.

World Meteorological Organization, (WMO).(1999), *Comprehensive Risk Assessment For Natural Hazards*. (Report Series: TD no. 955). WMO:Geneva.

Xie, J. & Mitchell, J. B. (1990). A back-projection method for imaging large-scale lateral variations of Lg coda Q with application to continental Africa. *Geophysical Journal International*, 100 (2): 161-181.

Xu, Guangyin, and Gao, Mengtan (1997), Study of the Non-uniform Distribution of Earthquake Risk within Potential Sources, *Earthquake Research in China*, 11, 69–75.

Yaghmaei-Sabegh S., Anbazhagan P., Neaz Sheikh M., Hing-Ho Tsang., (2010), A checking method for probabilistic seismic-hazard assessment: case studies on three cities. *Natural Hazards*, 58 (1), 67-84.

Zingoni, A. (2008). Report on the South African Eurocodes Summit. Pretoria:Joint Structural Division of South Africa, Available at http://www.eurocodes.uct.ac.za/downloads/South_African_Eurocode_Summit.pdf [Accessed on 2 May 2013]

Zuniga, F. R. & Wyss, M. (1995). Inadvertent changes in magnitude reported in earthquake catalogs: Their evaluation through *b*-value estimates. *Bulletin of the Seismological Society of America*, 85 (6): 1858–1866.